

Bayrische Julius Maximilians Universität
Würzburg



Diplomarbeit

von

Felix Keller

*Heavy Gauge Boson Scattering
in the
Electroweak Standard Model
and its
Extensions*

10. Oktober 2010

vorgelegt bei:

Prof. Dr. Thorsten Ohl

am

Institut für Theoretische Teilchenphysik und Astrophysik

Zusammenfassung

Die vorliegende Arbeit beschäftigt sich mit der Streuung schwerer Eichbosonen im Standard Model der Teilchenphysik und unter Berücksichtigung anormaler Eichbosonenkopplungen.

Dafür wird zunächst die Einführung schwerer Eichbosonen durch nicht abelsche $SU(2)_L$ Symmetriegruppe im Standard Model und die daraus resultierenden Selbstwechselwirkungen der Eichbosonen gezeigt und die entsprechenden Feynmanregeln abgeleitet.

Die Beschreibung des Standardmodel als effektive Theorie bei niedrigen Energien lässt die Formulierung von zusätzlichen Termen mit Massendimension vier zu, die in unitärer Eichung zusätzliche dreier und vierer Eichbosonen Vertizes in die Theorie einbringen. Die daraus resultierenden Feynman Graphen und damit Beiträge zur Eichbosonenstreuung werden berechnet.

Insgesamt werden mit diesen Feynman Regeln analytisch alle möglichen $V, V \rightarrow V, V$ totalen Wirkungsquerschnitte für Streuung im Standard Modell und mit eingeschaltetet anormaler dreier und vierer Eichbosonenkopplungen berechnet. Die analytischen Ergebnisse werden verwendet um den Monte Carlo Eventgenerator Whizard in diesen Prozessen zu testen. Dafür werden zunächst die Standard Modell Wirkungsquerschnitte verglichen.

Die anormalen Eichboson Kopplungen werden auf zwei Arten getestet. Zunächst werden die anormalen konstant gehalten und der totale Wirkungsquerschnitt in abhängigkeit der Schwerpunktsenergie untersucht. Als zweiter Test wird bei konstanter Schwerpunktsenergie der Wert der anormalen Kopplung in der Umgebung des Standardmodell Wertes variiert.

Der letzte Teil der Arbeit beschäftigt sich mit dem Prozess $e^+e^- \rightarrow l\nu_l q\bar{q}$ der Zugriff auf anormale Eichbosonen Kopplungen an Elektron/Positron Collidern wie dem zukünftigen Linearbeschleuniger (ILC) erlaubt. Die anormalen Kopplungen können hier bei voller Schwerpunktsenergie im Prozess $e^+e^- \rightarrow W^+W^-$ getestet werden. Die W Bosonen zerfallen dann in vier Fermionen, unter anderem in Endzustände der Form $l\nu_l q\bar{q}$. In dieser Arbeit werden die totalen Wirkungsquerschnitte für einige dieser Kopplungen mit Whizard berechnet.

Contents

1	Introduction	4
2	The electroweak Standard Model	6
2.1	Local U(1) and SU(2) Gauge Symmetry	6
2.2	Gauge Boson Self Interactions	8
2.3	GWS Gauge Bosons and Fermion interactions	9
2.4	Gauge Boson Masses	9
2.5	Fermions and Fermion Masses	12
2.6	Feynman Rules of GWS Theory	13
2.6.1	Gauge Boson Self Interactions	13
2.6.2	Gauge boson Propagator and Finite Particle Width	14
2.6.3	Fermion Gauge Boson interactions	15
2.6.4	Gauge Boson Higgs Interactions	16
3	Extensions to the Standard Model	17
3.1	Effective Lagrangian	18
3.2	Anomalous Couplings	22
3.3	Feynman Rules	22
3.3.1	Quartic Couplings	23
3.3.2	Triple Gauge Boson Vertex	24
4	Heavy Gauge Boson Scattering Cross Sections	26
4.1	Mandelstam variables	26
4.2	Center of Mass Frame	27
4.3	Crossing Symmetry	27
4.4	$2 \rightarrow 2$ cross sections	28
4.5	Standard Model scattering	29
4.5.1	$W^+ W^- \rightarrow W^+ W^-$	30
4.5.2	$W^+ W^- \rightarrow Z Z$	32
4.5.3	$Z Z \rightarrow Z Z$	33
4.6	Gauge Boson Scattering with Anomalous Couplings	34
5	Comparison of analytically and numerically calculated cross sections	37
5.1	Whizard - A Monte Carlo Event Generator	37
5.2	Interpretation of numerical results	38
5.3	Noise in analytic calculations	42
5.4	Standard Model Scattering	42

5.4.1	$ZZ \rightarrow ZZ$	42
5.4.2	Cross sections involving four charged gauge bosons	44
5.4.3	Cross sections involving two charged and two Z bosons	45
5.5	Gauge Boson Scattering with Anomalous Couplings	47
5.5.1	Variation of \sqrt{s} for Constant Anomalous Couplings	47
5.5.2	Variation of the Couplings at Constant Energy \sqrt{s}	50
6	Anomalous Couplings in cross section $e^+e^- \rightarrow 4f$	52
6.1	W production in $e^+e^- \rightarrow W^+W^-$	52
6.2	Total cross section of $e^+e^- \rightarrow l\nu_l q\bar{q}$	54
7	Conclusion	57
A	Tables	59
A.1	Standard Model Scattering	59
A.1.1	Cross sections involving four Z bosons	59
A.1.2	Cross sections involving four W bosons	61
A.1.3	Cross sections involving two Z and two W bosons	63
A.2	Scattering with anomalous couplings	65
A.2.1	Quartic couplings in four W boson cross sections	65
A.2.2	Quartic couplings in two Z and two W boson cross sections	67
A.2.3	Quartic couplings in four Z -boson cross section	71
A.2.4	Triple gauge boson couplings	73
A.3	$W^-W^- \rightarrow W^-W^-$ with different seeds and iterations	90
A.4	Scan of anomalous couplings at c.m. energy 1 TeV	91
B	Used Software	107

Chapter 1

Introduction

The Standard Model of particle physics with its underlying $SU(3)_C \times SU(2)_L \times U(1)_Y$ symmetry group is the widely accepted model that describes known particle interactions. It contains the QCD with its $SU(3)_C$ symmetry that describes the strong interactions of quarks. The $SU(2) \times U(1)$ is the symmetry of the unified theory of electromagnetic and weak interactions known as the Glashow Weinberg Salam Theory.

The weak interactions are mediated by heavy gauge bosons. They were predicted by Glashow and Salam as a consequence of non abelian $SU(2)$ symmetry and were found experimentally and their properties have been studied with high precision at the lepton collider LEP and LEP 2 and CERN. [2, 5, 6]

Although Standard Model processes have been tested, in some cases with high precision, the model itself cannot be the most fundamental theory of particle physics because of certain shortcomings. One would be the absence of neutrino masses Standard model in contrast to the fact that at least not all neutrinos are massless due to neutrino the measurement of neutrino oscillations. Besides, the forth of natures fundamental forces, gravity, is completely absent in the Model. A way of keeping the Standard Model physics but also extending it to possible new physics can be done via an effective theory approach. Doing so the Standard Model physics is expressed as a low energy theory, while new physics enter at a high energy scale and is suppressed at low energies.

This gives the possibility of introducing additional heavy gauge boson couplings which have to be tested in experiments at particle colliders. Measurements at OPAL or DELPHI at LEP have already given constraints on anomalous gauge boson couplings. [4, 7]. While LEP2 operated near production threshold of 2 W bosons around 190 GeV, the currently running Large Hadron collider (LHC) or future experiments like ILC work at center of mass energies beyond heavy gauge boson production threshold. Therefore they are expected to give new insights on physics beyond Standard Model, like anomalous gauge boson couplings.

In this thesis we review the Standard models electroweak sector and derive Feynman rules for heavy gauge boson scattering. Additionally, we give a description of Standard Model physics in an effective theory approach, which leads to additional triple and quartic gauge boson vertices with so called anomalous couplings. Using these vertices and the Standard Model gauge boson Feynman rules, we calculate all possible $VV \rightarrow VV$ ($V = W, Z$) total cross sections in chapter 4. We use these analytical calculated cross sections to validate

Whizard's numerical heavy gauge boson cross sections in Standard Model and with anomalous couplings in chapter 5. The tests are separated in two parts. First Whizard's calculations at different c.m. energies are tested while keeping constant anomalous couplings. Additionally we vary the anomalous couplings around their Standard Model value for constant c.m. energy $s = 1 \text{ TeV}$.

In chapter 6 we use Whizard to calculate the total cross section for the process $e^+e^- \rightarrow (W^+W^-) \rightarrow l\nu q\bar{q}$. This process gives the opportunity to probe the triple gauge boson couplings at full c.m. energy, because of s -channel diagrams in W production $e^+e^- \rightarrow W^+W^-$. Under assumed $SU(2) \times U(1)$ gauge invariance the set of anomalous couplings is reduced. For the remaining couplings, the total cross section for semi leptonic four fermion final states is calculated and compared to the Standard Model cross sections at LEP energy $\sqrt{s} = 190 \text{ GeV}$ and at ILC energies $\sqrt{s} = 500 \text{ GeV}$ and 1000 GeV .

Chapter 2

The electroweak Standard Model

The Standard Model of particle physics describes the weak, electromagnetic and strong interactions. The underlying gauge symmetry of this model is $SU(3)_c \times SU(2)_L \times U(1)_Y$. The $SU(3)_c$ describes the strong interactions of quarks and will not be considered further. The remaining $SU(2)_L \times U(1)_Y$ form a spontaneously broken gauge theory which gives the experimentally correct description of weak and electromagnetic interactions. This theory of electromagnetic and weak interactions was first introduced by Glashow, Weinberg and Salam [1], thus giving it its name Glashow, Weinberg and Salam (GWS) theory or the Electroweak Standard Model.

This section gives a brief overview about GWS theory focusing on local gauge symmetry that leads to the introduction of gauge boson fields. The gauge boson self interactions will be introduced and spontaneous symmetry breaking, which via the Higgs mechanism, leads to gauge boson masses will be discussed.

Finally the Feynman rules of the electroweak interactions with a focus on gauge boson scattering are presented.

2.1 Local U(1) and SU(2) Gauge Symmetry

Lets start with a local U(1) transformation, i.e. a local phase rotation through an angle $\alpha(x)$ acting on an Dirac spinor $\Psi(x)$.

$$\Psi(x) \rightarrow e^{i\alpha(x)}\Psi(x) \quad (2.1)$$

The angle $\alpha(x)$ may vary from point to point. Now the theory shall be invariant under a transformation like this. Bilinear terms like fermion mass terms $m\bar{\Psi}\Psi$ do not lead to difficulties since the phase simply cancels to a factor 1 with its complex conjugate. But considering derivatives like $\partial_\mu\Psi$ problems arise. This can be seen by looking at the definition of the derivative for example in direction n_μ

$$n^\mu\partial_\mu = \lim_{\epsilon \rightarrow 0} \frac{1}{\epsilon} [\Psi(x + \epsilon n) - \Psi(x)] \quad (2.2)$$

Here two fields are subtracted which transform differently under the transformation (2.1). A way out is the introduction of a factor that compensates the differences between different spacetime points. This is done by defining the covariant derivative

$$D_\mu = \partial_\mu - ieA_\mu(x) \quad (2.3)$$

After a straightforward calculation it can be shown (see Peskin [17], p.483) that the field A transforms under the local gauge transformation (2.1) like

$$A_\mu(x) \rightarrow A_\mu(x) - \frac{1}{e}\partial_\mu\alpha(x) \quad (2.4)$$

Transforming $D_\mu\Psi$ locally according to (2.1) and by using the transformation properties of A and the definition of the covariant derivative D_μ (2.3) we see that

$$D_\mu\Psi(x) \rightarrow D_\mu e^{i\alpha(x)}\Psi(x) = e^{i\alpha(x)}D_\mu\Psi(x) \quad (2.5)$$

holds. That means the covariant derivative transforms under this local $U(1)$ transformation like the Dirac field itself. In this way a new vector field, a so called gauge field is introduced to the theory. Now, by adding a kinetic term for $A(x)$ one can give this field a dynamical degree of freedom. This can be done in terms of the covariant derivative and one eventually arrives at the kinetic term [17]

$$ieF_{\mu,\nu} = [D_\mu, D_\nu] \quad (2.6)$$

which can be identified with the electromagnetic field tensor. The commutator of covariant derivatives itself transforms under local phase transformation

$$[D_\mu, D_\nu]\Psi(x) \rightarrow [D_\mu, D_\nu]e^{i\alpha(x)}\Psi(x) = e^{i\alpha(x)}[D_\mu, D_\nu]\Psi(x) \quad (2.7)$$

So by demanding the field Ψ to respect a local symmetry a new vector field occurred in the theory. Furthermore by assuming the Lagrangian to be invariant under parity and time reversal this leads to the Maxwell Dirac Lagrangian of QED [17].

$$\mathcal{L} = \bar{\Psi}(i\not{D})\Psi - \frac{1}{4}(F_{\mu\nu})^2 - m\bar{\Psi}\Psi \quad (2.8)$$

This method of imposing a local symmetry can be generalized to more complex theories. Yang and Mills proposed an generalization from local phase rotation of the principles from above to any continuous symmetry group. [20] In case of an $SU(2)$ group the starting point is an doublet of Dirac fields

$$\Psi = \begin{pmatrix} \Psi_1(x) \\ \Psi_2(x) \end{pmatrix} \quad (2.9)$$

This doublet shall transform under the local transformation

$$V(x) = \exp\left(i\alpha^i(x)\frac{\sigma^i}{2}\right) \quad (2.10)$$

where σ^i are the Pauli spin matrices, in a way that looks like (2.1)

$$\Psi(x) \rightarrow V(x)\Psi(x) \quad (2.11)$$

but which is not a rotation in physical space. In the original work of Yang and Mills [20] Ψ is a proton neutron doublet that transforms under isotopic spin. Now the Lagrangian has to be constructed like above to be invariant to this local SU(2) transformation. The difference is, that due to the Pauli matrices there are three orthogonal symmetry motions that do not commute with each other. So again a covariant derivative is defined

$$D_\mu = \partial_\mu - igA_\mu^i \frac{\sigma^i}{2} \quad (2.12)$$

with three vector fields A^i , one for each generator, and a coupling constant g . Again like in the $U(1)$ case, a field strength tensor can be defined using the commutator of the covariant derivative

$$[D_\mu, D_\nu] = -igF_{\mu\nu}^i \frac{\sigma^i}{2} \quad (2.13)$$

but because of the non commuting Pauli matrices, fulfilling the commutator relation

$$\left[\frac{\sigma^i}{2}, \frac{\sigma^j}{2} \right] = i\epsilon^{ijk} \frac{\sigma^k}{2} \quad (2.14)$$

with the SU(2) structure constants ϵ^{ijk} there occurs an extra term in F

$$F_{\mu\nu}^i = \partial_\mu A_\nu^i - \partial_\nu A_\mu^i + g\epsilon^{ijk} A_\mu^j A_\nu^k \quad (2.15)$$

And again a gauge invariant kinetic term for the field strength can added to the theory

$$\mathcal{L} = -\frac{1}{2} \text{Tr} \left[\left(F_{\mu\nu}^i \frac{\sigma^i}{2} \right)^2 \right] = -\frac{1}{4} \sum_i (F_{\mu\nu}^i)^2 \quad (2.16)$$

Together with fermions this leads to the Yang Mills Lagrangian

$$\mathcal{L} = -\frac{1}{4} \sum_i (F_{\mu\nu}^i)^2 + \bar{\Psi}(i\not{D})\Psi - m\bar{\Psi}\Psi \quad (2.17)$$

that contains the coupling constant g and the fermion mass as parameters.

2.2 Gauge Boson Self Interactions

A built-in feature of non abelian gauge theories is the occurrence of gauge boson self interactions. This can easily be seen by explicitly putting in the field strength tensor

$$F_{\mu\nu}^a = \partial_\mu A_\nu^a - \partial_\nu A_\mu^a + gf^{abc} A_\mu^b A_\nu^c \quad (2.18)$$

of a non abelian gauge theory with the structure constants f^{abc} into the kinetic term, (2.15). The index a will be summed over the generators of the gauge group.

In the expansion will occur terms that lead to three

$$\mathcal{L}_3 = -g f^{abc} (\partial_\kappa A_\lambda^a) A^{b\kappa} A^{c\lambda} \quad (2.19)$$

and four

$$\mathcal{L}_4 = -\frac{1}{4} g^2 (f^{eab} A_\kappa^a A_\lambda^b) (f^{ecd} A^{c\kappa} A^{d\lambda}) \quad (2.20)$$

gauge boson vertices. The Feynman rules for GWS theory including the gauge boson vertices will be derived below in chapter 2.6.

2.3 GWS Gauge Bosons and Fermion interactions

As mentioned above, the gauge group of GWS theory is $SU(2)_L \times U(1)_Y$. So following the arguments above by demanding local gauge invariance one has to define a covariant derivative that introduces gauge bosons into the theory. The general covariant derivative for a fermion field belonging to such a $SU(2)$ representation with a $U(1)$ charge Y is

$$D_\mu = \partial_\mu - ig A_\mu^a \tau^a - ig' Y B_\mu \quad (2.21)$$

where the A_μ^a are the three $SU(2)$ gauge bosons, τ^a are the generators of $SU(2)$ and B_μ the $U(1)$ boson.

2.4 Gauge Boson Masses

So far the three gauge bosons in this theory are massless. Mass terms of the form $m^2 A_\mu A^\mu$ are forbidden because of the $SU(2) \times U(1)$ gauge invariance of the Standard model. Using the transformation properties of the gauge field in this mass term

$$m^2 A_\mu A^\mu = m^2 (A_\mu - \partial_\mu \alpha(x)) (A^\mu - \partial^\mu \alpha(x)) \quad (2.22)$$

violates gauge invariance. The method of introducing gauge boson masses into GWS theory gauge boson masses is the Higgs mechanism. A new complex, scalar field, which is a spinor in case of $SU(2)$

$$\Phi = \begin{pmatrix} \Phi^a \\ \Phi^b \end{pmatrix} = \begin{pmatrix} \Phi_1^a + i\Phi_2^a \\ \Phi_1^b + i\Phi_2^b \end{pmatrix} \quad (2.23)$$

is postulated in the theory. The components of Φ are complex, so they are build up by two real fields each. The Lagrangian for Φ is

$$\mathcal{L} = (D_\mu \Phi)^\dagger (D^\mu \Phi) - \underbrace{\mu^2 \Phi^\dagger \Phi + \lambda (\Phi^\dagger \Phi)^2}_{=V} \quad (2.24)$$

where $\mu^2 < 0$ and $\lambda > 0$ so that the potential V of the field Φ is bounded from below. The total minimum of a potential like this is degenerate

$$\Phi(x) = \Phi_0 = \frac{-\mu^2}{2\lambda} e^{i\theta} \quad (2.25)$$

where θ defines a direction in the complex Φ plane. Choosing one particular state breaks the symmetry spontaneously. Because θ is arbitrary it is most convenient to chose $\theta = 0$ so that

$$\Phi_0 = \frac{-\mu^2 \frac{1}{2}}{2\lambda} = \frac{1}{\sqrt{2}v} \quad (2.26)$$

where v becomes the electroweak scale. Looking at deviations around this ground state leads to the occurrence of Goldstone bosons, which are massless, scalar and neutral. But since Goldstone bosons are not observed in nature, one has to get rid of them and the Higgs mechanism takes care of that in the following way.

The Higgs Mechanism choses the nonzero vacuum expectation value for the field Φ to spontaneously break the symmetry of V , i.e. the ground state becomes

$$\langle \Phi \rangle = \frac{1}{\sqrt{2}} \begin{pmatrix} 0 \\ v \end{pmatrix} \quad (2.27)$$

and the particle spectrum can be parametrized by expanding around this minimum

$$\Phi = \frac{1}{\sqrt{2}} \begin{pmatrix} \eta_1 + i\eta_2 \\ v + H + i\eta_3 \end{pmatrix} \quad (2.28)$$

with the three Goldstone boson $\eta_{1,2,3}$. These unphysical fields can be transformed away by going into unitary gauge where the field Φ takes the form

$$\Phi = \frac{1}{\sqrt{2}} \begin{pmatrix} 0 \\ v + H \end{pmatrix} \quad (2.29)$$

giving mass to the massless gauge bosons. The scalar, neutral field H - the Higgs Boson - survives. The Goldstone bosons are said to be 'eaten' by the gauge bosons giving them their third degree of freedom. This statement becomes plausible, when considering the actual degrees of freedom. Before applying the Higgs mechanism, the three massless gauge have two possible polarization states each. The $SU(2)$ field Φ with its complex components contributes four degrees of freedom. So together there are 10 degrees of freedom. After the Higgs mechanism each gauge boson acquired mass and therefore a third longitudinal polarization. So the gauge bosons in all have nine degrees of freedom plus the degree of freedom of the Higgs boson equals the 10 degrees of freedom before the Higgs mechanism was carried out.

In more detail the gauge boson mass terms are created by the VEV in the kinetic term of the scalar field $\Phi(2.29)$. Using the covariant derivative

$$D_\mu \Phi = \left(\partial_\mu - igA_\mu^a \tau^a - ig' \frac{1}{2} B_\mu \right) \Phi \quad (2.30)$$

where A_μ^a are the three SU(2) gauge bosons and B_μ is the U(1) gauge bosons there occur gauge boson mass terms. The relevant terms are [17]

$$\Delta\mathcal{L} = \frac{1}{2} \begin{pmatrix} 0 & v \end{pmatrix} \begin{pmatrix} gA_\mu^a\tau^a + g'\frac{1}{2}B_\mu \end{pmatrix} \begin{pmatrix} gA_\mu^b\tau^b + g'\frac{1}{2}B_\mu \end{pmatrix} \begin{pmatrix} 0 \\ v \end{pmatrix} \quad (2.31)$$

which, by inserting the Pauli matrices $\tau^i = \frac{\sigma^i}{2}$ lead to

$$\Delta\mathcal{L} = \frac{1}{2} \frac{v^2}{4} [g^2(A_\mu^1)^2 + g^2(A_\mu^2)^2 + (-gA_\mu^3 + g'B_\mu)^2] \quad (2.32)$$

By this Higgs mechanism three gauge bosons acquired mass while the fourth remains massless. This is most obvious in the notation of mass eigenstates of the gauge bosons.

$$W_\mu^\pm = \frac{1}{\sqrt{2}} (A_\mu^1 \mp iA_\mu^2) \quad \text{with} \quad m_W = g\frac{v}{2} \quad (2.33a)$$

$$Z_\mu = \frac{1}{\sqrt{g^2 + g'^2}} (gA_\mu^3 - g'B_\mu) \quad \text{with} \quad m_Z = \sqrt{g^2 + g'^2}\frac{v}{2} \quad (2.33b)$$

$$A_\mu = \frac{1}{\sqrt{g^2 + g'^2}} (gA_\mu^3 + g'B_\mu) \quad \text{with} \quad m_A = 0 \quad (2.33c)$$

The covariant derivative, (2.21) now takes the form

$$\begin{aligned} D_\mu = \partial_\mu - i\frac{g}{\sqrt{2}}(W_\mu^+\tau^+ + W_\mu^-\tau^-) - i\frac{1}{\sqrt{g^2 + g'^2}}Z_\mu(g^2\tau^3 - g^2Y) \\ - i\frac{gg'}{\sqrt{g^2 + g'^2}}A_\mu(\tau^3 + Y) \end{aligned} \quad (2.34)$$

where $\tau^\pm = (\tau^1 \pm i\tau^2)$. To simplify this expression one can identify the electron charge e with

$$e = \frac{gg'}{\sqrt{g^2 + g'^2}} \quad (2.35)$$

and the electric charge quantum number with

$$Q = T^3 + Y \quad (2.36)$$

and further more introduce the electroweak mixing angle θ_w that appears in the rotation of the interactions basis (A^3, B) to the mass basis (Z, A)

$$\begin{pmatrix} A^3 \\ B \end{pmatrix} = \begin{pmatrix} \cos\theta_w & -\sin\theta_w \\ \sin\theta_w & \cos\theta_w \end{pmatrix} \begin{pmatrix} Z \\ A \end{pmatrix} \quad (2.37)$$

with

$$\cos\theta_w = \frac{g}{\sqrt{g^2 + g'^2}}; \quad \sin\theta_w = \frac{g'}{\sqrt{g^2 + g'^2}} \quad (2.38)$$

Putting it all together, the covariant derivative takes the form

$$D_\mu = \partial_\mu - i\frac{g}{\sqrt{2}}(W_\mu^+T^+ + W_\mu^-T^-) - i\frac{g}{\cos\theta_w}Z_\mu(T^3 - \sin\theta_w Y) - ieA_\mu Q \quad (2.39)$$

with

$$g = \frac{e}{\sin \theta_w} \quad (2.40)$$

So by demanding local gauge invariance and introducing the covariant derivative one has brought gauge bosons into the theory. For the purpose of spontaneous symmetry breaking a scalar field was introduced into the theory and by assigning it an vacuum expectation value, i.e. introducing an electroweak scale v . Gauge boson masses for three of the four gauge bosons were created by the Higgs mechanism while the fourth remains massless. At the same time the $SU(2) \times U(1)$ invariance is retained since ad-hoc adding non invariant gauge boson mass terms to the Lagrangian becomes unnecessary. In this way GWS Theory predicts the existence of massive W and Z bosons by assumptions to the fundamental symmetry of the theory and indeed these gauge bosons have been found experimentally \square .

2.5 Fermions and Fermion Masses

Fermions in GWS Theory are categorized into Leptons and Quarks. While Leptons couple to the $SU(2) \times U(1)$ part of the gauge group, the quarks couple to the the whole $SU(3) \times SU(2) \times U(1)$ gauge group. The standard model quarks form triplets under the color charge. Besides, within the classification of leptons and quarks, the fermion coupling to gauge bosons distinguishes between left handed and right handed particles. Technically this can be realized by defining the projector

$$\Pi^\pm = \frac{1 \pm \gamma^5}{2} \quad (2.41)$$

So a left/right handed spinor can be expressed by

$$\Psi_{L/R} = \Pi^\pm \Psi = \frac{1 \pm \gamma^5}{2} \Psi \quad (2.42)$$

For both quarks and leptons there exist three generations with similar quantum numbers, but with different masses. The left handed fermions form $SU(2)$ Isospin doublets

$$L_L = \begin{pmatrix} l \\ \nu_l \end{pmatrix} \quad Q_L = \begin{pmatrix} u \\ d \end{pmatrix} \quad (2.43)$$

where l stands for the three lepton generations: electron (e), muon (μ) and tauon (τ) with their neutrino partners $\nu_{e,\mu,\tau}$. The three quark generations are pairs of up-type quarks (up (u), charm (c), top (t)) and down-type quarks (down (d), strange(s), bottom(b)). Except for the neutrinos to all leptons and quarks there exists a right handed particle. So finally the Lagrangian for fermion fields is

$$\mathcal{L}_{fermion} = \bar{\Psi}_{L_L, Q_L} i \not{D} \Psi_{L_L, Q_L} + \bar{\Psi}_{L_R, Q_R} i \tilde{\not{D}} \Psi_{L_R, Q_R} \quad (2.44)$$

where \not{D} is the covariant derivative (2.39). For the right handed particles the covariant derivative takes the form

$$\tilde{\not{D}}_\mu = \partial_\mu + ig' Y B_\mu \quad (2.45)$$

Fermion masses in the standard model can not be created by Dirac mass terms like $m\bar{\Psi}\Psi$ since these terms violate gauge invariance. This can be seen by using (2.42)

$$\bar{\Psi}\Psi = (\bar{\Psi}_L + \bar{\Psi}_R)((\Psi_L + \Psi_R)) = \bar{\Psi}_R\Psi_L + \bar{\Psi}_L\Psi_R \quad (2.46)$$

because the projector Π^\pm fulfills the equations

$$(\Pi^+)^2 = \Pi^+ \quad (2.47)$$

$$(\Pi^-)^2 = \Pi^- \quad (2.48)$$

$$\Pi^+\Pi^- = 0 \quad (2.49)$$

These terms are doublets which are not invariant under SU(2) gauge transformation and therefore forbidden in the Standard Model. The method of choice to introduce fermion masses in the standard model is again spontaneous symmetry breaking using the same field Φ that was used to introduce gauge boson masses. The Φ field here is used to create so called gauge invariant Yukawa interactions which take the form

$$\mathcal{L}_{Yukawa} = -\eta(\bar{\Psi}_L\Phi\Psi_R + \bar{\Psi}_R\Phi^\dagger\Psi_L) \quad (2.50)$$

where η are the Yukawa couplings.

2.6 Feynman Rules of GWS Theory

Now the total Lagrangian of the Standard Model can be expressed as

$$\mathcal{L} = \mathcal{L}_{gauge} + \mathcal{L}_{fermion} + \mathcal{L}_{Higgs} + \mathcal{L}_{Yukawa} \quad (2.51)$$

This can be used to derive the Feynman rules of GWS theory. Since this thesis focussed on heavy gauge boson scattering, only the Feynman rules for heavy gauge boson scattering and as far as needed, the gauge boson fermion and gauge boson Higgs vertices shall be derived. For a more detailed description see for example Mandl [14] or Peskin [17].

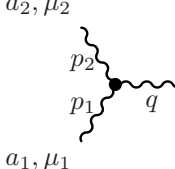
2.6.1 Gauge Boson Self Interactions

As already described in chapter 2.2 the non commuting generators of SU(2) lead to triple and quartic gauge boson self interactions. The relevant parts of the Lagrangian for this interaction in the interaction basis are

$$\mathcal{L}_{3/4} = -gf^{abc}(\partial_\kappa A_\lambda^a)A^{b\kappa}A^{c\lambda} - \frac{1}{4}g^2(f^{eab}A_\kappa^a A_\lambda^b)(f^{ecd}A^{c\kappa}A^{d\lambda}) \quad (2.52)$$

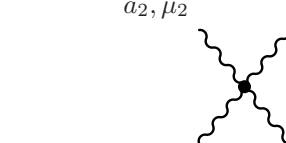
To derive the Feynman rule for the triple gauge boson vertex one has to choose a definite convention for the momenta since the first term of (2.52) contains derivatives. One possible convention is choosing all momenta going into the vertex. Now one has to assign the fields A to the impulses. For example contracting the field A^a with the momentum p_1 , the second field to the momentum p_2 and the third field to momentum q . The derivative contributes a factor $(-ik_\kappa)$ for a

momentum pointing into the diagram. There are 3! possibilities which alternate in sign due to the antisymmetry of the structure constants. The sum over all possibilities is shown in (2.53). The notation is chosen in a way that will allow a convenient construction of the $2 \rightarrow 2$ gauge boson cross sections in chapter 4



$$= g f^{a_1 a_2 b} (g^{\mu_1 \mu_2} (p_1 - p_2)^\nu + g^{\mu_2 \nu} (p_2 - q)^{\mu_1} + g^{\nu \mu_1} (q - p_1)^{\mu_2}) \quad (2.53)$$

The second term in (2.52) leads to the four gauge boson vertex. The same way as for the three gauge boson vertex, the fields A have to be assigned to the momenta but since the term does not contain derivatives, the vertex does not explicitly depend on them. Again there has to be summed over all possible contractions. In all there are 4! possibilities. The vertex is given in (2.54)



$$= -i g^2 [f^{a_1 a_2 b} f^{a_3 a_4 b} (g^{\mu_1 \mu_3} g^{\mu_2 \mu_4} - g^{\mu_1 \mu_4} g^{\mu_2 \mu_3}) + f^{a_2 a_3 b} f^{a_1 a_4 b} (g^{\mu_2 \mu_4} g^{\mu_1 \mu_3} - g^{\mu_1 \mu_2} g^{\mu_3 \mu_4}) + f^{a_2 a_4 b} f^{a_1 a_3 b} (g^{\mu_2 \mu_3} g^{\mu_1 \mu_4} - g^{\mu_1 \mu_2} g^{\mu_3 \mu_4})] \quad (2.54)$$

2.6.2 Gauge boson Propagator and Finite Particle Width

For the calculation of realistic scattering cross sections, at least in the energy range near particle resonances, finite particle widths for massive particles have to be included into the calculation. The simplest approach is using a Breit Wigner Formula. Considering gauge bosons a propagator (in unitary gauge) like

$$\frac{-i}{q^2 - m^2 + im\Gamma_m} \left(g^{\mu\nu} - \frac{k^\mu k^\nu}{k^2} \right) \quad (2.55)$$

with the mass of the intermediate gauge boson m^2 , violates gauge invariance. Mathematically this can be seen in the violation of Ward identities [18].

To avoid this there exist several possibilities, of which two shall be sketched here.

fudge factor scheme In this scheme the amplitude is calculate neglecting the width, i.e. maintaining gauge invariance. Next the complete matrix element is multiplied by a factor [18]

$$\frac{q^2 - m^2}{q^2 - m^2 + im\Gamma_m} \quad (2.56)$$

for every diagram that can become resonant. This method treats resonant diagrams correctly.

Another method of restoring gauge invariance is the

complex mass scheme Here the width is included in the square of the particle mass. This is done by setting

$$m^2 \rightarrow m^2 - im\Gamma_m \quad (2.57)$$

in the whole theory. This implies the use of a complex Weinberg angle [18]

$$\cos\theta_W = \frac{m_W^2 - im_W\Gamma_W}{m_Z^2 - im_Z\Gamma_Z} \quad (2.58)$$

This scheme is gauge invariant at the cost of questionable changes of the physical content of the Feynman rules.

2.6.3 Fermion Gauge Boson interactions

The fermion gauge boson interactions come from the fermion Lagrangian

$$\mathcal{L}_{fermion} = \bar{\Psi}(i\not{D})\Psi \quad (2.59)$$

that couples the gauge bosons via the covariant derivative, (2.39) to the fermions. They are in general separated in interactions that mediate charged and neutral gauge bosons. In the so called charged current the exchanged particles are (W^\pm) bosons.

$$\mathcal{L}_{cc} = -\frac{g}{2\sqrt{2}} \bar{f} (i\gamma^\mu(1 - \gamma_5)) f W_\mu^+ + \text{h.c.} \quad (2.60)$$


In contrast, the neutral current exchanges neutral gauge bosons (Z) and the electromagnetic interaction exchanging a photon.

$$\mathcal{L}_{NC} = -\frac{g}{2\cos(\theta_w)} \bar{f} \gamma^\mu (v - a\gamma_5) f Z_\mu \quad (2.61)$$


with $v = T_3 - 2Q_f \sin(\theta_W)^2$ and $a = T_3$

$$\mathcal{L}_{em.} = -eQ_f \bar{f} \gamma^\mu f A_\mu \quad (2.62)$$

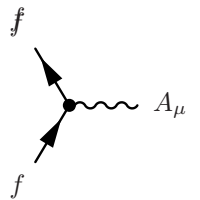
From the charged and neutral current Lagrangian (2.60) and (2.61) and the electromagnetic Lagrangian, (2.62) one easily gets the Feynman Rule for the fermion gauge boson vertex shown in (2.63), (2.64) and (2.65),



$$= -i\frac{g}{2\sqrt{2}}(\gamma^\mu(1 - \gamma_5)) \quad (2.63)$$



$$= -i\frac{g}{2\cos(\theta_w)}\gamma^\mu(v - a\gamma_5) \quad (2.64)$$



$$= ieQ_f\gamma^\mu \quad (2.65)$$

2.6.4 Gauge Boson Higgs Interactions

While the kinetic term of the Higgs field with the covariant derivative D_μ , (2.39) and the given VEV (2.27) creates mass terms for the gauge bosons, the description of the Higgs as excitations as

$$\Phi = \begin{pmatrix} 0 \\ v + H \end{pmatrix} \quad (2.66)$$

leads to Gauge Boson Higgs Interactions. The Lagrangian for the triple vertices becomes

$$(D_\mu \Phi)(D^\mu \Phi) = \frac{2}{v} (m_W^2 W_\mu^+ W^{-\mu} + m_Z^2 Z_\mu Z^\mu) H \quad (2.67)$$

and from this the Higgs gauge boson vertices becomes

$$\begin{array}{c} \mu_2 \\ \text{wavy line} \\ \bullet \\ \text{wavy line} \\ \mu_1 \end{array} \text{---} H = i \frac{2m_{W/Z}^2}{v} g^{\mu_1 \mu_2} \quad (2.68)$$

There are also quartic gauge boson - Higgs interactions but since they do not contribute on $2 \rightarrow 2$ gauge boson scattering, they shall be neglected here.

The Yukawa sector creates Higgs fermion interactions, which depend on the fermion mass of the participating particle. In this thesis, the Feynman rules would be needed for the analysis of $e^+e^- \rightarrow W^+W^-$ cross sections. But by setting the electron to zero which is justified in a high energy limit, these interactions do not give a contribution to the cross section. Therefore the Feynman rules shall be neglected as well as Higgs self interactions.

For a complete collection of the GWS Feynman rules see for example Mandl [14]. With the Feynman rules described in this chapter is possible to calculate heavy gauge boson scattering in the electroweak standard model. This will be shown in chapter 4.

Chapter 3

Extensions to the Standard Model

So far, the Standard Model gives a precise description for all known particle interactions, that were tested in experiments. In the next years LHC data will show, if there actually exists a Standard Model Higgs boson. By this, the Standard Model would be found to give a correct description of the physics within the testable energy range up to the TeV scale and therefore push the energy range for new beyond Standard Model physics to higher energies.

Finding no Higgs could from the physical point of view be considered a more interesting case. It would give a direct hint on new physics. Especially the breaking of electroweak symmetry and the introduction of fermion and gauge boson masses into the model would be open and still are for discussion.

Theories beyond Standard Model physics always have to build in a way that contain the known physics. This can be done in terms of effective Lagrangians where the area of new physics is suppressed up to a certain energy scale.

Such an approach was formulated to describe electroweak symmetry in a bottom up approach. Here the starting point is Fermi's theory where the weak interactions are described by higher dimensional, and therefore low energy suppressed, operators.

We will review this approach of constructing an effective Lagrangian of the electroweak sector by operators with increasing dimension. A detailed discussion of this access to electroweak symmetry breaking was written down in [11].

Demanding the electroweak symmetry $SU(2) \times U(1)$, a new field Σ is introduced. The choice of representation of this field gives the possibility of constructing a Higgsless theory as well as a theory that contains a Higgs boson.

Additionally, simply by constructing all possible (CP invariant) dimension 4 operators, new terms can be added to the Lagrangian as will be shown in chapter 3.2. They lead to anomalous gauge boson couplings, such as a 4 Z boson quartic vertex, which is not contained in the Standard Model.

Finally, the Feynman rules for the quartic and triple gauge boson vertices are derived to be able to calculate gauge boson scattering with anomalous couplings.

3.1 Effective Lagrangian

The operators in the effective Lagrangian that shall describe the electroweak sector are ordered by increasing dimension. The lowest terms in the Lagrangian include information on the mass spectrum of the particles. Using the doublet notation for left and right handed particle fields following Kilian [11]

$$\begin{aligned} Q_L &= \begin{pmatrix} U_L \\ D_L \end{pmatrix}, Q_R = \begin{pmatrix} U_R \\ D_R \end{pmatrix}, \\ L_L &= \begin{pmatrix} N_L \\ E_L \end{pmatrix}, L_R = \begin{pmatrix} N_R \\ E_R \end{pmatrix}, \end{aligned} \quad (3.1)$$

the fermion mass terms, i.e. bilinear terms in the Lagrangian are

$$\mathcal{L} = -(\bar{Q}_L M_Q Q_R + \bar{L}_L M_L L_R + h.c) - (\bar{L}_L^c M_{L_L} \frac{1 + \tau^3}{2} L_L + \bar{L}_R^c M_{N_R} \frac{1 + \tau^3}{2} L_R). \quad (3.2)$$

Here U stands for the up-type quarks u,c,t and D for the down type quarks d,s,b respectively. E describes the leptons e, μ, τ with their neutrino partners ν_e, ν_μ, ν_τ . M_i are the mass matrices and τ_i the Pauli matrices.

Next in this approach will be electromagnetic interactions. With the covariant derivative given in (2.3) and the field strength tensor $A_{\mu\nu}$ we obtain the dimension four operators

$$\mathcal{L}_4 = \bar{Q}_L i \not{D} Q_L + \bar{Q}_R i \not{D} Q_R + \bar{L}_L i \not{D} L_L + \bar{L}_R i \not{D} L_R - \frac{1}{4} A_{\mu\nu} A^{\mu\nu} \quad (3.3)$$

So far \mathcal{L}_3 and \mathcal{L}_4 contain all operators that agree with conservation of fermion number and local U(1) gauge invariance.

Dimension five operators, which follow next in this expansion are of the form

$$\mathcal{L} = \bar{Q}_R \mu_Q \sigma_{\mu\nu} A^{\mu\nu} Q_L + \bar{L} \mu_L \sigma_{\mu\nu} A^{\mu\nu} + h.c \quad (3.4)$$

Their couplings $\mu_{Q/L}$ are of mass dimension -1 , which means their effects are suppressed by a factor $\mu_{Q/L} \propto 1/\Lambda$. These operators occur for example when radiative corrections are calculated. Famous examples would be corrections to the electron's g factor or the operator $\bar{s} \sigma_{\mu\nu} A^{\mu\nu} b$ which is one of the operators that describe a flavor changing neutral current and therefore can be used to describe $b \rightarrow s\gamma$ decays.

The dimension six operators in this effective theory approach describe neutral current and charged current interactions at low energies and thus involve heavy gauge bosons. They can be described by the Lagrangian [11]

$$\mathcal{L}_6 = -4\sqrt{2}G_F(2J_\mu^+ J^{-\mu} + \rho_* J_\mu^0 J^{0\mu}) \quad (3.5)$$

where the neutral and charged currents are given by

$$J_\mu^\pm = \frac{1}{\sqrt{2}} \bar{Q}_L \tau^\pm \gamma_\mu V_{CKM} Q_L + \bar{L}_L \tau^\pm \gamma_\mu L_L \quad (3.6)$$

$$\begin{aligned} J_\mu^0 &= \bar{Q}_L \left(-q_Q \sin(\theta_W)^2 + \frac{\tau^3}{2} \right) \gamma_\mu Q_L + \bar{Q}_R \left(-q_Q \sin(\theta_W)^2 \right) \gamma_\mu Q_R \\ &+ \bar{L}_L \left(-q_L \sin(\theta_W)^2 + \frac{\tau^3}{2} \right) \gamma_\mu Q_L + \bar{L}_R \left(-q_L \sin(\theta_W)^2 \right) \gamma_\mu L_R \end{aligned} \quad (3.7)$$

To implement the local gauge symmetry of the interactions, one introduces the vector fields W^\pm and Z [11]

$$\mathcal{L}_6 = -g_W (W^{+\mu} J_\mu^+ + W^{-\mu} J_\mu^-) - g_Z (Z^\mu J_\mu^0) + \mathcal{L}_{2W} \quad (3.8)$$

with mass terms

$$\mathcal{L}_{2W} = M_W^2 W^{+\mu} W_\mu^- + \frac{1}{2} M_Z^2 Z^\mu Z_\mu . \quad (3.9)$$

Because so far the heavy gauge bosons are no dynamical degrees of freedom and thus are unobservable, i.e. no kinetic terms in the Lagrangian, the field equations for W^\pm and Z read

$$W_\mu^\pm = \frac{g_W}{M_W^2} J_\mu^\mp, Z_\mu = \frac{g_Z}{M_Z^2} J_\mu^0 . \quad (3.10)$$

By inserting the solutions back into 3.8 the original form of \mathcal{L}_6 , (3.7), can be recovered if the coupling parameters and the mass parameters are related to each other by

$$g_W^2 = \frac{4M_W^2}{v^2}, \quad g_Z^2 = \rho_* \frac{4M_Z^2}{v^2} \quad (3.11)$$

Here the electroweak scale v is introduced which is related to the Fermi constant by

$$v = \left(\sqrt{2} G_F \right)^{\frac{1}{2}} . \quad (3.12)$$

If one demands a local gauge symmetry one has to specify the covariant derivative that couples the gauge bosons to fermions. For the left and right handed fermions it is [11]

$$D_{L\mu} = \partial_\mu + ieqA_\mu + i \left(-q \sin(\theta_w)^2 + \frac{\tau^3}{2} \right) Z_\mu + i \frac{g_W}{\sqrt{2}} \left(\tau^+ W_\mu^+ V_{CKM}^\dagger + \tau^- W_\mu^- V_{CKM} \right) , \quad (3.13a)$$

$$D_{R\mu} = \partial_\mu + ieqA_\mu + ig_Z \left(-q \sin(\theta_w)^2 \right) Z_\mu . \quad (3.13b)$$

To make these suitable covariant derivatives one has to identify the corresponding gauge symmetry. So the τ^\pm have to fulfill the relation $[\tau^+, \tau^-] = \tau^3$ and thereby relating the neutral and the charged currents. Doing so the W^\pm contain two components

$$W^\pm = A^1 \mp iA^2 , \quad (3.14)$$

while the third component A^3 has to form the Z field in a linear combination with another U(1) field B . Then analog to the standard model, the photon field and the Z boson are generated by a rotation from the (A^3, B) basis in (2.37). This is not the most general ansatz for the Z and the photon. For a more general ansatz see Kilian [11] chapter 2.1. Finally with a single hypercharge coupling g' the covariant derivatives take the form

$$D_{L\mu} = \partial_\mu + ig' \left(q - \frac{\tau^2}{2} \right) B_\mu + ig A_\mu^a \frac{\tau^a}{2} , \quad (3.15a)$$

$$D_{R\mu} = \partial_\mu + ig' q B_\mu . \quad (3.15b)$$

Putting it all together the Lagrangian for electromagnetic and weak interactions in this bottom up approach is

$$\mathcal{L} = \bar{Q}_L i \not{D}_L Q_L + \bar{Q}_R i \not{D}_R Q_R + \bar{L}_L i \not{D}_L L_L + \bar{L}_R i \not{D}_R L_R - \frac{1}{4} A_{\mu\nu} A^{\mu\nu} + \mathcal{L}_{2W} + \mathcal{L}_3 \quad (3.16)$$

Since the W and Z bosons are known and their masses have been measured in experiments, they are identified with the known gauge bosons and they are given the physical masses

$$M_W = 80.419 \text{ GeV} , \quad M_Z = 91.2 \text{ GeV} . \quad (3.17)$$

To make them physical degrees of freedom at energies above $E \approx M_W$ kinetic terms have to be added in terms of field strength tensors [11]

$$\mathcal{L}_{4W} = -\frac{1}{2} tr [\mathbf{W}_{\mu\nu} \mathbf{W}^{\mu\nu}] - \frac{1}{2} tr [\mathbf{B}_{\mu\nu} \mathbf{B}^{\mu\nu}] \quad (3.18)$$

with

$$\mathbf{W}_{\mu\nu} = \partial_\mu \mathbf{W}_\nu - \partial_\nu \mathbf{W}_\mu + ig [\mathbf{W}_\mu, \mathbf{W}_\nu] , \quad (3.19)$$

$$\mathbf{B}_{\mu\nu} = \partial_\mu \mathbf{B}_\nu - \partial_\nu \mathbf{B}_\mu \quad (3.20)$$

and

$$\mathbf{W}_\mu = W_\mu^a \frac{\tau^a}{2} \quad \mathbf{B}_\mu = B_\mu \frac{\tau^3}{2} . \quad (3.21)$$

Up to now this is a model that contains all Standard Model particles, except the Higgs boson. But a problem is, that the fermion and gauge boson mass terms in (3.2) and (3.9) are not $SU(2) \times U(1)$ gauge invariant. Therefore a field Σ is introduced into the theory that transforms under local $SU(2)_L$ transformations $U(x)$ and $U(1)_Y$ transformations $V(x)$ like [11]

$$\Sigma(x) \rightarrow U(x) \Sigma(x) V^\dagger(x) \quad (3.22)$$

By inserting extra field Σ into the fermion and gauge boson mass terms, we can restore gauge symmetry. The fermion mass terms (3.2) become

$$\mathcal{L} = -(\bar{Q}_L \Sigma M_Q Q_R + \bar{L}_L \Sigma M_L L_R + h.c) \quad (3.23)$$

which becomes now has the required $SU(2)_L \times U(1)_Y$ transformation properties. The boson mass term, (3.9) is replaced by a kinetic energy term for the Σ field. With

$$V_\mu = \Sigma (D_\mu \Sigma)^\dagger \quad \text{and} \quad T = \Sigma \tau^3 \Sigma^\dagger \quad (3.24)$$

and the covariant derivative is determined by the field transformations properties of the sigma field itself,(3.22)

$$D_\mu \Sigma = \partial_\mu \Sigma + ig \mathbf{W}_\mu \Sigma - ig' \Sigma \mathbf{B}_\mu . \quad (3.25)$$

So the gauge boson mass terms can be written as [11]

$$\mathcal{L}_{2W} = -\frac{v^2}{4} tr [V_\mu V^\mu] - \beta' \frac{v^2}{8} tr [TV_\mu] tr [TV^\mu] \quad (3.26)$$

with a free parameter β' .

Since the dimension four part \mathcal{L}_4 (3.3) and the kinetic terms of the gauge bosons (3.13b) already have the required symmetry there is no need for inserting the Σ field. Instead there is the possibility of adding a potential term for the Σ field to the Lagrangian.

$$\mathcal{L} = -\frac{\mu^2 v^2}{4} \text{tr} [\Sigma^\dagger \Sigma] + \frac{\lambda^4 v^4}{16} \text{tr} [\Sigma^\dagger \Sigma]^2 + \dots \quad (3.27)$$

So eventually the Lagrangian that is invariant under the electroweak $\text{SU}(2) \times \text{U}(1)$ symmetry group is

$$\mathcal{L} = \mathcal{L}_{2W} + \mathcal{L}_3 + \mathcal{L}_4 + \mathcal{L}_\Sigma . \quad (3.28)$$

A question that has yet to be answered is the effect of the Σ field in the low energy effective Lagrangian. In order to obtain the known fermion and gauge boson masses the field σ has to obtain a VEV. By this there is no additional information in the modified Lagrangian and it is done by giving a nonzero expectation value to the operator

$$\text{tr} [\Sigma^\dagger \Sigma] \quad (3.29)$$

which can be realized by giving the potential in 3.27 a nontrivial minimum. With the right normalization this can be expressed as

$$\left\langle \frac{1}{2} \text{tr} [\Sigma^\dagger \Sigma] \right\rangle = 1 . \quad (3.30)$$

For calculations one has to select a particular field by hand. For lowest order calculations the choice of unitary gauge, where [11]

$$\Sigma(x) = 1 \quad (3.31)$$

is most convenient, because in this gauge the Lagrangian (3.16) keeps its form of the absence of the Σ field and the vector field V_μ , (3.24) becomes a linear combination of W and Z bosons

$$V_\mu = -ig\mathbf{W}_\mu + ig'B_\mu \quad (3.32)$$

A Higgsless model is realized by imposing the relation [11]

$$\Sigma^\dagger \Sigma = 1 \quad (3.33)$$

where a suitable parametrization for the Σ is

$$\Sigma(x) = \exp\left(-\frac{i}{v}\mathbf{w}(x)\right) \quad \text{with} \quad \mathbf{w}(x) = w^a(x)\tau^a, \quad a = 1, 2, 3 . \quad (3.34)$$

By allowing fluctuations of $\text{tr}[\Sigma^\dagger \Sigma]$, i.e. introducing the replacement

$$\Sigma \rightarrow \left(1 + \frac{1}{v}H\right) \Sigma \quad (3.35)$$

a Higgs boson can be introduced in the theory.

In this thesis the Σ field is defined in unitary gauge, since this gives a convenient

form of the vector fields V_μ in (3.32) for calculations. Finally one arrives at the so called chiral Lagrangian that describes the electroweak interactions in an energy range, where the W and Z boson are dynamical degrees of freedom [11]. But the terms in the Lagrangian considered so far are not all possible terms that respect the electroweak $SU(2)_L \times U(1)_Y$ symmetries, as shall be seen in the next chapter.

3.2 Anomalous Couplings

The construction of the chiral Lagrangian in the preceding chapter is not complete. There are more dimension four operators that can be constructed and that introduce anomalous gauge boson couplings. They are needed as counter terms in loop calculations to make the theory finite at next to leading order. Making the restriction of demanding CP invariance there are the 11 terms shown in 3.36. The first ten terms can be found in [13] while the parity violating eleventh term was investigated in [1].

$$\mathcal{L}_1 = \frac{1}{2} \alpha_1 g' B_{\mu\nu} \text{tr}(TW^{\mu\nu}) , \quad (3.36a)$$

$$\mathcal{L}_2 = \frac{1}{2} i \alpha_2 g' B_{\mu\nu} \text{tr}(T[V^\mu, V^\nu]) , \quad (3.36b)$$

$$\mathcal{L}_3 = i \alpha_3 g \text{tr}(W_{\mu\nu}[V^\mu, V^\nu]) , \quad (3.36c)$$

$$\mathcal{L}_4 = \alpha_4 (\text{tr}(V_\mu V_\nu))^2 , \quad (3.36d)$$

$$\mathcal{L}_5 = \alpha_5 (\text{tr}(V_\mu V^\nu))^2 , \quad (3.36e)$$

$$\mathcal{L}_6 = \alpha_6 \text{tr}(V_\mu V_\nu) \text{tr}(TV^\mu) \text{tr}(TV^\nu) , \quad (3.36f)$$

$$\mathcal{L}_7 = \alpha_7 \text{tr}(V_\mu V^\mu) \text{tr}(TV_\nu) \text{tr}(TV^\nu) , \quad (3.36g)$$

$$\mathcal{L}_8 = \frac{1}{4} \alpha_8 g^2 [\text{tr}(TW_{\mu\nu})]^2 , \quad (3.36h)$$

$$\mathcal{L}_9 = \frac{1}{2} i \alpha_9 \text{tr}(TW_{\mu\nu}) \text{tr}(T[V^\mu, V^\nu]) , \quad (3.36i)$$

$$\mathcal{L}_{10} = \frac{1}{2} \alpha_{10} (\text{tr}(TV_\mu) \text{tr}(TV_\nu))^2 , \quad (3.36j)$$

$$\mathcal{L}_{11} = \alpha_{11} g \epsilon^{\mu\nu\rho\sigma} \text{tr}(TV_\mu) \text{tr}(V_\nu W_{\rho\sigma}) . \quad (3.36k)$$

3.3 Feynman Rules

To derive the Feynman rules for the additional terms in the Lagrangian one has insert the equation for the V_μ (3.32) into the Lagrangian (3.36). In the mass basis V_μ takes the form

$$V_\mu = -i \frac{g_W}{\sqrt{2}} (W_\mu^+ \tau^+ + W_\mu^- \tau^-) - i g_Z Z_\mu \frac{\tau_3}{2} \quad (3.37)$$

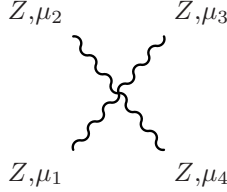
Doing this for example for \mathcal{L}_5 this leads to

$$\begin{aligned}\mathcal{L}_5 &= \frac{\alpha_5 g_W^4}{4} (W_\mu^+ W^{\mu-} + W_\mu^- W^{\mu+}) (W_\nu^+ W^{\nu-} + W_\nu^- W^{\nu+}) \\ &+ 2 \frac{\alpha_5 g_W^2 g_Z^2}{4} (W_\mu^+ W^{\mu-} + W_\mu^- W^{\mu+}) (Z_\nu Z^\nu) \\ &+ \frac{\alpha_5 g_Z^4}{4} (Z_\mu Z^\mu) (Z_\nu Z^\nu)\end{aligned}\quad (3.38)$$

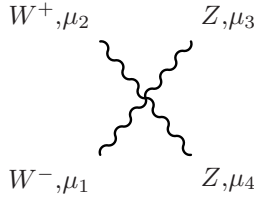
In this case quartic gauge boson couplings occur which can be almost immediately read of the Lagrangian. For example the last term in (3.38) couples directly 4 Z bosons in a quartic vertex proportional to α_5 . Doing so for all additional Lagrangians leads to triple and quartic gauge boson vertices described in the following sections.

3.3.1 Quartic Couplings

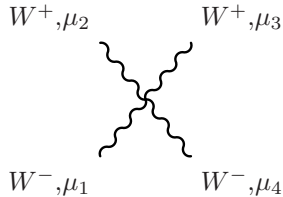
The method described in the previous paragraph was used to derive the quartic couplings from the Lagrangians \mathcal{L}_4 , \mathcal{L}_5 , \mathcal{L}_6 , \mathcal{L}_7 and \mathcal{L}_{10} . Since, due to charge conservation, the only possible particle combinations involve 4 W bosons, 4 Z bosons or 2 W and 2 Z bosons, the Feynman rules can be grouped together in the following three main quartic vertices.



$$= 2i \frac{g^4}{c_w^4} [\alpha_4 + \alpha_5 + 2(\alpha_6 + \alpha_7 + \alpha_{10})] (g^{\mu_1 \mu_2} g^{\mu_3 \mu_4} + g^{\mu_1 \mu_4} g^{\mu_2 \mu_3} + g^{\mu_1 \mu_3} g^{\mu_2 \mu_4}) \quad (3.39)$$



$$= i \frac{g^4}{c_w^2} [(\alpha_4 + \alpha_6) (g^{\mu_1 \mu_4} g^{\mu_2 \mu_3} + g^{\mu_1 \mu_3} g^{\mu_2 \mu_4}) + 2(\alpha_5 + \alpha_7) (g^{\mu_1 \mu_2} g^{\mu_3 \mu_4})] \quad (3.40)$$



$$= ig^4 [2\alpha_4 g^{\mu_1\mu_3} g^{\mu_2\mu_4} + (\alpha_4 + 2\alpha_5) (g^{\mu_1\mu_2} g^{\mu_3\mu_4} + g^{\mu_1\mu_4} g^{\mu_2\mu_3})] \quad (3.41)$$

3.3.2 Triple Gauge Boson Vertex

The triple gauge boson vertex that can be derived from the additional terms in the Lagrangian (3.36a) to (3.36k) can be expressed as the effective Lagrangian in (3.42) as can be found in [9]. The Lagrangian is

$$\begin{aligned} \frac{\mathcal{L}_{WWV}}{g_{WWV}} &= ig_1^V (W_{\mu\nu}^+ W^{-\mu} V^\nu - W_{\mu\nu}^- W^{+\mu} V^\nu) + i\kappa_V W_\mu^+ W_\nu^- V^{\mu\nu} \\ &- g_4^V W_\mu^+ W_\nu^- V^{\mu\nu} + \frac{i\lambda}{m_W^2} W_{\lambda\mu}^+ W_\nu^{-\mu} V^{\nu\lambda} \\ &+ g_5^V \epsilon^{\mu\nu\rho\lambda} (W_\mu^+ (\partial_\rho W_\nu^-) - (\partial_\rho W_\mu^+) W_\nu^-) V_\lambda \\ &+ i\tilde{\kappa}_V W_\mu^+ W_\nu^- \tilde{V}^{\mu\nu} + \frac{i\tilde{\lambda}_V}{m_W^2} W_{\lambda\mu}^+ W_\nu^{-\mu} \tilde{V}^{\nu\lambda} , \end{aligned} \quad (3.42)$$

where V stands for the Z boson and the photon A , $W_{\mu\nu} = \partial_\mu W_\nu - \partial_\nu W_\mu$, $V_{\mu\nu} = \partial_\mu V_\nu - \partial_\nu V_\mu$ and $\tilde{V}_{\mu\nu} = \frac{1}{2}\epsilon_{\mu\nu\rho\sigma} V^{\rho\sigma}$. These are all Lorentz invariant operators when neglecting the scalar component of the vector bosons

$$\partial_\mu V^\mu = 0 , \quad \partial_\mu W^\mu = 0 \quad (3.43)$$

and by using on shell W bosons. In (3.42) there are all dimension four operators except the λ and $\tilde{\lambda}$ terms. These terms come from dimension six operators which have the form [11]

$$tr [\mathbf{W}_\mu^\nu \mathbf{W}_\nu^\rho \mathbf{W}_\rho^\sigma] \quad (3.44)$$

with

$$\mathbf{W}_{\mu\nu} = \partial_\mu \mathbf{W}_\nu - \partial_\nu \mathbf{W}_\mu + ig[\mathbf{W}_\mu, \mathbf{W}_\nu] \quad \text{and} \quad (3.45)$$

$$\mathbf{W}_\mu = W_\mu^a \frac{\tau^a}{2} \quad (3.46)$$

The coupling constants in (3.42) are related to the α_i in 3.36 by [1]

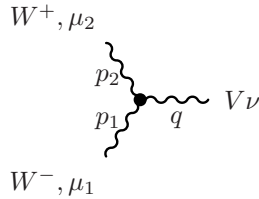
$$\kappa_\gamma - 1 = g^2\alpha_2 + g^2\alpha_3 + g^2\alpha_9 , \quad (3.47a)$$

$$\kappa_Z - 1 = -g^2\alpha_2 + g^2\alpha_3 + g^2\alpha_9 , \quad (3.47b)$$

$$g_1^Z - 1 = \frac{1}{\cos(\theta_W)^2} g^2\alpha_3 , \quad (3.47c)$$

$$g_5^Z - 1 = \frac{1}{\cos(\theta_W)^2} g^2\alpha_{11} . \quad (3.47d)$$

From this Lagrangian the triple gauge vertex can be expressed as



$$\begin{aligned}
&= g_{WWV}(g_1^V g^{\mu_1\mu_2}(p_1 - p_2)^\nu + g^{\mu_2\nu}(g_1^V p_2 - \kappa_V q)^{\mu_1} + g^{\nu\mu_1}(\kappa_V q - g_1^V p_1)^{\mu_2}) \\
&+ \lambda_V \frac{s}{2m_W^2}(g^{\mu_1\mu_2}(p_1 - p_2)^\nu - \frac{\lambda_V}{m_W^2}(p_1 - p_2)^\nu q^{\mu_1} q^{\mu_2} + \lambda_V(q^{\mu_1} g^{\mu_2\nu} - q^{\mu_2} g^{\mu_1\nu}) \\
&+ ig_4^V(g^{\mu_1\nu} q^{\mu_2} + g^{\mu_2\nu} q^{\mu_1}) + ig_5^V \epsilon^{\nu\mu_1\mu_2\rho}(p_1 - p_2)_\rho - \tilde{\kappa}_V \epsilon^{\nu\mu_1\mu_2\rho} q_\rho \\
&+ \tilde{\lambda}_V \epsilon^{\nu\mu_1\mu_2\rho} q_\rho + \frac{\tilde{\lambda}_V}{2m_W^2}(p_1 - p_2)^\nu \epsilon^{\mu_1\mu_2\rho\sigma} q_\rho (p_1 - p_2)_\sigma , \tag{3.48}
\end{aligned}$$

with all momenta pointing into the vertex. The standard model triple gauge boson vertex can be recovered setting the couplings to

$$g_1^V = \kappa_V = 1 \quad \text{and} \quad g_4^V = g_5^V = \tilde{\kappa}_V = \tilde{\lambda}_V = 0 . \tag{3.49}$$

For the photon couplings the g_1^γ is usually called the minimal coupling term of the W while the κ_γ is referred to as the anomalous magnetic moment of the W [9]. Together with the λ_γ the magnetic moment μ_W and the quadrupole moment Q_W can be describe as [9]

$$\mu_W = \frac{e}{2m_W}(1 + \kappa_\gamma + \lambda_\gamma) , \tag{3.50a}$$

$$Q_W = -\frac{e}{m_W^2}(\kappa_\gamma - \lambda_\gamma) . \tag{3.50b}$$

The parity violating couplings $\tilde{\lambda}_\gamma$ and $\tilde{\kappa}_\gamma$ are related to the electric dipole moment of the W^+ by

$$d_W = \frac{e}{2m_W}(\tilde{\kappa}_\gamma + \tilde{\lambda}_\gamma) , \tag{3.51a}$$

$$\tilde{Q}_W = -\frac{e}{m_W^2}(\tilde{\kappa}_\gamma - \tilde{\lambda}_\gamma) . \tag{3.51b}$$

and finally the couplings g_4^γ and g_5^γ violate charge conjugation symmetry. By demanding any of these symmetries, the couplings would automatically be zero. But to remain the most general formulation of the triple gauge vertex, all the factors shall be retained.

Using the Feynman rules describe in this chapter, anomalous couplings can be introduced in the calculation of the heavy gauge boson scattering.

Chapter 4

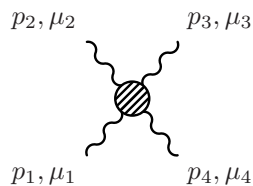
Heavy Gauge Boson Scattering Cross Sections

Using the Feynman rules of GWS theory of chapter 2.6 and including the Feynman rules of the Standard Model extension in chapter 3.3, the cross sections for heavy gauge boson scattering shall be calculated. Thus the external particles involved are four W bosons, four Z bosons or two W and two Z bosons in all possible combinations. Processes involving only one Z are forbidden due to charge conservation.

In the first part of this chapter the kinematic variables and index conventions are defined. After that the construction of Feynman amplitudes out of the Feynman rules in the previous chapters will be given for the Standard Model cross sections and including the anomalous couplings.

4.1 Mandelstam variables

The momenta and the indices at the Feynman diagrams are chosen in a symmetric way with momenta p_1 to p_4 and indices μ_1 to μ_4 .


$$(4.1)$$

Choosing all momenta going into the diagram and applying momentum conservation to the processes this leads to

$$p_1 + p_2 + p_3 + p_4 = 0 \quad (4.2)$$

We define the Mandelstam variables by

$$s = (p_1 + p_2)^2 = (p_3 + p_4)^2 \quad (4.3a)$$

$$t = (p_1 + p_4)^2 = (p_2 + p_3)^2 \quad (4.3b)$$

$$u = (p_1 + p_3)^2 = (p_2 + p_4)^2 \quad (4.3c)$$

which fulfill the useful relation, that relates the kinematic invariants to the particle masses

$$s + t + u = \sum_{i=1}^4 m_i^2 \quad (4.4)$$

where the m_i are the masses of the external particles. Furthermore, following from (4.4) one of the three Mandelstam variables is redundant and can be expressed by the other two and the masses of the external particles.

4.2 Center of Mass Frame

Going to a special frame of reference, namely the center of mass frame (CoM), the amplitudes will be expressed in terms of observables, instead of expressing the amplitudes by two of the Mandelstam variables. The choice taken here are the square of the CoM energy s and the cosine of the angle θ between the beam direction and the outgoing particle. With

$$p_i^2 = m_i^2 \quad (4.5)$$

the variable t and u can be expressed by s and $\cos \theta$. By choosing the beam axis along the z axis so that

$$-p_{1,2} = \begin{pmatrix} \frac{\sqrt{s}}{2} \\ 0 \\ 0 \\ \pm p \end{pmatrix}, \quad p_{3,4} = \begin{pmatrix} \frac{\sqrt{s}}{2} \\ \pm \vec{p}' \end{pmatrix} \quad (4.6)$$

they can be expressed as

$$t = -s/2 + m_1^2 + m_3^2 + 2|\vec{p}||\vec{p}'| \cos \theta, \quad (4.7a)$$

$$u = -s/2 + m_1^2 + m_4^2 - 2|\vec{p}||\vec{p}'| \cos \theta. \quad (4.7b)$$

So for example for $W^+ W^- \rightarrow W^+ W^-$ the mandelstam variables in terms of s and $\cos \theta$ are

$$t = -\left(\frac{s}{2} - 2m_W^2\right)(1 - \cos \theta), \quad (4.8a)$$

$$u = -\left(\frac{s}{2} - 2m_W^2\right)(1 + \cos \theta). \quad (4.8b)$$

4.3 Crossing Symmetry

While calculating cross sections, there is a useful method, called crossing symmetry, to relate cross sections which have particle and corresponding anti particle in final and initial state. It states that the S matrix element for any process involving a particle with momentum p in the initial state is equal to the S matrix element of an otherwise identical process but with an antiparticle of momentum $k = -p$ in the final state. [17].

Applying this symmetry on heavy gauge boson cross sections where the only

external particles are Z bosons W^- and W^+ boson, we see that the amplitudes containing particles in the initial(final) state can be crossed to amplitudes with its antiparticles in the final (initial) state. For example, the cross section $W^+W^- \rightarrow W^+W^-$ can be crossed into the cross section $W^-W^- \rightarrow W^-W^-$ using the conventions below, by flipping the final state W^+ to the initial state and the initial state W^+ to final state, making them both W^- bosons.

$$(4.9)$$

This becomes even more useful in terms of Mandelstam variables. Using the definitions in (4.3) by exchanging $p_2 \leftrightarrow p_3$

$$\begin{aligned} s &= (p_1 + p_2)^2 \rightarrow (p_1 + p_3)^2 = u \\ t &= (p_1 + p_4)^2 \rightarrow (p_1 + p_4)^2 = t \\ u &= (p_1 + p_3)^2 \rightarrow (p_1 + p_2)^2 = s \end{aligned} \quad (4.10a)$$

So when the amplitude for $W^+W^- \rightarrow W^+W^-$ has been calculated in terms of Mandelstam variables, the amplitude for $W^-W^- \rightarrow W^-W^-$ is derived by exchanging $s \leftrightarrow u$ while t remains unchanged.

4.4 $2 \rightarrow 2$ cross sections

The general form of $2 \rightarrow 2$ cross sections is given as

$$d\sigma = \frac{1}{4\sqrt{(p_1 p_2)^2 - m_1^2 m_2^2}} \frac{1}{\prod_i n_i} |\mathcal{M}|^2 \delta^{(4)}(p_1 + p_2 + p_3 + p_4) d\tilde{p}_3 d\tilde{p}_4 \quad (4.11)$$

with

$$d\tilde{p} = \frac{d^3 \vec{p}}{2\pi^3 2p_0} \Big|_{p_0 = \sqrt{\vec{p}^2 + m^2}} \quad (4.12)$$

p_1 and p_2 are the momenta of the initial state particles. The symmetry factor n_i has to be multiplied for because identical particles in the final state are indistinguishable. The phase space integral can be transformed to

$$\frac{d^3 \vec{p}_3}{2\pi^3 2E_3} \frac{d^3 \vec{p}_4}{2\pi^3 2E_4} = \frac{1}{16\pi^2} \frac{|\vec{p}_3|}{E} d\cos\theta d\phi, \quad (4.13)$$

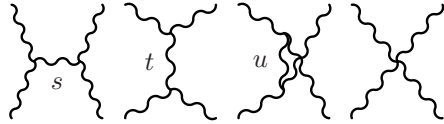
which leads to the formula for the differential cross section

$$\frac{d\sigma}{d\Omega} = \frac{1}{16\pi^2} \frac{1}{4\sqrt{(p_1 p_2)^2 - m_1^2 m_2^2}} \frac{1}{\prod_i n_i} \frac{|p_f|}{E} |\mathcal{M}(p_1, p_2 \rightarrow p_3, p_4)|^2 \quad (4.14)$$

To calculate the total cross section σ one has to do the phase space integration over ϕ and $\cos\theta$. Since the cross sections are symmetric around the z -axis, the ϕ integration gives a factor of 2π .

4.5 Standard Model scattering

Now the Feynman rules for the scattering of heavy gauge bosons shall be evaluated. In general $2 \rightarrow 2$ cross sections can contain in lowest order diagrams of the following form:


(4.15)

The possible heavy gauge boson scattering process can be separated into three different 'families' of processes from which the other processes can be derived using crossing symmetry described in chapter 4.3. The processes are

$$W^+W^- \rightarrow W^+W^- , \quad (4.16a)$$

$$W^+W^- \rightarrow ZZ , \quad (4.16b)$$

$$ZZ \rightarrow ZZ . \quad (4.16c)$$

From the first line in (4.16a) the derivable processes are

$$W^\pm W^\pm \rightarrow W^\pm W^\pm \quad (4.17)$$

Using crossing symmetry the amplitudes for the processes

$$W^\pm Z \rightarrow W^\pm Z \quad (4.18a)$$

$$ZZ \rightarrow W^+W^- \quad (4.18b)$$

can be computed from the second line in (4.16b). In the Standard Model the third process involving four Z bosons is only possible via Higgs exchange because a triple or quartic Z vertex is not contained and the exchange of a charged vector boson is forbidden due to charge conservation. As was shown in chapter 3.3 there exists a quartic vertex involving four external Z bosons with anomalous couplings.

On the following pages we will construct the amplitudes for the processes (4.16) by evaluating the Standard Model Feynman rules that are given in chapter 2.6 and with anomalous couplings given in chapter 3.3.

The amplitudes for the remaining processes in (4.17) and (4.18) will be derived from these amplitudes using crossing symmetry. Since we consider heavy gauge bosons as external particles only, these processes exhaust the possibilities for heavy gauge boson scattering.

To calculate the physical process one has to switch to the mass eigenstates and contract the gauge indices. For $SU(2)$ the combinations of structure constants are

$$f^{a_i a_j b} f^{a_k a_l b} = \delta^{a_i a_k} \delta^{a_j a_l} - \delta^{a_i, a_l} \delta^{a_j, a_k} \quad (4.19)$$

where the components in the interaction basis are related to the mass eigenstates via

$$W^\pm(p_i) = \frac{1}{\sqrt{2}}(\delta_{1, a_i} \mp \delta_{2, a_i})W^{a_i}(p_i) , \quad i = 1, 2, 3, 4 \quad (4.20)$$

Because all the momenta are pointing inwards, the final state has to be charge conjugated, so in fact the calculated amplitude is the amplitude for 4 particles annihilating into the vacuum. Applying the idea of crossing symmetry this process is equal to the calculation of a $2 \rightarrow 2$ processes.

The amplitudes for gauge boson scattering can be expressed as $\mathcal{M}^{\mu_1\mu_2\mu_3\mu_4}$ which have to be contracted with the external polarization vectors.

$$\mathcal{M}^{\mu_1\mu_2\mu_3\mu_4} \epsilon_{\mu_1}(p_1) \epsilon_{\mu_2}(p_2) \epsilon_{\mu_3}^*(p_3) \epsilon_{\mu_4}^*(p_4) \quad (4.21)$$

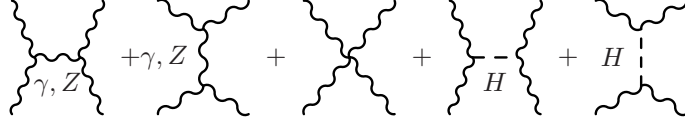
For unpolarized cross sections one has to sum over all polarizations, which can be expressed in the physical polarization sum

$$\sum_{r,r'=1}^3 \epsilon_{\mu_1}^r(p_1) \epsilon_{\mu_1'}^{r'}(p_1) = g_{\mu\mu'} - \frac{p_1^\mu p_1^{\mu'}}{p_1^2} \quad (4.22)$$

for each polarization vector. The amplitudes given on the following pages are the uncontracted amplitudes $\mathcal{M}^{\mu_1\mu_2\mu_3\mu_4}$. In the further calculation the square of these amplitudes is contracted with the polarization sums to the full squared amplitudes which then are integrated to unpolarized total cross sections.

4.5.1 $W^+ W^- \rightarrow W^+ W^-$

For the amplitude involving four W bosons one has to take into account the contact diagram and an s and t channel diagram each with the possibility of photon and Z boson exchange. Since the final state particles can be distinguished, no u channel diagram contributes because the final state particles are distinguishable.



Because the final state particles are incoming one has to charge conjugate them in order to treat them as outgoing particles. Contracting the structure constants lead to

$$f^{a_1 a_2 b} f^{a_3 a_4 b} = -1 \quad (4.23a)$$

$$f^{a_2 a_3 b} f^{a_4 a_1 b} = -1 \quad (4.23b)$$

$$f^{a_2 a_4 b} f^{a_3 a_1 b} = 0 \quad (4.23c)$$

for $W^+ W^- \rightarrow W^+ W^-$. The easiest diagram to evaluate is the contact diagram. Omitting the last line in (3.41) because of (4.23c) it becomes

$$\begin{aligned} M_{contact} &= -ig^2 [f^{a_1 a_2 b} f^{a_3 a_4 b} ((g^{\mu_1 \mu_3} g^{\mu_2 \mu_4} - g^{\mu_1 \mu_4} g^{\mu_2 \mu_3}) \\ &\quad + f^{a_2 a_3 b} f^{a_4 a_1 b} (g^{\mu_2 \mu_4} g^{\mu_1 \mu_3} - g^{\mu_1 \mu_2} g^{\mu_3 \mu_4}))] \\ &= -ig^2 [(-1)(2g^{\mu_1 \mu_3} g^{\mu_2 \mu_4} - g^{\mu_1 \mu_4} g^{\mu_2 \mu_3} - g^{\mu_1 \mu_2} g^{\mu_3 \mu_4})] \end{aligned} \quad (4.24)$$

There are two possible s channel diagrams. One exchanges a photon while in the second diagram, a Z boson is exchanged. With $g = e/s_W$ and using the

cyclic notation these two s -channel diagrams can be combined to

$$\begin{aligned}
M_{s,A,Z} &= gf^{a_1 a_2 b} (g^{\mu_1 \mu_2} (p_1 - p_2)^\nu + g^{\mu_2 \nu} (p_2 - q)^{\mu_1} + g^{\nu \mu_1} (q - p_1)^{\mu_2}) \\
&\times \left(\frac{-ic_w^2}{s - m_Z^2} \left(g^{\nu \rho} - \frac{q^\nu q^\rho}{m_Z^2} \right) + \frac{-s_w^2 g^{\nu \rho}}{s} \right) \\
&\times gf^{a_3 a_4 b} (g^{\mu_3 \mu_4} (p_3 - p_4)^\rho + g^{\mu_4 \rho} (p_4 - q)^{\mu_3} + g^{\rho \mu_3} (q - p_3)^{\mu_4}) \quad (4.25)
\end{aligned}$$

where s_w and c_w are the sine and cosine of the Weinberg angle. The cyclic notation of the amplitude now pays off since the t -channel diagram can be constructed from this amplitude by turning the s channel diagram on the side and cycling the indices

$$\begin{array}{ccc}
\begin{array}{c} \mu_2 \qquad \mu_3 \\ \diagdown \quad \diagup \\ \text{---} s \text{---} \\ \diagup \quad \diagdown \\ \mu_1 \qquad \mu_4 \end{array} & \longrightarrow & \begin{array}{c} \mu_1 \rightarrow \mu_2 \qquad \mu_2 \rightarrow \mu_3 \\ \diagdown \quad \diagup \\ \text{---} t \text{---} \\ \diagup \quad \diagdown \\ \mu_4 \rightarrow \mu_1 \qquad \mu_3 \rightarrow \mu_4 \end{array} \quad (4.26)
\end{array}$$

where $1 \rightarrow 2, 2 \rightarrow 3, 3 \rightarrow 4, 4 \rightarrow 1$ in the indices. So the t -channel amplitude can be expressed as

$$\begin{aligned}
M_{t,W} &= gf^{a_2 a_3 b} (g^{\mu_2 \mu_3} (p_2 - p_3)^\nu + g^{\mu_3 \nu} (p_3 - q)^{\mu_2} + g^{\nu \mu_2} (q - p_2)^{\mu_3}) \\
&\times \frac{-ic_w^2}{t - m_Z^2} \left(g^{\nu \rho} - \frac{q^\nu q^\rho}{m_Z^2} \right) \\
&\times gf^{a_4 a_1 b} (g^{\mu_4 \mu_1} (p_4 - p_1)^\rho + g^{\mu_1 \rho} (p_1 - q)^{\mu_4} + g^{\rho \mu_4} (q - p_4)^{\mu_1}) \quad (4.27)
\end{aligned}$$

These are the gauge boson amplitudes that contribute to this process. Besides them there are two Higgs exchange diagrams via the s and the t channel possible. These diagrams are in a first approximation proportional to $\frac{s}{v^2}$ and cancel the contributions linear in s from the pure gauge boson diagrams [3]. Using the Feynman rule (2.68) the s channel diagram becomes

$$M_{s,H} = i \frac{2m_W^2}{v} g^{\mu_1 \mu_2} \times \frac{i}{s - m_H^2} \times i \frac{2m_W^2}{v} g^{\mu_3 \mu_4} . \quad (4.28)$$

Here the first and the third factor are the gauge boson Higgs vertices and the second is the Higgs propagator. The t -channel diagram can be derived from the s -channel amplitude again by cycling the indices. It reads

$$M_{t,H} = i \frac{2m_W^2}{v} g^{\mu_2 \mu_3} \times \frac{i}{t - m_H^2} \times i \frac{2m_W^2}{v} g^{\mu_4 \mu_1} \quad (4.29)$$

Finally all parts have to be put together to form the amplitude \mathcal{M} that is used in (4.14) to

$$\mathcal{M} = M_{s,A,Z} + M_{t,A,Z} + M_{s,H} + M_{t,H} + M_{contact} \quad (4.30)$$

Using crossing symmetry the amplitude for $W^\pm W^\pm \rightarrow W^\pm W^\pm$ can be calculated from this amplitude by exchanging the Mandelstam variable $s \leftrightarrow u$.

This can be seen by looking at the looking at the Feynman diagrams. The s -channel diagram is forbidden due to charge conservation. But now, besides the t -channel diagram, a u channel diagram contributes because the two W^- bosons in the final state are indistinguishable. The corresponding Feynman diagrams that contribute to the amplitude of $W^\pm W^\pm \rightarrow W^\pm W^\pm$ are

$$\mathcal{M} = \gamma, Z + \gamma, Z + \text{t-channel} + H + H \quad (4.31)$$

4.5.2 $W^+ W^- \rightarrow Z Z$

This cross section and its derived relatives involve two Z bosons. Due to charge conservation at the vertices and the absence of a triple Z -boson vertex in the Standard Model, the intermediate particle has to be another W boson or a Higgs boson. The contributing diagrams are a t -channel and a u -channel diagram.

$$\mathcal{M} = W + W + \text{t-channel} + H + H \quad (4.32)$$

The vertex parts of the t channel diagram can be reused while replacing the propagator by a W -boson propagator.

$$\begin{aligned} M_{t,W} &= g f^{a_2 a_3 b} (g^{\mu_2 \mu_3} (p_2 - p_3)^\nu + g^{\mu_3 \nu} (p_3 - q)^{\mu_2} + g^{\nu \mu_2} (q - p_2)^{\mu_3}) \\ &\times \frac{-i c_w^2}{t - m_W^2} \left(g^{\nu \rho} - \frac{q^\nu q^\rho}{m_W^2} \right) \\ &\times g f^{a_4 a_1 b} (g^{\mu_4 \mu_1} (p_4 - p_1)^\rho + g^{\mu_1 \rho} (p_1 - q)^{\mu_4} + g^{\rho \mu_4} (q - p_4)^{\mu_1}) \end{aligned} \quad (4.33)$$

The u -channel amplitude can immediately be written down by exchanging $3 \leftrightarrow 4$ in the t -channel

$$\begin{aligned} M_{u,W} &= g f^{a_2 a_4 b} (g^{\mu_2 \mu_4} (p_2 - p_4)^\nu + g^{\mu_4 \nu} (p_4 - q)^{\mu_2} + g^{\nu \mu_2} (q - p_2)^{\mu_4}) \\ &\times \frac{-i c_w^2}{t - m_W^2} \left(g^{\nu \rho} - \frac{q^\nu q^\rho}{m_W^2} \right) \\ &\times g f^{a_3 a_1 b} (g^{\mu_3 \mu_1} (p_3 - p_1)^\rho + g^{\mu_1 \rho} (p_1 - q)^{\mu_3} + g^{\rho \mu_3} (q - p_3)^{\mu_1}) \end{aligned} \quad (4.34)$$

Contracting the structure constants for this process one gets

$$f^{a_1 a_2 b} f^{a_3 a_4 b} = 0 \quad (4.35a)$$

$$f^{a_2 a_3 b} f^{a_4 a_1 b} = -1 \quad (4.35b)$$

$$f^{a_2 a_4 b} f^{a_3 a_1 b} = -1 \quad (4.35c)$$

which gives the contact diagram for this process

$$\begin{aligned} M_{contact} &= -i g^2 [f^{a_2 a_3 b} f^{a_1 a_4 b} (g^{\mu_2 \mu_4} g^{\mu_1 \mu_3} - g^{\mu_1 \mu_2} g^{\mu_3 \mu_4}) \\ &\quad + f^{a_2 a_4 b} f^{a_1 a_3 b} (g^{\mu_2 \mu_3} g^{\mu_1 \mu_4} - g^{\mu_1 \mu_2} g^{\mu_3 \mu_4})] \\ &= -i g^2 [(-1)(g^{\mu_2 \mu_4} g^{\mu_1 \mu_3} + g^{\mu_2 \mu_3} g^{\mu_1 \mu_4} - 2g^{\mu_1 \mu_2} g^{\mu_3 \mu_4})] \end{aligned} \quad (4.36)$$

Because the Higgs does not carry charge the only possible Higgs gauge boson diagram that contributes is via the s -channel which is

$$M_{s,H} = i \frac{2m_W^2}{v} g^{\mu_1 \mu_2} \times \frac{i}{s - m_H^2} \times i \frac{2m_Z^2}{v} g^{\mu_3 \mu_4} \quad (4.37)$$

All together the standard model amplitude for this process is the sum of all contributions

$$\mathcal{M} = M_{t,W} + M_{u,W} + M_{contact} + M_{s,H} \quad (4.38)$$

This again leads to a amplitude depending on s , t , u and the particle masses, which can be used to derive the other cross sections involving 2 Z bosons.

The Feynman diagrams contributing to the cross section for $ZZ \rightarrow W^+W^-$ are equal to the diagrams shown in (4.32). Because we calculate unpolarized cross sections the summation over all polarization states is carried out we can exchange the masses of initial and final state in polarization sum of $W^+W^- \rightarrow ZZ$ to calculate the amplitude the squared amplitude for this process. With the correct flux factor in (4.14), we easily calculate the total cross section.

The amplitudes with one W boson and one Z boson in the initial state can be constructed by flipping the momentum p_1 to the final and the momentum p_3 to the initial state. Looking at the definitions of the Mandelstam variables this means the amplitude for $W^\pm Z \rightarrow W^\pm Z$ can be derived from $W^+W^- \rightarrow ZZ$ by exchanging $s \leftrightarrow t$, while u remains unchanged. The corresponding diagrams are

$$\mathcal{M} = \text{[Diagram 1]} + \text{[Diagram 2]} + \text{[Diagram 3]} + \text{[Diagram 4]} \quad (4.39)$$

This exhausts the possibilities of the scattering of two W and two Z bosons.

4.5.3 $Z Z \rightarrow Z Z$

Finally we study two Z -bosons scattering into two Z -bosons. Simply looking at the vertices in the interaction basis and contracting the structure constants one finds

$$f^{a_1 a_2 b} f^{a_3 a_4 b} = 0 \quad (4.40a)$$

$$f^{a_2 a_3 b} f^{a_4 a_1 b} = 0 \quad (4.40b)$$

$$f^{a_2 a_4 b} f^{a_3 a_1 b} = 0 \quad (4.40c)$$

the structure constants cancel to zero. This can be understood easily. Charge conservation forbids charged gauge bosons in the intermediate state because all external particles are neutral. Additionally, because of the absence of γZZ and ZZZ vertices in the standard model, there exists no diagram involving gauge bosons in the intermediate state for this process. Nonetheless the Higgs channel contributes a s -, t -, and u -channel diagram to the amplitude.

$$\mathcal{M} = \text{[Diagram 1]} + \text{[Diagram 2]} + \text{[Diagram 3]} \quad (4.41)$$

The three amplitudes are

$$M_{s,H} = i \frac{2m_W^2}{v} g^{\mu_1 \mu_2} \times \frac{i}{s - m_H^2} \times i \frac{2m_W^2}{v} g^{\mu_3 \mu_4} \quad (4.42a)$$

$$M_{t,H} = i \frac{2m_W^2}{v} g^{\mu_2 \mu_3} \times \frac{i}{t - m_H^2} \times i \frac{2m_W^2}{v} g^{\mu_4 \mu_1}$$

$$M_{u,H} = i \frac{2m_W^2}{v} g^{\mu_2 \mu_4} \times \frac{i}{u - m_H^2} \times i \frac{2m_W^2}{v} g^{\mu_3 \mu_1} \quad (4.42b)$$

Thus the amplitude for this process is the sum over these three channels


$$\mathcal{M} = M_{s,H} + M_{t,H} + M_{u,H} \quad (4.43)$$

4.6 Gauge Boson Scattering with Anomalous Couplings

When the Feynman rules for anomalous gauge boson couplings are taken into account, there are new possible diagrams that contribute to the scattering cross sections. They have to be added to the Standard Model amplitudes.

$$\mathcal{M} = \mathcal{M}_{SM} + \mathcal{M}_{ac} \quad (4.44)$$

Still the possible diagrams are s , t , u , and contact diagrams. They are constructed the same way like the previous chapter but using the Feynman rules from chapter 3.3. To treat them diagrammatically we introduce a new triple gauge boson vertex for each anomalous coupling



$$\propto \Delta g_1^V, \Delta \kappa_V, g_4^V, \lambda_V, g_5^V, \tilde{\kappa}_V, \tilde{\lambda}_V \quad (4.45)$$

and contact term



$$\alpha_i \quad (4.46)$$

which is proportional to the anomalous couplings α_i in the quartic vertices. Here Δg_1^V and $\Delta \kappa_V$ are the deviation of the couplings $\Delta g_1^V = g_1^V - 1$ and $\Delta \kappa_V = \kappa_V - 1$.

With these vertices the amplitude for $W^+ W^- \rightarrow W^+ W^-$ becomes

$$\mathcal{M}_{BSM} = \mathcal{M}_{SM} + \begin{array}{c} \text{c} \quad \text{c} \quad \text{c} \\ \text{+} \quad \text{+} \quad \text{+} \\ \text{c} \quad \text{c} \quad \text{c} \\ \text{+} \quad \text{+} \quad \text{+} \\ \text{c} \quad \text{c} \quad \text{c} \\ \text{+} \quad \alpha_i \end{array} \quad (4.47)$$

with s - and t - channel diagrams where the c stands for the couplings according to the triple gauge boson vertex (3.48)

$$c = \Delta g_1^V, \Delta \kappa_V, g_4^V, \lambda_V, g_5^V, \tilde{\kappa}_V, \tilde{\lambda}_V \quad (4.48)$$

and contact diagrams are added proportional to

$$\alpha_i = \alpha_4, \alpha_5 \quad (4.49)$$

as can be seen from the Feynman rule (3.41). Analog the cross section $W^+ W^- \rightarrow Z Z$ receives additional t - and u -channel diagrams from the triple gauge boson vertex

$$\mathcal{M}_{BSM} = \mathcal{M}_{SM} + \begin{array}{c} \text{c} \quad \text{c} \quad \text{c} \\ \text{+} \quad \text{+} \quad \text{+} \\ \text{c} \quad \text{c} \quad \text{c} \\ \text{+} \quad \text{+} \quad \text{+} \\ \text{c} \quad \text{c} \quad \text{c} \\ \text{+} \quad \alpha_i \end{array} \quad (4.50)$$

with the couplings α_i

$$\alpha_i = \alpha_4, \alpha_6, \alpha_5, \alpha_7 \quad (4.51)$$

and the c are the same as in (4.48) since they come from the same triple gauge vertex (3.48).

Finally the $Z Z \rightarrow Z Z$ cross section receives a new contact diagram

$$\mathcal{M}_{BSM} = \mathcal{M}_{SM} + \alpha_i \begin{array}{c} \text{wavy lines} \\ \text{+} \\ \text{wavy lines} \end{array} \quad (4.52)$$

where the contributing α_i are

$$\alpha_i = \alpha_4, \alpha_5, \alpha_6, \alpha_7, \alpha_{10} \quad (4.53)$$

The triple gauge vertex does not contribute to this process. Again the remaining processes involving external heavy gauge bosons can be derived from the first two via crossing symmetry as described in the previous chapter. Finally these amplitudes can be used to calculate the differential and total cross sections. For the cross section (4.14) the square has to be taken

$$|\mathcal{M}|^2 = \mathcal{M}\mathcal{M}^* \quad (4.54)$$

So in the total cross section not only the single diagrams contribute but interferences between all possible diagrams have to be included in the calculations.

Chapter 5

Comparison of analytically and numerically calculated cross sections

5.1 Whizard - A Monte Carlo Event Generator

The calculation of simple processes, e.g. in QED or in $2 \rightarrow 2$ gauge boson scattering of chapter 4, can be handled analytically with moderate effort. As soon as theories get more complex or multiple final states are allowed, these calculations quickly become very extensive and therefore an analytic calculation becomes at least very time consuming. In contrast to this, the detailed phenomenological analysis of certain processes at particle colliders usually involves a whole lot of background processes that have to be included correctly to make reliable predictions for experiments.

Often, besides the evaluation of Feynman rules additional information has to be included in the calculation, like parton distribution functions in QCD processes. Finally, being able to simulate the experiments by creating events in a format that can be fed into detectors gives the opportunity to test their sensitivity in detector simulations.

To to all this in an effective and productive way Monte Carlo Event Generators like Whizard [12] exist. It is able to generate and analyze events of multiple particle cross sections in a variety of models. It includes the electroweak Standard Model as well as QCD and some of their extensions like Little Higgs, Three Site Higgsless Model, anomalous couplings and Super Symmetry [12].

Matrix elements for multiple particle scattering amplitudes are generated with the matrix element generator O'Mega [15]. To calculate the total cross sections, the phase space integration is carried out by adaptive multi channel integration [16]. So in general Monte Carlo event generator are powerful tools to calculate cross sections and generate events in context of a certain model to make phenomenological predictions for collider experiments. To ensure the reliability of these tools it is important to test them against analytically handable processes.

The way of calculating heavy gauge boson scattering cross sections was outlined

in chapter 4. Now we use these analytic calculations to compare the numeric results calculated by Whizard against them. Two features of Whizard that have been useful in particular shall be presented here.

For comparing cross sections at different energies \sqrt{s} the `testsuite.m4` which is part of Whizard's self-tests, was used. It uses the preprocessor `m4` to generate input files for Whizard that calculate the *pull* (5.2) automatically for a given analytic value of the cross section.

To vary the anomalous couplings or other parameters, Whizard has a function to scan them and record the cross section with corresponding error. With this function and Whizard's built in scripting language `Sindarin` it is possible to automatically sweep the anomalous couplings and record the corresponding values for the total cross sections. The Whizard model file that is used is `SM.mdl` for the Standard Model cross sections and `SM_ac.mdl` for the anomalous couplings. The numerical integration in Whizard is carried out with 2:100000 iterations which is sufficient for $2 \rightarrow 2$ cross sections to produce stable results with reasonable errors.

5.2 Interpretation of numerical results

To interpret the quality of the numeric results the so called *pull* is calculated. It sets the deviation of a certain value σ to its expectation value $\langle\sigma\rangle$ in a relation to the sum of their error estimates δ_σ and $\delta_{\langle\sigma\rangle}$ respectively.

$$\text{Pull} = \left| \frac{\sigma - \langle\sigma\rangle}{\sqrt{\delta_\sigma^2 + \delta_{\langle\sigma\rangle}^2}} \right| \quad (5.1)$$

In case of this comparison, the analytic calculation of the cross section shall be interpreted as the expectation value $\langle\sigma\rangle = \sigma_{an}$. It is assumed to be exact, so its error vanishes $\delta_{\langle\sigma\rangle} = 0$.

The deviation of Whizard numeric result is tested against this expectation value $\sigma = \sigma_{num}$ where the error estimate δ_σ is the error calculated by Whizard. With (5.1) this reduces to

$$\text{Pull} = \left| \frac{\sigma_{num} - \sigma_{an}}{\delta_{\sigma_{num}}} \right| \quad (5.2)$$

A numerical result is considered valid when the *pull*'s absolute value is smaller than three. The reason for this lies in the fact, that the *pull* squared follows a χ^2 distribution.

In general the χ^2 distribution with $(k - 1)$ degrees of freedom is defined as the sum over set of normally distributed independent random variables squared $\{X_i\}$ with k degrees of freedom. For this, the random variable [19]

$$\chi^2 = \left(\frac{x_i - \langle x_i \rangle}{dx_i} \right)^2 \quad (5.3)$$

with the expectation value $\langle x_i \rangle$ and the error dx_i is defined. Picking N of these random variables out of the normal distributed population leads to the

χ^2 distribution. Because in our case (5.3) is nothing else than the square of the *pull* defined in (5.2), the *pull* squared is expected to be χ^2 squared distributed where the probability density function is given by

$$P_{\chi^2} = \frac{2^{-\frac{\nu}{2}} e^{-\frac{x}{2}} x^{-1+\frac{\nu}{2}}}{\Gamma(\frac{\nu}{2})} \quad (5.4)$$

with the random variable x and ν degrees of freedom. The *pull* as defined in (5.2) has two degrees of freedom, the numerical calculated cross section and its error and is tested against the analytical results. Assuming the probability of Whizard's cross section σ_{num} to be gaussian distributed around its expectation value σ_{an} , the *pull* is expected to be χ^2 distributed with one degree of freedom. The reason why the *pull* < 3 is chosen as maximum value can be understood easily by taking a look at the probability density function of the χ^2 distribution. The cumulative probability of a certain value of χ^2 is given by the area under the curve of the χ^2 probability function shown in fig 5.2. It gives the probability that a certain χ^2 value A falls between 0 and the value A . So when setting the critical value of the *pull* to three or $\chi^2 = 9$ of one degree of freedom, the corresponding cumulative probability is 0.997. This means 99.7 per cent of the Whizard's cross sections compared with the analytical ones should give a value of a *pull* smaller than or equal to three.

During our calculations we found the *pull* to have a strong unbalance to one sign

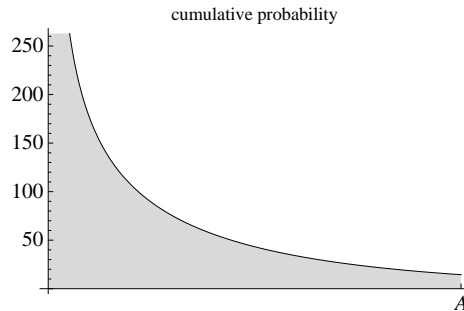


Figure 5.1: Probability distribution function of a χ^2 distribution. The area under the curve, i.e. the integral to a χ^2 of A gives the cumulative probability.

for some of the test runs as can be seen for example in table 5.1. Additionally the *pull* lies within a small range around *pull* = 1.5. This behavior can be a sign of unwanted correlations in the random numbers.

First of all it turned out that in Whizard's implemented self test routine the seed of the random number generator is set to an equal start value *seed* = 0. This is done to ensure that, when Whizard's self tests are executed, the results are stable. Allowing random seeds in this tests might, due to statistics, lead to results that produce *pulls* bigger than three, which would make the test fail although there are no errors in the program.

For the purpose of the tests in this thesis this is not wanted. So we disabled this feature to allow random seed values for the each integration. Because the *pull*'s statistical distribution as well as its sign is of interest, the random number generator is initiated with different seeds for every process. When recalculating

$Z Z \rightarrow Z Z$ Abs($\cos(\theta)$) < 0.95				
\sqrt{s} [GeV]	$\sigma_{an}(s)$ [fb]	$\sigma_{num}(s)$ [fb]	Error[fb]	Pull
200	2.04368E+04	2.04379E+04	2.97072E+00	0.374
300	6.71853E+03	6.71706E+03	1.21773E+00	-1.21
400	3.54704E+03	3.54624E+03	6.56512E-01	-1.22
500	2.21957E+03	2.21900E+03	3.52831E-01	-1.61
700	1.11584E+03	1.11555E+03	1.71440E-01	-1.68
1000	5.44211E+02	5.44061E+02	8.10324E-02	-1.85
2000	1.35973E+02	1.35937E+02	1.97950E-02	-1.82
5000	2.17682E+01	2.17625E+01	3.17050E-03	-1.79
7000	1.11071E+01	1.11041E+01	1.62166E-03	-1.84
10000	5.44270E+00	5.44132E+00	7.97045E-04	-1.74
20000	1.36072E+00	1.36038E+00	2.00190E-04	-1.72

Table 5.1: Cross section for $ZZ \rightarrow ZZ$. The calculated *pulls* are with one exception entirely smaller than zero and are very close together around -1.5. The seed of Whizard's random number generator was set to equal start value $seed = 0$ in the input file

$Z Z \rightarrow Z Z$ Abs($\cos(\theta)$) < 0.95				
\sqrt{s} [GeV]	$\sigma_{an}(s)$ [fb]	$\sigma_{num}(s)$ [fb]	Error[fb]	Pull
200	2.04368E+04	2.04371E+04	2.96828E+00	0.103
300	6.71853E+03	6.71907E+03	1.22787E+00	0.44
400	3.54704E+03	3.54608E+03	6.61347E-01	-1.45
500	2.21957E+03	2.21919E+03	3.04802E-01	-1.26
700	1.11584E+03	1.11598E+03	1.65961E-01	0.839
1000	5.44211E+02	5.44185E+02	8.19803E-02	-0.323
2000	1.35973E+02	1.35984E+02	1.85525E-02	0.574
5000	2.17682E+01	2.17736E+01	2.49319E-03	2.18
7000	1.11071E+01	1.11075E+01	1.71161E-03	0.245
10000	5.44270E+00	5.44305E+00	6.64204E-04	0.528
20000	1.36072E+00	1.36057E+00	1.70855E-04	-0.882

Table 5.2

the above example as shown in table 5.2 we see that the pull is distributed over a wider range around zero. Although the *pull* was initiated with random seeds, in another test for $W^-W^- \rightarrow W^-W^-$ seen in appendix A.3 again the *pull* for every c.m. energy was negative. Rerunning the test with manually set

seed ($seed = 143, seed = 13$) as can be seen in appendix A.3 the *pulls* are more distributed around zero. Additionally the test was run again with more iteration steps (iterations = 2:1000000) in the integration. Higher precision is expected to lead to smaller deviations from the analytic results and with corresponding smaller errors the *pull* stays of the the same order and is well distributed as shown in the last table in A.3.

In conclusion the entirely negative *pulls* of this testrun are of statistical nature which is not impossible, although very unlikely.

To reliably verify the statistical distribution the *pull*, it was recorded for all of the following calculations. The histograms in fig. 5.2(a) show the *pull*'s distribution around zero, in fig. 5.2(b) the *pull* is squared to check the χ^2 distribution behavior. It contains roughly 2000 values from the tested processes below. First of all we fit a gaussian function of the form into the histogramm in fig. 5.2(a)

$$P_{gauss} = ae^{\frac{(x-b)^2}{2c^2}} \quad (5.5)$$

The parameters a,b, and c are set to

$$a = 300, \quad b = 0.2, \quad c = 1.3 \quad (5.6)$$

With the right normalization a gaussian function gives the probability density function of a normally distributed random variable. Then these parameters correspond to the mean value (b), normalization constant (a) and standard deviation (c). The fittet gaussian curve in fig. 5.2(a) shows that the *pull* is

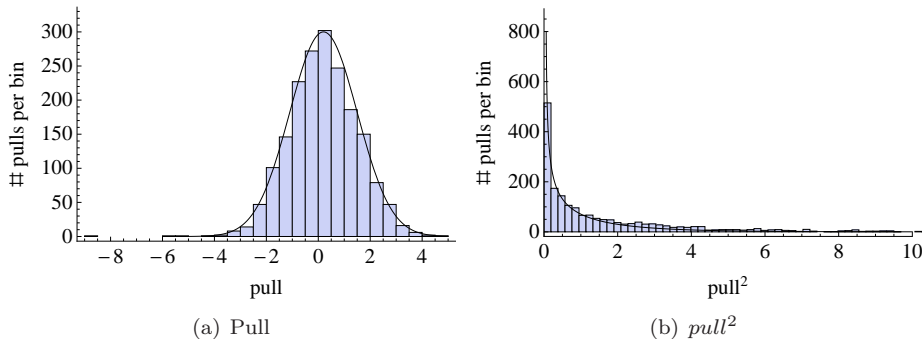


Figure 5.2: Histograms of the calculated *pull* and *pull*² values. Fig. 5.2(a) shows the gaussian distribution of the *pull* around zero. Fig. 5.2(b) shows the χ^2 distribution of the *pull*²

normally distributed around zero with a slight deviation of $b = 0.2$ and a FWHM of $2c^2 = 1.3$. In fig. 5.2(b) we fitted the χ^2 probability density function of one degree of freedom from (5.4), which as well as the gaussian fit, reproduces the histograms shape. Thus we conclude that the Whizard's numerical integration behaves as expected and proceed with the actual comparison of analytic and numeric cross sections of heavy gauge boson scattering.

5.3 Noise in analytic calculations

In the previous section, the analytic calculations are assumed to be exact, making the error $\delta_{\langle\sigma\rangle}$ in (5.1) vanish. At least for the Standard Model calculations, this statement has to be constrained. At high energies, namely above 10 TeV, the analytical calculations showed up a numerical noise, shown in fig. 5.3, which increases with increasing energies. This noise is not due to problems coming from the integrating the total cross section, but is already present in the squared matrix element. Fig. 5.3(a) shows the c.m. energy dependence of the differential cross section for $W^+W^- \rightarrow W^+W^-$ in the minimum $\cos\theta = 0$ and the influence of this noise on the resulting total cross section 5.3(b). We see that the

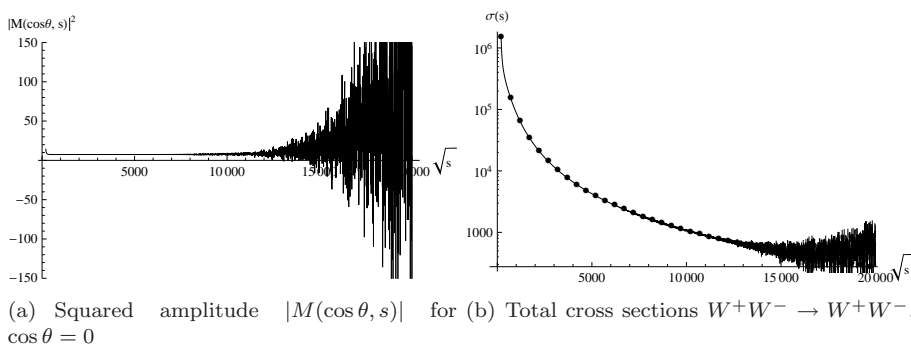


Figure 5.3: Numerical noise in the squared amplitude and its influence on the total cross section.

numerical noise in the differential cross section occurs again in the total cross section when its value, due to the cross sections $1/s$ decay, reaches values which are of the same order which occurred at energies above 10 TeV. When the noise in the amplitude shown in fig. 5.3(a) becomes of order 100, the noise becomes dominant, when the total cross sections becomes of the same order in fig 5.3(b). The cross sections for anomalous couplings do not show these oscillations because of the unitarity violating growth of the cross sections, the noise of the standard model amplitude is suppressed. Fig. 5.4(a) shows the squared amplitude for the same process but with anomalous coupling $\alpha_4 = 0.1$. This amplitude rises with s , thus the noise becomes suppressed with higher energies. This results in a smooth total cross section shown in fig. 5.4(b). As a consequence, for the Standard Model scattering cross sections we neglect the results for the total cross section for c.m. energies $\sqrt{s} > 10TeV$. For cross sections involving anomalous couplings we are able to test the numeric cross sections up to $\sqrt{s} > 20TeV$.

5.4 Standard Model Scattering

5.4.1 $ZZ \rightarrow ZZ$

We start off with the four Z boson amplitude 4.43. Because in this to amplitude contribute Higgs exchange diagrams, it will be uses to compare the Higgs width. Squaring the amplitude and integrating it with 4.14 gives the total cross section

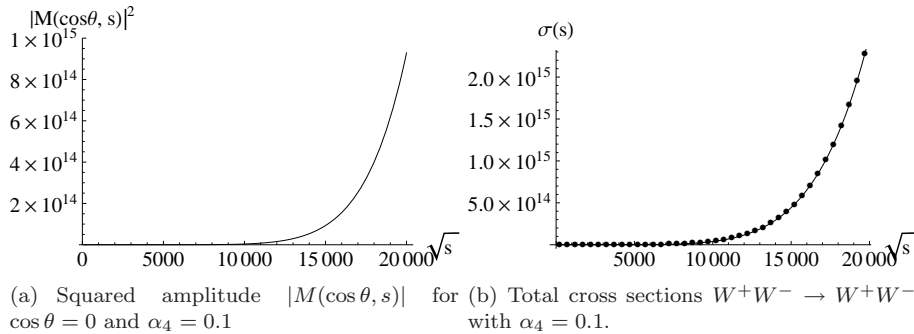


Figure 5.4: Dominance of the anomalous coupling terms suppress noise in analytic calculations.

as was described in the previous chapter. The explicit numerical values used for the calculations are

$$m_W = 80.419 \text{ GeV} , \quad \Gamma_W = 0 \text{ GeV} \quad (5.7a)$$

$$m_Z = 91.1882 \text{ GeV} , \quad \Gamma_Z = 0 \text{ GeV} \quad (5.7b)$$

$$m_H = 300 \text{ GeV} , \quad \Gamma_H = 1.419 \text{ GeV} \quad (5.7c)$$

The Higgs mass is set to 300 GeV to push it above the threshold to be able to raster the Higgs resonance. This is an arbitrary choice ignoring the fact that the Higgs boson's width is not independent of its mass and depending on the particles it decays to. In case of decays into gauge bosons $H \rightarrow VV$ with $V = W, Z$, the Higgs width is proportional to the third power of its mass [8]

$$\Gamma_H = \frac{1}{2} m_H^3 \quad (5.8)$$

This means for $m_H \approx 1\text{TeV}$ is of the same order as its mass $\Gamma \approx m_H$. The results are shown in fig. 5.5(a) and fig. 5.5(b). The data points correspond to the cross section calculated by Whizard and the continuous line is the result of the analytic calculation. Cuts have been set on $\cos(\theta)$ to avoid the denominator of the t- and u- channel diagram to vanish for $\cos(\theta) = \pm 1$. The graph in fig. 5.5(a) corresponds to cuts $|\cos(\theta)| < 0.95$ and in fig. 5.5(b) cut $|\cos(\theta)| < 0.99$ where set. The data that corresponds to the black circles in fig. 5.5(a) and fig. 5.5(b) can be found in the appendix A.1.1.

Like the figures above already indicate, the numerical results agree with the analytic calculations within the statistical error and the *pull* calculated as described in (5.2) is within the set limit of three as can be seen from the tables.

To check the width of the Higgs the total cross sections is calculated around the set Higgs mass in a range $m_H \pm 1$. The results are shown in fig. 5.5(c) and fig. 5.5(d) for the different cuts and the data tables can be found in the appendix A.1.1. Again Whizard gives reliable results within the statistical errors. And the tables in the appendix A.1.1 show a *pull* for both cuts well beneath the limit of three.

For the following amplitudes the Higgs mass is set to $m_H = 115 \text{ GeV}$ and the width is set to zero.

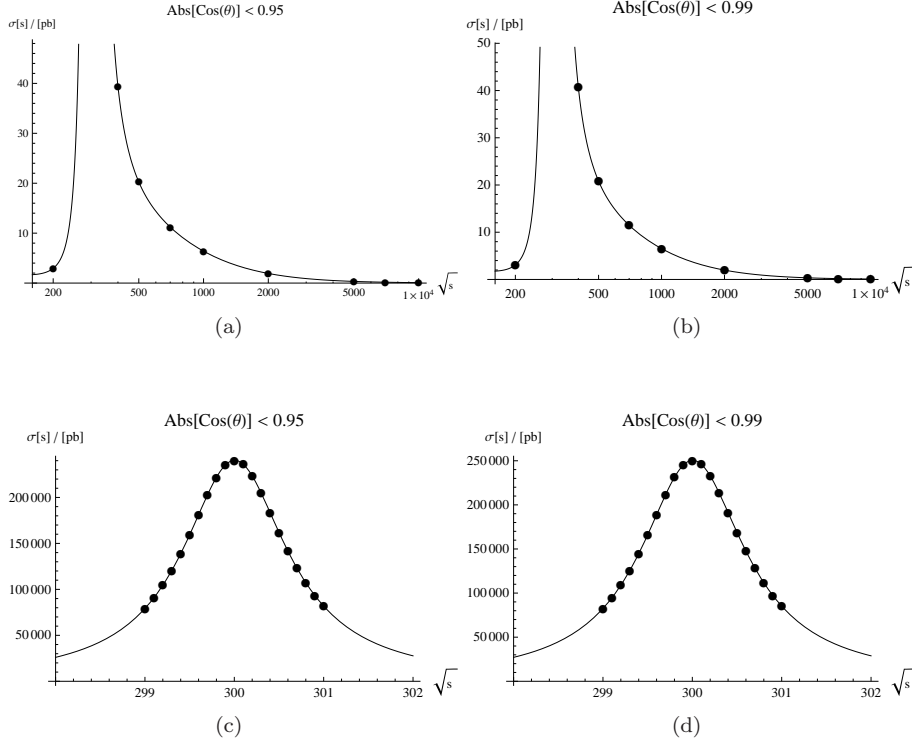


Figure 5.5: Detailed comparison of Higgs resonance in $ZZ \rightarrow ZZ$ for 5.5(c): $\cos \theta < 0.95$ and 5.5(d): $\cos \theta < 0.99$

5.4.2 Cross sections involving four charged gauge bosons

Next we examine the cross sections involving four W bosons calculated from amplitude $W^+W^- \rightarrow W^+W^-$ (4.30). The Z-width Γ_Z can be set to zero because the process takes place at energies well above the Z resonance, so its effect is negligible. With the Higgs mass m_H set to 115 GeV, the cross sections shows neither a resonance nor a threshold but the $1/s$ dependence. There is no threshold because of the identical masses in the initial and final state which allows an immediate production of a $W^+ W^-$ pair when the center of mass energy reaches $\sqrt{s} = 2m_W$.

The graphs are shown in fig. 5.6(a) and fig. 5.6(b) Again the numerical results agree with the calculations up to the limit where our calculation breaks down. As describe above the amplitude involving four W^- bosons can be derived from the previous amplitude by exchanging s and u . The result is equal to the calculation of amplitude (4.31). The results are shown in fig. 5.7(a) and fig. 5.7(b) for the two cuts at $|\cos(\theta)| < 0.95$ and $|\cos(\theta)| < 0.99$. Again for high energies, the numeric noise in the analytic calculations produces a deviation bigger than the numeric error. Besides this the numeric results agree with the analytic calculation.

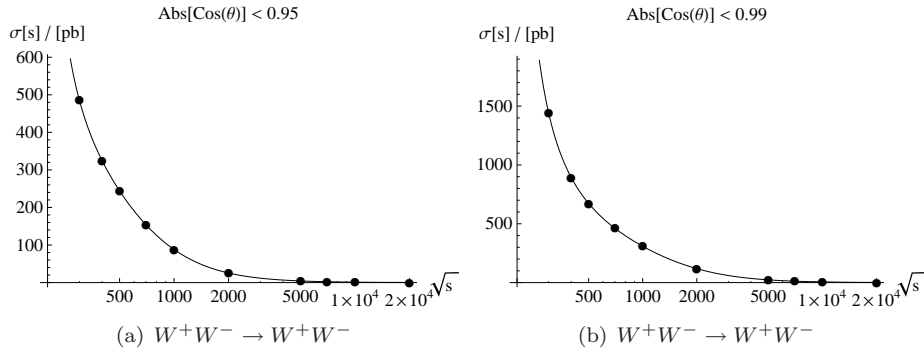


Figure 5.6

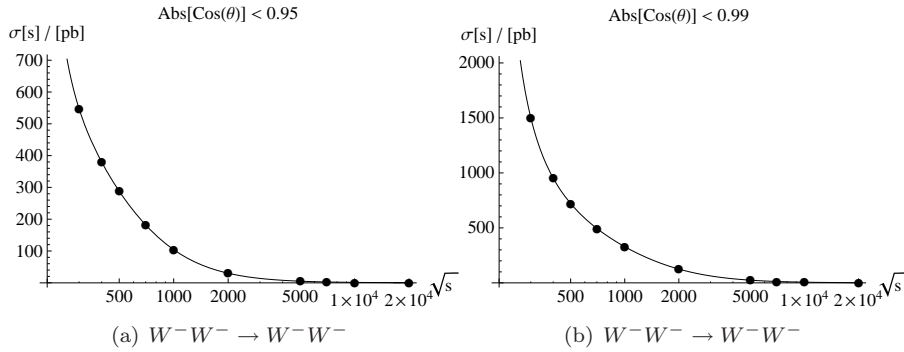


Figure 5.7

5.4.3 Cross sections involving two charged and two Z bosons

Proceeding to the the processes involving two charged gauge bosons and two Z -bosons. As above the cross sections are compared for two cuts on $\cos(\theta)$. The results for $W^+W^- \rightarrow ZZ$, that were calculated from amplitude (4.32) are shown in fig. 5.8(a) and fig. 5.8(b) with tables in the appendix A.1.3.

For this cross section the analytic calculation again became unstable at high energies. And the noise lead to deviations to the Whizard's results, that were bigger than the numerical error. The, by crossing symmetry related amplitudes, (4.39) and $ZZ \rightarrow W^+W^-$, where derived from this one, squared and integrated to the total cross sections shown in 5.9 and 5.10 for the process $W^-Z \rightarrow W^-Z$ and for the process $ZZ \rightarrow W^+W^-$ in fig. 5.11(a) and fig. 5.11(b). Comparing the graphs and the results in the appendix A.1.3, again agreement can be seen. The process $W^+Z \rightarrow W^+Z$ differs from $W^-Z \rightarrow W^-Z$ only in the direction of charge flow but besides gives identical cross section results.

The amplitude for the process $ZZ \rightarrow W^+W^-$, which simply exchanges initial and final state of the amplitude and the corresponding tables in the appendix A.1.3, also show agreement between analytic and numeric calculation.

With this cross section, all heavy gauge boson scattering cross sections involv-

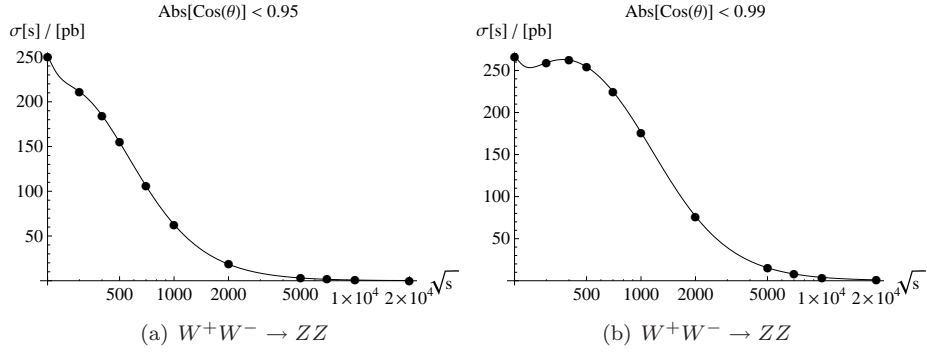


Figure 5.8

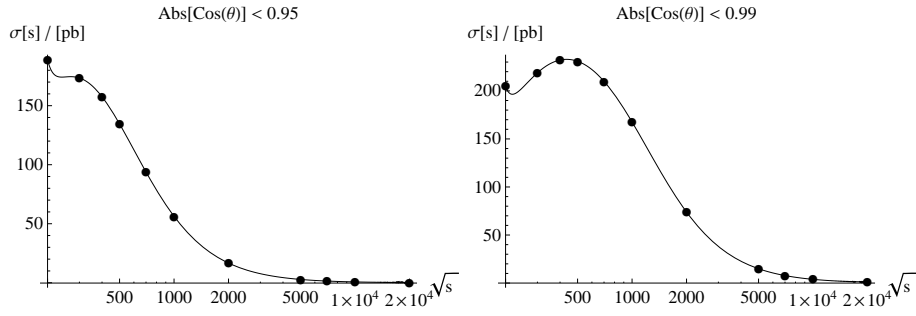
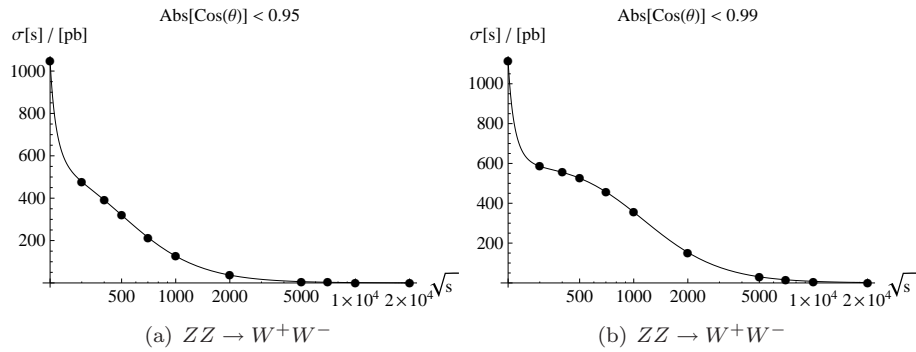


Figure 5.9: $W^-Z \rightarrow W^-Z$

Figure 5.10: $W^-Z \rightarrow W^-Z$



(a) $ZZ \rightarrow W^+W^-$

(b) $ZZ \rightarrow W^+W^-$

ing external W and Z bosons have been calculated and were compared against numeric calculations of Whizard. Despite the high energy deviations caused by noise in the analytic calculations, all analytic cross sections show agreement to their numeric equivalents.

So it was shown that Whizard gives reliable results for heavy gauge boson scattering in the Standard Model.

5.5 Gauge Boson Scattering with Anomalous Couplings

In this section the anomalous couplings are switched on. Thus the cross sections are calculated from the amplitudes in chapter 4.6. For constant anomalous couplings, the center of mass energy dependence of the total cross sections will be compared for the triple and quartic gauge boson couplings. In the second part, the energy is set to a constant value and the couplings will be scanned using Whizard's `scan` function.

5.5.1 Variation of \sqrt{s} for Constant Anomalous Couplings

Quartic Couplings

The quartic vertices are collected in (3.39) for four Z -bosons, (3.40) for two Z - and two charged gauge bosons and in (3.41) for four W -bosons. The couplings α_i are set to the constant value $\alpha_i = 0.1$ one at a time and the energy range 200 GeV to 20 TeV is scanned like in the previous chapter. Since the Feynman rules for some anomalous couplings α_i are equal, the following abbreviations are used in tables and graphics for the presentation of the results

$$(\alpha_4 + \alpha_5) = \alpha_{4,5} , \quad (5.9a)$$

$$(\alpha_4 + \alpha_6) = \alpha_{4,6} , \quad (5.9b)$$

$$(\alpha_5 + \alpha_7) = \alpha_{5,7} , \quad (5.9c)$$

$$(\alpha_4 + \alpha_6 + \alpha_{10}) = \alpha_{4,6,10} . \quad (5.9d)$$

The lower indices on the right and side of 5.9 mean, that energy scans for equal constant α_i give equal results. To show the full range of compared energies, a log-log plot is chosen for presentation. Plots are shown with quartic couplings for $|\cos\theta| < 0.95$. In fig. 5.11 the cross section $W^+W^- \rightarrow ZZ$ bosons are compared for couplings $\alpha_{4,6}$ in fig. 5.11(c) and $\alpha_{5,7}$ in fig. 5.11(d). The cross sections with anomalous couplings of four Z -bosons $\alpha_{4,5}$ and $\alpha_{6,7,10}$ are shown in fig. 5.12(a) and fig 5.12(b) while the anomalous quartic couplings for cross sections with 4 W bosons are shown in fig. 5.13. Since graphics for the remaining cross sections are similar in shape and do not present new information, they are omitted here. Nonetheless the results of the testruns with quartic gauge boson couplings in all possible heavy gauge boson cross sections for two different cuts are presented in the appendix A.2.3, A.2.1 and A.2.2.

The results show good agreement between Whizard and the analytic calculations up to very high energies. As mentioned above the noise is suppressed by the growth of the cross section with s . Our tests are successful over the whole c.m. energy range. In some cases the pull exceeds the critical limit of three. As

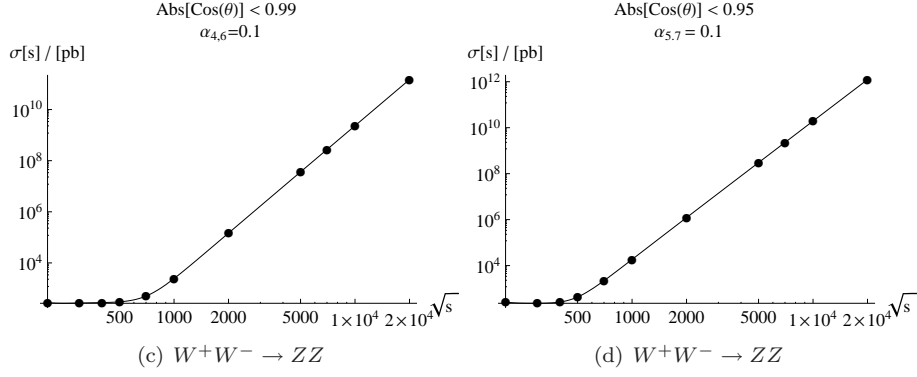


Figure 5.11: anomalous couplings $\alpha_{4,6} = 0.1$ and $\alpha_{5,7} = 0.1$ for heavy gauge boson scattering of $W^+W^- \rightarrow ZZ$

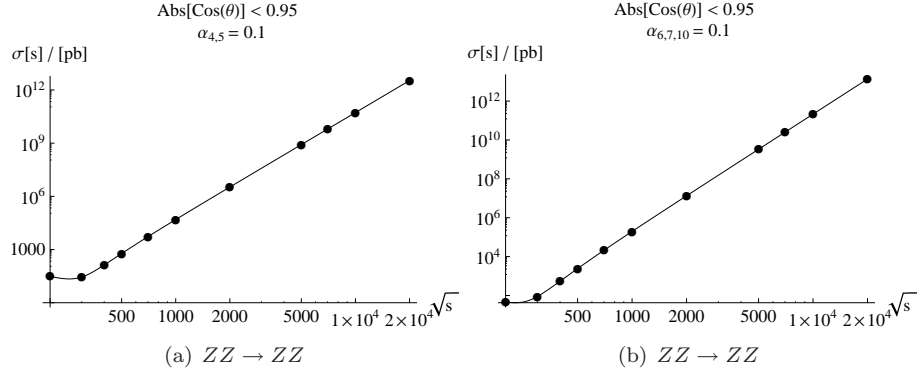


Figure 5.12: anomalous couplings $\alpha_{4,5} = 0.1$ and $\alpha_{6,7,10} = 0.1$ for heavy gauge boson scattering involving four Z - bosons

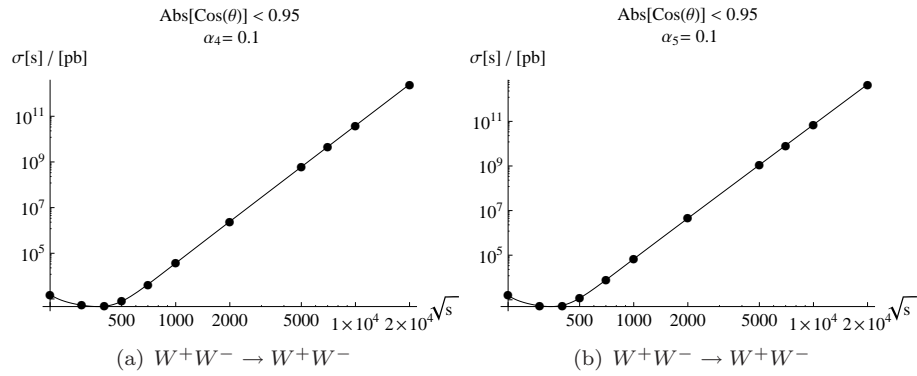


Figure 5.13: anomalous couplings $\alpha_4 = 0.1$ and $\alpha_5 = 0.1$ for heavy gauge boson scattering $W^+W^- \rightarrow W^+W^-$

analyzed in section 5.2 the reason for this lies in the statistic distribution of the pull.

Triple Gauge Couplings

The second part of this energy scanning will test the triple gauge couplings in (3.42). Again the coupling will be set to a constant value of 0.1 while the center of mass energy \sqrt{s} will be scanned for values up to 20 TeV. The cut on the angle is set on $|\cos\theta| < 0.95$ and $|\cos\theta| < 0.95$.

The amplitude for 4 external Z-bosons does not receive any contributions from the triple gauge boson vertex. The amplitude with two external Z bosons and two charged W bosons, in which besides the Higgs, only W-boson propagators occur, receives contributions from WWZ vertex and finally the four W amplitudes receive contributions from the WWZ as well as the WWA vertex.

Again we restrict the presentation of plots to a small sample and direct the reader to the appendix A.2.4 where the full results of the tests are shown in tables. One more log-log plots are chosen for presentation. We show plots for the triple gauge couplings $g_{A,Z}^1$ and $\kappa_{A,Z}$ in the process $W^+W^- \rightarrow W^+W^-$ for a cut on $|\cos\theta| < 0.95$. The plots in principle show the same behavior as the quartic couplings. For low energies, the Standard Model parts are still

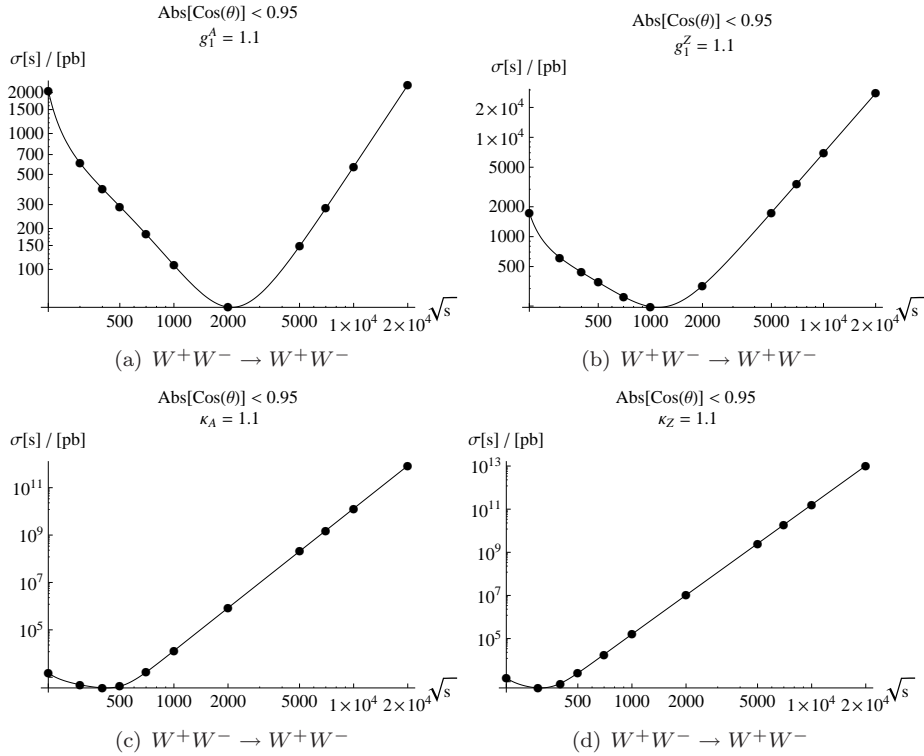


Figure 5.14: anomalous couplings $g_1^{Z,A} = 1.1$ and $\kappa_{Z,A} = 1.1$ for $W^+W^- \rightarrow W^+W^-$

dominant. For high energies the unitarity violating anomalous part takes over and we see the rise of the total cross section with s .

The *pull* values in the appendix for the triple gauge couplings show the expected behaviour. Within the statistical limits the anomalous triple gauge couplings are tested successfully.

In all, the tests of triple and quartic anomalous couplings in heavy gauge boson cross sections at different c.m. energies were successful. Whizard gives equal results within the limits of the statistical errors in our analytic and Whizards numeric calculations.

5.5.2 Variation of the Couplings at Constant Energy \sqrt{s}

In this section we vary the anomalous couplings in our analytic calculations as well as in Whizard. To do so Whizard's `scan` function becomes useful. It is able to scan a parameter in a given range for certain steps and stores the information for further evaluation. We chose to compare the heavy gauge boson cross sections in a range of $\Delta c = \Delta\alpha_i = \pm 0.1$ in steps of 0.02 around the coupling's Standard Model value. c are the anomalous triple gauge couplings as defined in (4.48) and α_i are the quartic couplings.

Since the triple gauge boson vertex is linear in the couplings c , the amplitude shows a quadratic dependence on the anomalous couplings in highest order. Therefore the total cross sections is a polynomial of order four in terms of the anomalous couplings.

The quartic vertex is linear as well in the couplings α_i but also occurs once in the total amplitude for each coupling in $2 \rightarrow 2$ processes. For this reason total cross section, containing the amplitude squared, is parabolic in terms of the quartic couplings.

This behaviour can clearly be seen in fig. 5.15 and 5.16, where we plotted the total cross section of $W^+W^- \rightarrow W^+W^-$ against the triple gauge couplings $0.9 < g_{Z,A}^1 < 1.1$ and the quartic couplings $-0.1 < a_{4,5} < 0.1$ at constant c.m. energy $s = 1$ TeV. In fig. 5.15 and fig. 5.16 we see the couplings total cross

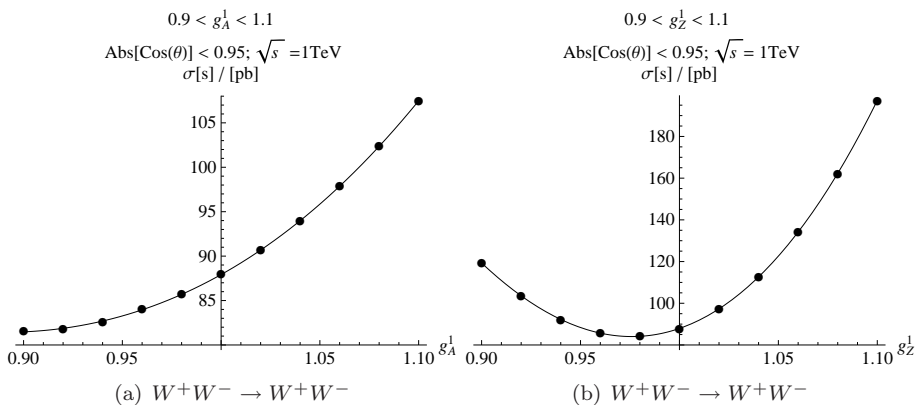


Figure 5.15: anomalous couplings $0.9 < g_1^{Z,A} < 1.1$ at $\sqrt{s} = 1$ TeV for $W^+W^- \rightarrow W^+W^-$

sections for g_A^1 and g_Z^1 at c.m. energy of $\sqrt{s} = 1$ TeV and the quartic couplings α_4 and α_5 . For this couplings Whizard produces results within the statistical

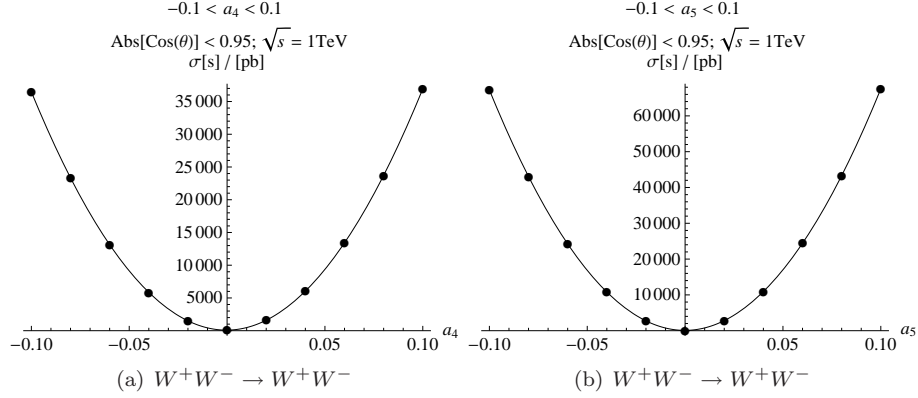


Figure 5.16: anomalous couplings $-0.1 < \alpha_{4,5} < 0.1$ at $\sqrt{s} = 1\text{TeV}$ for $W^+W^- \rightarrow W^+W^-$

limits as the tables in appendix A.4 show. Additionally the other triple and quartic gauge boson couplings were scanned. The results are shown as well in the appendix. Since the other triple and quartic anomalous couplings show the same polynomial dependence as indicated in the plots above, we avoid plotting all of the total cross sections.

Nonetheless, for the remaining anomalous couplings in the heavy gauge boson cross sections, Whizard's results agree within our analytic calculations.

In all our extensive tests have shown that Whizard produces reliable results for the scattering of heavy gauge boson cross sections. It was shown that the *pull* behaves as a random variable with two degrees of freedom. Looking at the pulls distribution which would correspond to a statistic experiment of pulling N times a pull, we see in Fig. 5.2(a) the pulls's normal distribution around zero. As statistics predict, we see a χ^2 distribution with one degree of freedom in fig. 5.2(b), when picking N times picking from a normal distributed random variable with two degrees of freedom. In our case doing ≈ 2000 calculations of cross sections and calculations of the corresponding pulls. This shows that Whizard's integrations works perfectly within the statistical limits.

Chapter 6

Anomalous Couplings in cross section $e^+e^- \rightarrow 4f$

6.1 W production in $e^+e^- \rightarrow W^+W^-$

The cross sections that were calculated in the last chapter are useful to test the reliability of the Whizard software. In physical experiments, these processes can not be studied directly, mainly for two reasons. On the one hand beams of gauge bosons cannot be prepared to produce the initial states for gauge boson scattering. On the other hand, heavy gauge bosons do not occur as stable particle in the final state, but decay further in either charged leptons and neutrinos or quarks which themselves lead to hadron jets in the final state.

To study the gauge boson couplings, a good process is process $e^+e^- \rightarrow W^+W^- \rightarrow 4f$. Besides the clean environment, that leptons provide in the initial state, it gives direct access at full c.m. energy on the gauge boson vertex. Neglecting the electron mass, the lowest order diagrams that produce two charge W bosons are

$$\begin{array}{c}
 \text{Diagram 1: } \gamma \\
 \text{Diagram 2: } Z \\
 \text{Diagram 3: } \nu_e
 \end{array}
 \quad (6.1)$$

At LEP II it was already used to study the gauge boson properties. Constraints on anomalous couplings have been extracted from measurements of this cross section by the OPAL collaboration [7] and DELPHI [4]. The total cross section in the Standard Model falls off like $1/s$ due to cancellations between the s - and t -channel diagrams. These cancellations are nontrivial, because the production of longitudinal gauge bosons. This can be seen easily by replacing the polarization sum by the approximation for longitudinal gauge bosons.

$$\epsilon_L^\mu(p) \rightarrow \frac{p^\mu}{m} + \mathcal{O}(m/E_p) \quad (6.2)$$

Then, the amplitude becomes

$$M = M_{\mu\nu} \epsilon^\mu(p_3) \epsilon^\nu(p_4) \rightarrow M_{\mu\nu} \frac{p_3^\mu \cdot p_4^\nu}{m_W^2} \approx \frac{s}{m_W^2} . \quad (6.3)$$

Without these cancellations this would lead to a cross section growing at least proportional to s and therefore would violate unitarity. But luckily when making the replacement (6.3) in the $e^+e^- \rightarrow W^+W^-$ amplitude becomes

$$M = -\frac{g^4 m_Z^4 (8sw^4 - 4sw^2 + 1)(m_W^4 - 2m_W^2 t + t(s+t))}{4m_W^2 (m_Z^2 - s)^2}, \quad (6.4)$$

which leads to the total cross section in fig. 6.1, which drops off like $\sigma \approx 1/s$ and thereby preserves unitarity. For high energies, where the gauge boson masses

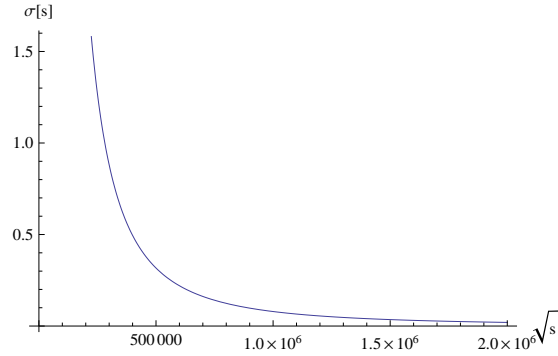


Figure 6.1: Total cross section for $e^+e^- \rightarrow W_L^+W_L^-$. Cancellations between s and t channel diagrams lead to $1/s$ decay of the cross section, preserving unitarity

can be neglected, this is equal to the Ward identity

$$M_{\mu\nu}\epsilon^\mu(p_3)\epsilon^\nu(p_4) \rightarrow M_{\mu\nu}p_3^\mu p_4^\nu = 0, \quad (6.5)$$

which itself is a special case of the Goldstone boson equivalence theorem. It states that the production of longitudinal gauge bosons is equal to the production of Goldstone bosons for high energies.

These cancellations also take place when allowing only one external longitudinal gauge boson.

When the anomalous couplings are included, analog to section 4.6, additional s and t -channel diagrams have to be included in the scattering amplitude.

$$(6.6)$$

Here c_i stands for the anomalous triple gauge couplings

$$c_V = g_1^V, \kappa_V, g_4^V, g_5^V, \kappa_5^V, \lambda_V, \lambda_5^V \quad (6.7)$$

where V is either a photon A or a Z boson.

The additional terms in the amplitude do not produce the standard model cancellations and therefore the total cross section does not preserve unitarity. Fig. 6.2(a) show the energy dependence of the total cross section for the couplings

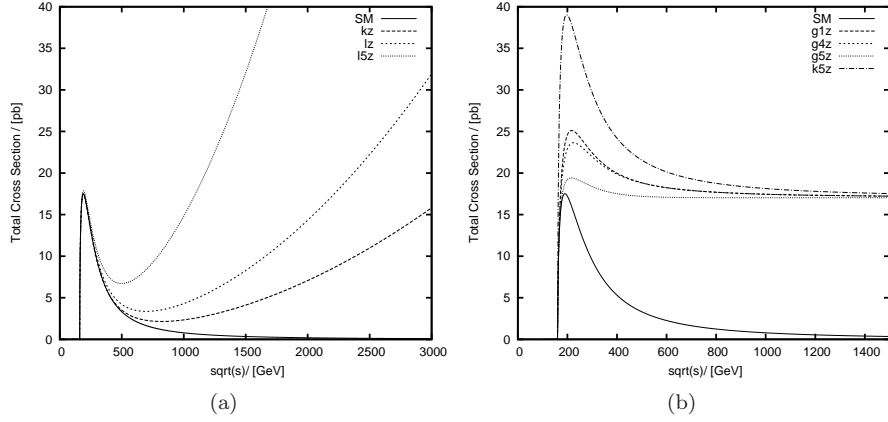


Figure 6.2: Energy dependence of the total cross section of the anomalous Couplings a) $\kappa_Z, \lambda_Z^Z, \lambda_5^Z = 0.1$ and b) $g_1^Z, g_4^Z, g_5^Z, \kappa_5^Z = 2$ in $e^+e^- \rightarrow W^+W^-$. The couplings in a) grow with increasing s while the couplings in b) cancel the $1/s$ dependence of the standard model cross section and saturate at a constant value.

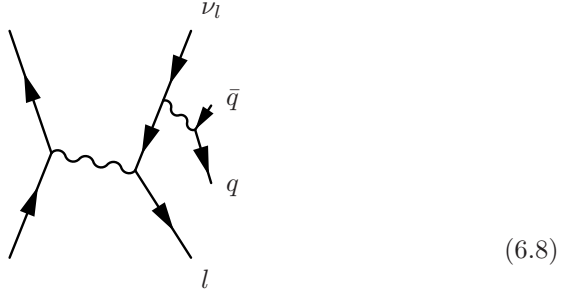
λ_Z, λ_5^Z coming from dimension 6 operators and for the anomalous magnetic moment κ_Z . They show an increasing total cross section with increasing c.m. energy \sqrt{s} . In contrast the remaining triple gauge boson couplings $g_1^Z, g_4^Z, g_5^Z, \kappa_5^Z$ in fig. 6.2(b) cancel the $1/s$ behavior which leads to convergence of the total cross section to a constant value for high energies. For a detailed plot they are set to a high value of two in fig. 6.2(b).

6.2 Total cross section of $e^+e^- \rightarrow l\nu_l q\bar{q}$

In this section we calculate the total cross section for the scattering process $e^+e^- \rightarrow 2W \rightarrow l\nu_l q\bar{q}$. The W bosons from the underlying process $e^+e^- \rightarrow W^+W^-$ have three general possible decay topologies. They can decay

- **leptonic** : both W decay in a lepton and a neutrino $l\nu_l$
- **semileptonic**: one of the W bosons decays into lepton and neutrino while the other one decays hadronic in a $q\bar{q}$ jet.
- **hadronic**: both W decay hadronically into quark jets $q\bar{q}q\bar{q}$

In this thesis we investigate processes with the semileptonic final state $l\nu_l q\bar{q}$. In collider detectors this final state is recognized as a single lepton and two hadron jets. For leptons in the final state we consider electrons e and muons μ with corresponding neutrinos ν_e and ν_μ . For final state quarks up (u), down (d), charm (c) and strange (s) quarks are considered. Background diagrams to processes with similar final state are processes like



(6.8)

where a final state lepton decays in a final state neutrino and a unstable W^+ boson, which decays further into a $q\bar{q}$ pairs.

Besides this, the main background processes are processes with $q\bar{q}\tau\nu$ final state where the τ decays further into muons and electrons and neutral current interactions with two leptons and two quarks in the final state.

To reduce the number of possible couplings, we assume electro magnetic gauge invariance, so the couplings

$$\Delta g_1^\gamma = g_5^\gamma = 0 \quad (6.9)$$

are set to zero. Further more $SU(2) \times U(1)$ gauge invariance shall be preserved. This leads to the constraints on the couplings [4]

$$\Delta\kappa_z = g_1^Z - \tan^2\theta_W \Delta\kappa_\gamma \quad (6.10a)$$

$$\lambda_z = \lambda_\gamma \quad (6.10b)$$

$$\tilde{\kappa}_z = -\tan^2\theta_W \tilde{\kappa}_\gamma \quad (6.10c)$$

$$\tilde{\lambda}_Z = \tilde{\lambda}_\gamma \quad (6.10d)$$

With this constraints there remain three CP violating couplings g_Z^4 , κ_Z^5 , and λ_Z^5 and three CP conserving couplings Δg_Z^1 , λ_Z and $\Delta\kappa_\gamma$ for which we use the fit values that can be found in [4]

$$g_Z^4 = -0.39_{-0.20}^{+0.19} \quad \Delta g_Z^1 = 0.07_{-0.12}^{+0.08} \quad (6.11)$$

$$\kappa_Z^5 = -0.09_{-0.05}^{+0.08} \quad \lambda_Z = 0.16_{-0.13}^{+0.12} \quad (6.12)$$

$$\lambda_Z^5 = -0.08 \pm 0.07 \quad \Delta\kappa_A = -0.32_{-0.15}^{+0.17} \quad (6.13)$$

With these values the process the total cross section $e^+e^+ \rightarrow l\nu_l q\bar{q}$ will be calculated at LEP c.m. energy 190 GeV and ILC energy 500 GeV and 1000 GeV. For the analyzing the couplings at higher energies than the fitted values from (6.13), we assume the independence of the couplings of the c.m. energy. In our analysis the following cuts are applied

- $|\cos\theta| < 0.95$ for all particles
- $\theta > 5degree$ for all particles
- $p_T, E > 10GeV$ for the final state particles
- $M > 10GeV$ for the final state particles

\sqrt{s}/GeV	Total cross section [fb] for process $e^+e^- \rightarrow l\nu_l q\bar{q}$		
	190 GeV	500GeV	1000 GeV
SM	2762.29 ± 4.43	1433.04 ± 7.39	995.87 ± 1.83
g_Z^1	3004.88 ± 5.07	2209.50 ± 3.34	2137.73 ± 3.38
g_Z^4	2802.42 ± 4.52	1582.36 ± 2.3	1273.74 ± 2.17
κ_Z^5	2770.26 ± 4.59	1445.91 ± 2.22	1002.83 ± 1.88
λ_Z	2828.50 ± 4.39	2739.11 ± 4.25	6881.76 ± 11.2
λ_Z^5	2791.85 ± 4.4	1772.63 ± 2.54	2457.57 ± 4.27
κ_A	2830.36 ± 4.37	2015.00 ± 2.87	3120.76 ± 3.84

Table 6.1: Total cross section for process $e^+e^- \rightarrow l\nu_l q\bar{q}$ for the anomalous triple gauge boson couplings given in 6.13 for c.m. energy $\sqrt{s} = 190 GeV, 500 GeV, 1000 GeV$.

where θ is the angle between beam axis and final state particle, p_T is the transverse impuls and E the energy of the particle and M is the invariant mass.

With these cuts the total cross sections are calculated for the full process $e^+e^- \rightarrow l\nu_l q\bar{q}$, first at $\sqrt{s} = 190 GeV$ which roughly corresponds to the maximum in the total cross section of $e^+e^- \rightarrow W^+W^-$, second at ILC c.m.energy $\sqrt{s} = 500 GeV$ and third at $\sqrt{s} = 1 TeV$ which corresponds to a high ILC energy.

As we see in table 6.1 the total cross sections for the full process follow the W -production curves in fig 6.2. Saturation of the W production process for g_Z^1, g_Z^4, κ_Z^5 in fig 6.2(b) produces almost no difference in the total cross sections for the full process in the step from 500 GeV to 1000 GeV.

In contrast, the remaining couplings $\lambda_{Z,A}^5, \lambda_A$ and κ in the W production, shown in fig. 6.2(a), produce increasing total cross sections from 500 GeV to 1000 TeV corresponding to an increasing W production for $e^+e^- \rightarrow W^+W^-$

The standard model total cross sections at this energies drop with increasing c.m. energies. This leads to almost doubled total cross sections for the full process at 1 TeV compared to the expected Standard Model cross section.

Chapter 7

Conclusion

In this thesis the heavy gauge boson scattering in the Standard Model, in particular in GWS theory, and with anomalous gauge boson couplings was studied. Therefore we derived the Standard Model Feynman rules for gauge boson scattering. Additionally we showed a description of the Standard Model as an effective theory by step by step building the Lagrangian from operators with increasing dimension. Doing so, the Lagrangian describing the standard model particles can be written down. An additional Σ field was introduced into the theory which introduced additional dimension four operators. These operator in unitary gauge describe anomalous gauge boson couplings.

By deriving the corresponding Feynman rules for the anomalous gauge boson couplings and with the Standard Model Feynman rules we were able to calculate $V, V \rightarrow V, V$ scattering cross sections, with $V = W, Z$ in the initial and final state.

The analytic standard model calculations broke down for energies above 10 TeV because numeric noise occurred in the calculated matrix element. At energies above 10 TeV the total cross section for Standard model scattering became, due to the $1/s$ dependence, of the order of this noise, so the results were not reliable anymore.

The cross sections including anomalous couplings did not show this behavior. The reason for this lies in the unitarity violation of the anomalous couplings terms. With increasing energy, the additional terms coming from the anomalous couplings became dominant and the cross sections rose with c.m. energy. Thus the noise in the Standard Model amplitude was suppressed by these terms and we were able to calculate the total cross sections up to $\sqrt{s} = 20TeV$

We compared the analytical calculated gauge boson cross section against the Monte Carlo event generator Whizard [12]. Monte Carlo Event generators are used for phenomenological predictions at currently operating colliders like LHC or future particle colliders like a linear lepton collider ILC. The heavy gauge boson cross sections were used to test the internal calculation of these processes in Whizard. Although these cross sections are not directly observable, they are important as sub processes and a valid numerical treatment is important for predictions for physics beyond Standard Model, in particular heavy gauge boson couplings, at colliders where the electroweak scale is accessible, like the LHC or a future linear collider (ILC).

To treat the statistics of Wizard's numerical integration in this comparison

properly, we calculated the *pull* (5.2) from the total cross sections, with the assumption of exact analytic results. With respect to the noise in our calculations we had to restrict this assumption to c.m. energies below 10 TeV for the standard model cross sections as mentioned above. In all, ≈ 2000 tests were made resulting in the calculation of the same amount of *pull* values. We were able to show that the *pull* is normally distributed around zero by fitting Gaussian function to the *pull* histogram. Looking at the square of the *pull* values we saw that they are distributed like the probability density function of χ^2 distribution of one degree of freedom. From this we have shown that the pull squared itself behaves like a Gaussian random variable with two degrees of freedom.

In the test runs, a test was counted successful when the corresponding *pull* was smaller than three. This corresponds to a cumulative probability of 99.7 per cent. Indeed our tests were successful, although slight excitations of *pull* > 3 occurred. They have to be of statistical nature, because although unlikely, events like this are not impossible.

Additionally in some test runs the sign of the pulls was almost equal. This was found to be of statistical origin, too. Rerunning the tests with different seeds or different integrations steps could not reproduce this but showed the expected behavior.

Summing all this together, in our extensive tests of heavy gauge boson scattering cross sections Whizard was found to produce reliable results for heavy gauge boson scattering in Standard Model and with anomalous couplings.

With this knowledge, we calculated the cross section $e^+e^- \rightarrow (W^+W^-) \rightarrow l\nu_l q\bar{q}$ with anomalous couplings at LEP energies $s = 190$ GeV and at assumed ILC c.m. energy $s = 500$ GeV and 1 TeV. We have shown, that the underlying W production $e^+e^- \rightarrow W^+W^-$ preserves unitarity in Standard Model, due to cancellations between s and t channel diagrams. The anomalous couplings violate these cancellations and thus the total cross section of W production increases with energy \sqrt{s} for the couplings $\lambda_Z, \lambda_Z^5, \kappa_A$ or saturates at constant value for the couplings g_Z^1, g_Z^4, κ_Z^5 .

This behavior reproduces in the total cross section for semi leptonic four fermion production. At LEP energy $\sqrt{s} = 190$ GeV, which roughly corresponds to the maximum in W production cross section, the total cross section in Standard Model and with anomalous couplings was found to be of same order. Going away from the maximum to ILC energy $\sqrt{s} = 500$ GeV gives reduced total cross sections for all couplings.

Increasing the c.m. energy further up to 1 TeV, leads to an increase of the total cross sections for the full process for the couplings $\lambda_Z, \lambda_Z^5, \kappa_A$ while the anomalous couplings that lead to saturation of the W production cross section, give total cross sections of the same order of the full process at 500 GeV.

Appendix A

Tables

The section shows the tables cited in the text for the comparison of the analytic calculations with numerical results from Whizard. In the tables σ_{an} is the analytic result for the cross section and σ_{num} gives the result from Whizard. The error is the numerical error calculated by Whizard. The pull is calculated according to (5.2).

A.1 Standard Model Scattering

A.1.1 Cross sections involving four Z bosons

\sqrt{s} [GeV]	$\sigma_{an}(s)[fb]$	$ZZ \rightarrow ZZ$ Abs(cos(θ)) < 0.95		Pull
		$\sigma_{num}(s)[fb]$	Error[fb]	
200	2.95061E+03	2.95076E+03	4.23539E-01	0.351
300	2.40344E+08	2.40332E+08	3.64603E+04	-0.316
400	3.94193E+04	3.94193E+04	4.56172E+00	0.00571
500	2.02510E+04	2.02543E+04	2.00865E+00	1.64
700	1.12113E+04	1.12125E+04	9.79551E-01	1.26
1000	6.39041E+03	6.39162E+03	5.62956E-01	2.14
2000	1.92628E+03	1.92627E+03	2.10511E-01	-0.0239
5000	3.33216E+02	3.33240E+02	4.57896E-02	0.516
7000	1.71457E+02	1.71381E+02	2.46691E-02	-3.07
10000	8.44037E+01	8.44176E+01	7.20243E-03	1.93

$ZZ \rightarrow ZZ$ Abs(cos(θ)) < 0.99				
\sqrt{s} [GeV]	$\sigma_{an}(s)$ [fb]	$\sigma_{num}(s)$ [fb]	Error[fb]	Pull
200	3.07785E+03	3.07810E+03	4.59423E-01	0.538
300	2.50464E+08	2.50416E+08	3.00435E+04	-1.6
400	4.07304E+04	4.07289E+04	4.15948E+00	-0.358
500	2.08206E+04	2.08210E+04	1.72828E+00	0.212
700	1.14754E+04	1.14746E+04	9.81526E-01	-0.829
1000	6.53078E+03	6.53119E+03	4.53795E-01	0.895
2000	1.97590E+03	1.97584E+03	1.69700E-01	-0.336
5000	3.45200E+02	3.45311E+02	4.14108E-02	2.67
7000	1.78058E+02	1.78038E+02	2.51898E-02	-0.786
10000	8.77950E+01	8.78010E+01	5.66518E-03	1.05

$ZZ \rightarrow ZZ$ Abs(cos(θ)) < 0.95				
\sqrt{s} [GeV]	$\sigma_{an}(s)$ [fb]	$\sigma_{num}(s)$ [fb]	Error[fb]	Pull
299	7.91896E+07	7.92027E+07	8.43565E+03	1.56
299.1	9.07788E+07	9.08134E+07	1.36140E+04	2.54
299.2	1.04430E+08	1.04427E+08	6.22514E+03	-0.475
299.3	1.20378E+08	1.20410E+08	1.34407E+04	2.42
299.4	1.38714E+08	1.38724E+08	1.47103E+04	0.699
299.5	1.59214E+08	1.59227E+08	2.47570E+04	0.53
299.6	1.81104E+08	1.81115E+08	1.07153E+04	1.05
299.7	2.02805E+08	2.02823E+08	2.57726E+04	0.712
299.8	2.21849E+08	2.21870E+08	2.82719E+04	0.737
299.9	2.35233E+08	2.35290E+08	3.51393E+04	1.63
300	2.40344E+08	2.40320E+08	3.39930E+04	-0.716
300.1	2.36093E+08	2.36030E+08	3.42607E+04	-1.83
300.2	2.23457E+08	2.23501E+08	3.28419E+04	1.33
300.3	2.04982E+08	2.05005E+08	2.99785E+04	0.782
300.4	1.83657E+08	1.83615E+08	2.62187E+04	-1.61
300.5	1.61975E+08	1.62017E+08	2.26068E+04	1.86
300.6	1.41557E+08	1.41576E+08	2.07531E+04	0.904
300.7	1.23218E+08	1.23239E+08	1.77817E+04	1.15
300.8	1.07212E+08	1.07196E+08	1.57059E+04	-1.05
300.9	9.34720E+07	9.34939E+07	1.34363E+04	1.63
301	8.17779E+07	8.17897E+07	1.21987E+04	0.965

\sqrt{s} [GeV]	$ZZ \rightarrow ZZ$ Abs(cos(θ)) < 0.99			Pull
	$\sigma_{an}(s)$ [fb]	$\sigma_{num}(s)$ [fb]	Error[fb]	
299	8.25321E+07	8.25362E+07	1.70173E+03	2.38
299.1	9.46095E+07	9.46461E+07	1.21342E+04	3.02
299.2	1.08836E+08	1.08850E+08	8.09057E+03	1.69
299.3	1.25456E+08	1.25475E+08	1.36298E+04	1.42
299.4	1.44563E+08	1.44562E+08	8.16273E+03	-0.139
299.5	1.65926E+08	1.65919E+08	1.68321E+04	-0.41
299.6	1.88737E+08	1.88692E+08	2.08702E+04	-2.17
299.7	2.11351E+08	2.11391E+08	2.95982E+04	1.36
299.8	2.31195E+08	2.31227E+08	1.29946E+04	2.49
299.9	2.45141E+08	2.45104E+08	2.27428E+04	-1.61
300	2.50464E+08	2.50447E+08	3.20865E+04	-0.52
300.1	2.46031E+08	2.46075E+08	2.94431E+04	1.48
300.2	2.32861E+08	2.32898E+08	1.63176E+04	2.26
300.3	2.13606E+08	2.13699E+08	3.06542E+04	3.03
300.4	1.91382E+08	1.91338E+08	2.51661E+04	-1.74
300.5	1.68787E+08	1.68807E+08	1.14958E+04	1.78
300.6	1.47509E+08	1.47519E+08	2.17776E+04	0.48
300.7	1.28397E+08	1.28407E+08	1.23844E+04	0.824
300.8	1.11718E+08	1.11716E+08	7.19611E+03	-0.339
300.9	9.73990E+07	9.73871E+07	1.22334E+04	-0.971
301	8.52128E+07	8.52309E+07	6.10849E+03	2.97

A.1.2 Cross sections involving four W bosons

\sqrt{s} [GeV]	$W^+W^- \rightarrow W^+W^-$ Abs(cos(θ)) < 0.95			Pull
	$\sigma_{an}(s)$ [fb]	$\sigma_{num}(s)$ [fb]	Error[fb]	
200	1.54138E+06	1.54111E+06	6.42791E+02	-0.421
300	4.85272E+05	4.85167E+05	1.98021E+02	-0.529
400	3.24887E+05	3.24764E+05	1.34012E+02	-0.92
500	2.43911E+05	2.43889E+05	9.47832E+01	-0.234
700	1.53531E+05	1.53428E+05	9.09674E+01	-1.13
1000	8.79222E+04	8.79246E+04	5.85955E+01	0.0414
2000	2.53570E+04	2.53318E+04	1.88859E+01	-1.34
5000	4.24929E+03	4.24434E+03	3.29294E+00	-1.5
7000	2.17750E+03	2.17954E+03	1.44625E+00	1.41
10000	1.07069E+03	1.07095E+03	8.56250E-01	0.299

$W^+W^- \rightarrow W^+W^-$ $\text{Abs}(\cos(\theta)) < 0.99$				
$\sqrt{s}[\text{GeV}]$	$\sigma_{an}(s)[fb]$	$\sigma_{num}(s)[fb]$	Error[fb]	Pull
200	5.93538E+06	5.93428E+06	3.77840E+03	-0.292
300	1.43934E+06	1.44042E+06	1.14069E+03	0.948
400	8.93903E+05	8.95293E+05	6.04400E+02	2.3
500	6.72900E+05	6.73011E+05	4.48635E+02	0.248
700	4.61549E+05	4.61060E+05	2.97247E+02	-1.64
1000	3.08622E+05	3.08613E+05	2.29624E+02	-0.0374
2000	1.18586E+05	1.18520E+05	1.13524E+02	-0.585
5000	2.32347E+04	2.32095E+04	2.81012E+01	-0.897
7000	1.21234E+04	1.21388E+04	1.46678E+01	1.05
10000	6.00988E+03	6.01164E+03	8.48699E+00	0.208

$W^-W^- \rightarrow W^-W^-$ $\text{Abs}(\cos(\theta)) < 0.95$				
$\sqrt{s}[\text{GeV}]$	$\sigma_{an}(s)[fb]$	$\sigma_{num}(s)[fb]$	Error[fb]	Pull
200	1.61322E+06	1.61249E+06	9.10854E+02	-0.801
300	5.47603E+05	5.47302E+05	2.59165E+02	-1.16
400	3.79574E+05	3.79904E+05	2.02384E+02	1.63
500	2.87927E+05	2.87804E+05	1.49559E+02	-0.825
700	1.81905E+05	1.81906E+05	8.35727E+01	0.016
1000	1.04100E+05	1.04097E+05	6.08406E+01	-0.0548
2000	2.99728E+04	2.99842E+04	2.26245E+01	0.505
5000	5.01988E+03	5.02524E+03	4.69681E+00	1.14
7000	2.57142E+03	2.57191E+03	2.26746E+00	0.215
10000	1.27358E+03	1.26261E+03	1.26548E+00	-8.67

$W^-W^- \rightarrow W^-W^-$ $\text{Abs}(\cos(\theta)) < 0.99$				
$\sqrt{s}[\text{GeV}]$	$\sigma_{an}(s)[fb]$	$\sigma_{num}(s)[fb]$	Error[fb]	Pull
200	6.02473E+06	6.01834E+06	4.76452E+03	-1.34
300	1.50374E+06	1.50317E+06	1.11675E+03	-0.508
400	9.52232E+05	9.52053E+05	6.47708E+02	-0.276
500	7.21275E+05	7.21625E+05	4.44478E+02	0.787
700	4.94506E+05	4.94500E+05	3.37920E+02	-0.0174
1000	3.28773E+05	3.28616E+05	2.33688E+02	-0.672
2000	1.25114E+05	1.25047E+05	1.31623E+02	-0.51
5000	2.44119E+04	2.43407E+04	3.80533E+01	-1.87
7000	1.27323E+04	1.27180E+04	1.70132E+01	-0.843
10000	6.31059E+03	6.30398E+03	8.49266E+00	-0.779

A.1.3 Cross sections involving two Z and two W bosons

$W^+W^- \rightarrow ZZ$ Abs(cos(θ)) < 0.95				
\sqrt{s} [GeV]	$\sigma_{an}(s)[fb]$	$\sigma_{num}(s)[fb]$	Error[fb]	Pull
200	2.50028E+05	2.50052E+05	2.01587E+01	1.19
300	2.11321E+05	2.11255E+05	4.64313E+01	-1.41
400	1.84810E+05	1.84850E+05	4.52426E+01	0.892
500	1.54865E+05	1.54887E+05	3.51094E+01	0.622
700	1.05911E+05	1.05938E+05	4.01706E+01	0.664
1000	6.27813E+04	6.27793E+04	2.80040E+01	-0.0698
2000	1.84104E+04	1.84121E+04	8.54271E+00	0.199
5000	3.09359E+03	3.09690E+03	2.07218E+00	1.6
7000	1.58591E+03	1.58556E+03	1.05843E+00	-0.335
10000	7.79330E+02	7.79594E+02	4.11287E-01	0.643

$W^+W^- \rightarrow ZZ$ Abs(cos(θ)) < 0.99				
\sqrt{s} [GeV]	$\sigma_{an}(s)[fb]$	$\sigma_{num}(s)[fb]$	Error[fb]	Pull
200	2.65982E+05	2.65996E+05	1.37442E+01	0.985
300	2.59168E+05	2.59217E+05	4.45289E+01	1.09
400	2.62449E+05	2.62558E+05	5.40865E+01	2.01
500	2.54320E+05	2.54352E+05	6.01311E+01	0.527
700	2.24980E+05	2.25020E+05	5.56632E+01	0.716
1000	1.76450E+05	1.76324E+05	6.59214E+01	-1.91
2000	7.65338E+04	7.65455E+04	4.35455E+01	0.27
5000	1.53747E+04	1.53745E+04	1.03789E+01	-0.0183
7000	8.03543E+03	8.03010E+03	6.55601E+00	-0.812
10000	3.98898E+03	3.99382E+03	3.02982E+00	1.6

$W^-Z \rightarrow W^-Z$ Abs(cos(θ)) < 0.95				
\sqrt{s} [GeV]	$\sigma_{an}(s)[fb]$	$\sigma_{num}(s)[fb]$	Error[fb]	Pull
200	1.89249E+05	1.89225E+05	3.03273E+01	-0.776
300	1.73464E+05	1.73572E+05	5.28424E+01	2.05
400	1.57555E+05	1.57614E+05	6.16066E+01	0.959
500	1.34571E+05	1.34513E+05	5.16914E+01	-1.13
700	9.38201E+04	9.38006E+04	3.41900E+01	-0.571
1000	56272.5	5.63062E+04	3.00313E+01	-1.114
2000	1.66578E+04	1.66680E+04	1.00988E+01	1.01
5000	2.80701E+03	2.80486E+03	1.92744E+00	-1.12
7000	1.43923E+03	1.44098E+03	1.02219E+00	1.71
10000	7.10314E+02	7.07552E+02	5.14731E-01	-5.37

$W^-Z \rightarrow W^-Z$ Abs(cos(θ)) < 0.99				
\sqrt{s} [GeV]	$\sigma_{an}(s)$ [fb]	$\sigma_{num}(s)$ [fb]	Error[fb]	Pull
200	2.04799E+05	2.04888E+05	3.68682E+01	2.4
300	2.18800E+05	2.18875E+05	4.89336E+01	1.53
400	2.32098E+05	2.32082E+05	6.68919E+01	-0.239
500	2.30784E+05	2.30792E+05	7.17170E+01	0.111
700	2.09923E+05	2.10093E+05	1.00090E+02	1.7
1000	1.67691E+05	1.67727E+05	9.58522E+01	0.371
2000	7.39076E+04	7.39603E+04	5.68828E+01	0.926
5000	1.49242E+04	1.49441E+04	1.27905E+01	1.56
7000	7.80423E+03	7.81263E+03	8.42521E+00	0.997
10000	3.87846E+03	3.87347E+03	4.34859E+00	-1.15

$ZZ \rightarrow W^+W^-$ Abs(cos(θ)) < 0.95				
\sqrt{s} [GeV]	$\sigma_{an}(s)$ [fb]	$\sigma_{num}(s)$ [fb]	Error[fb]	Pull
200	1.04860E+06	1.04860E+06	8.90735E+01	-0.0266
300	4.77706E+05	4.77575E+05	1.05745E+02	-1.24
400	3.91178E+05	3.91176E+05	9.48140E+01	-0.0203
500	3.20294E+05	3.20211E+05	7.11059E+01	-1.17
700	2.15251E+05	2.15232E+05	8.32817E+01	-0.223
1000	1.26523E+05	1.26531E+05	5.42595E+01	0.154
2000	3.68895E+04	3.68676E+04	1.55027E+01	-1.42
5000	6.18900E+03	6.18781E+03	3.67910E+00	-0.323
7000	3.17217E+03	3.17526E+03	1.80973E+00	1.71
10000	1.56174E+03	1.55726E+03	1.00415E+00	4.461

$ZZ \rightarrow W^+W^-$ Abs(cos(θ)) < 0.99				
\sqrt{s} [GeV]	$\sigma_{an}(s)$ [fb]	$\sigma_{num}(s)$ [fb]	Error[fb]	Pull
200	1.11551E+06	1.11555E+06	7.25703E+01	0.588
300	5.85868E+05	5.86000E+05	1.04096E+02	1.27
400	5.55514E+05	5.55322E+05	1.13113E+02	-1.69
500	5.25987E+05	5.26103E+05	1.24668E+02	0.931
700	4.57242E+05	4.57161E+05	1.30256E+02	-0.62
1000	3.55599E+05	3.55441E+05	1.34186E+02	-1.18
2000	1.53353E+05	1.53310E+05	8.39315E+01	-0.51
5000	3.07584E+04	3.07261E+04	2.19497E+01	-1.47
7000	1.60732E+04	1.60714E+04	1.23790E+01	-0.147
10000	7.98154E+03	7.97277E+03	5.53635E+00	-1.58

A.2 Scattering with anomalous couplings

A.2.1 Quartic couplings in four W boson cross sections

$W^+W^- \rightarrow W^+W^-$ Abs($\cos(\theta)$) < 0.95 anomalous coupling $a_4 = 0.1$				
\sqrt{s} [GeV]	$\sigma_{an}(s)[fb]$	$\sigma_{num}(s)[fb]$	Error[fb]	Pull
200	1.58322E+06	1.58304E+06	6.99588E+02	-0.258
300	5.32612E+05	5.32277E+05	2.17533E+02	-1.54
400	4.78581E+05	4.78632E+05	2.25409E+02	0.228
500	7.84872E+05	7.84920E+05	2.72463E+02	0.176
700	4.31736E+06	4.31770E+06	8.44914E+02	0.405
1000	3.69472E+07	3.69411E+07	6.47892E+03	-0.946
2000	2.45436E+09	2.45421E+09	4.40229E+05	-0.351
5000	6.06739E+11	6.06869E+11	9.58091E+07	1.35
7000	4.57393E+12	4.57502E+12	6.29534E+08	1.74
10000	3.89025E+13	3.88941E+13	6.39839E+09	-1.31
20000	2.49091E+15	2.49106E+15	4.23951E+11	0.351

$W^+W^- \rightarrow W^+W^-$ Abs($\cos(\theta)$) < 0.99 anomalous coupling $a_4 = 0.1$				
\sqrt{s} [GeV]	$\sigma_{an}(s)[fb]$	$\sigma_{num}(s)[fb]$	Error[fb]	Pull
200	5.99102E+06	5.99521E+06	3.87936E+03	1.08
300	1.50431E+06	1.50475E+06	1.09884E+03	0.401
400	1.08361E+06	1.08326E+06	6.28589E+02	-0.552
500	1.29176E+06	1.29228E+06	5.48194E+02	0.946
700	4.99010E+06	4.99279E+06	1.01061E+03	2.66
1000	3.97991E+07	3.97950E+07	3.54422E+03	-1.16
2000	2.61679E+09	2.61722E+09	2.18849E+05	1.95
5000	6.46591E+11	6.46444E+11	6.04501E+07	-2.43
7000	4.87427E+12	4.87517E+12	4.62639E+08	1.94
10000	4.14567E+13	4.14637E+13	3.70277E+09	1.88
20000	2.65444E+15	2.65465E+15	2.90929E+11	0.72

$W^+W^- \rightarrow W^+W^-$ Abs($\cos(\theta)$) < 0.95 anomalous coupling $a_5 = 0.1$				
\sqrt{s} [GeV]	$\sigma_{an}(s)[fb]$	$\sigma_{num}(s)[fb]$	Error[fb]	Pull
200	1.58448E+06	1.58435E+06	6.94206E+02	-0.193
300	5.38466E+05	5.38397E+05	2.25292E+02	-0.308
400	5.62016E+05	5.62170E+05	2.13986E+02	0.719
500	1.17897E+06	1.17891E+06	3.41656E+02	-0.165
700	7.71491E+06	7.71575E+06	1.03219E+03	0.81
1000	6.75725E+07	6.75651E+07	1.01859E+04	-0.722
2000	4.49051E+09	4.49143E+09	7.64735E+05	1.21
5000	1.10891E+12	1.10895E+12	1.48015E+08	0.247
7000	8.35861E+12	8.35761E+12	1.04271E+09	-0.961
10000	7.10878E+13	7.11053E+13	1.03600E+10	1.69
20000	4.55150E+15	4.55148E+15	6.63442E+11	-0.0259

$W^+W^- \rightarrow W^+W^-$
 $\text{Abs}(\cos(\theta)) < 0.99$
anomalous coupling $a_5 = 0.1$

\sqrt{s} [GeV]	$\sigma_{an}(s)[fb]$	$\sigma_{num}(s)[fb]$	Error[fb]	Pull
200	5.99341E+06	5.99142E+06	3.89800E+03	-0.512
300	1.50692E+06	1.50704E+06	9.65887E+02	0.124
400	1.16277E+06	1.16267E+06	6.77131E+02	-0.15
500	1.68953E+06	1.68964E+06	5.73501E+02	0.197
700	8.50788E+06	8.51067E+06	1.07919E+03	2.59
1000	7.17120E+07	7.17146E+07	5.09286E+03	0.511
2000	4.74279E+09	4.74299E+09	3.68920E+05	0.547
5000	1.17101E+12	1.17113E+12	9.45413E+07	1.22
7000	8.82664E+12	8.82646E+12	7.42537E+08	-0.247
10000	7.50681E+13	7.50591E+13	5.91608E+09	-1.53
20000	4.80634E+15	4.80652E+15	4.85150E+11	0.368

$W^-W^- \rightarrow W^-W^-$
 $\text{Abs}(\cos(\theta)) < 0.95$
anomalous coupling $a_4 = 0.1$

\sqrt{s} [GeV]	$\sigma_{an}(s)[fb]$	$\sigma_{num}(s)[fb]$	Error[fb]	Pull
200	1.57816E+06	1.57980E+06	8.37485E+02	1.96
300	5.23928E+05	5.24380E+05	2.52521E+02	1.79
400	4.12294E+05	4.12370E+05	2.04874E+02	0.369
500	6.03233E+05	6.03127E+05	2.36976E+02	-0.448
700	3.51603E+06	3.51706E+06	5.80260E+02	1.77
1000	3.17875E+07	3.17849E+07	4.18227E+03	-0.627
2000	2.14935E+09	2.14943E+09	2.85390E+05	0.272
5000	5.31670E+11	5.31550E+11	8.71756E+07	-1.38
7000	4.00785E+12	4.00813E+12	6.25424E+08	0.453
10000	3.40869E+13	3.40927E+13	4.75024E+09	1.21
20000	2.18251E+15	2.18263E+15	2.91327E+11	0.408

$W^-W^- \rightarrow W^-W^-$
 $\text{Abs}(\cos(\theta)) < 0.99$
anomalous coupling $a_4 = 0.1$

\sqrt{s} [GeV]	$\sigma_{an}(s)[fb]$	$\sigma_{num}(s)[fb]$	Error[fb]	Pull
200	5.97625E+06	5.98531E+06	5.27000E+03	1.72
300	1.46453E+06	1.46391E+06	1.10726E+03	-0.564
400	9.62141E+05	9.61288E+05	6.23170E+02	-1.37
500	1.01411E+06	1.01333E+06	4.12050E+02	-1.89
700	3.92366E+06	3.92228E+06	6.70587E+02	-2.06
1000	3.35096E+07	3.35142E+07	2.28385E+03	2.01
2000	2.26217E+09	2.26179E+09	1.78973E+05	-2.13
5000	5.59719E+11	5.59719E+11	4.82133E+07	0.000649
7000	4.21929E+12	4.21901E+12	3.84984E+08	-0.724
10000	3.58852E+13	3.58853E+13	2.96995E+09	0.0396
20000	2.29765E+15	2.29736E+15	2.12949E+11	-1.35

$W^-W^- \rightarrow W^-W^-$ $\text{Abs}(\cos(\theta)) < 0.95$ anomalous coupling $a_5 = 0.1$				
$\sqrt{s}[\text{GeV}]$	$\sigma_{an}(s)[fb]$	$\sigma_{num}(s)[fb]$	Error[fb]	Pull
200	1.57403E+06	1.57430E+06	7.95786E+02	0.337
300	5.28578E+05	5.28665E+05	2.49409E+02	0.349
400	3.70701E+05	3.70584E+05	1.84829E+02	-0.635
500	3.37716E+05	3.37613E+05	1.39155E+02	-0.74
700	9.42128E+05	9.42349E+05	2.58406E+02	0.854
1000	7.82979E+06	7.83114E+06	1.34339E+03	1
2000	5.36579E+08	5.36700E+08	8.88608E+04	1.36
5000	1.33151E+11	1.33180E+11	2.67852E+07	1.09
7000	1.00394E+12	1.00392E+12	2.01386E+08	-0.0945
10000	8.53953E+12	8.53886E+12	1.45827E+09	-0.461
20000	5.46811E+14	5.46837E+14	9.27974E+10	0.277

$W^-W^- \rightarrow W^-W^-$ $\text{Abs}(\cos(\theta)) < 0.99$ anomalous coupling $a_5 = 0.1$				
$\sqrt{s}[\text{GeV}]$	$\sigma_{an}(s)[fb]$	$\sigma_{num}(s)[fb]$	Error[fb]	Pull
200	5.97079E+06	5.97220E+06	5.30602E+03	0.265
300	1.47263E+06	1.47295E+06	9.79687E+02	0.323
400	9.26305E+05	9.25915E+05	6.10752E+02	-0.639
500	7.50633E+05	7.50663E+05	3.86109E+02	0.0781
700	1.27351E+06	1.27435E+06	4.61735E+02	1.82
1000	8.64631E+06	8.64456E+06	8.91175E+02	-1.96
2000	5.84600E+08	5.84712E+08	5.52208E+04	2.03
5000	1.45127E+11	1.45115E+11	1.85852E+07	-0.67
7000	1.09423E+12	1.09399E+12	1.42264E+08	-1.71
10000	9.30746E+12	9.30871E+12	1.04034E+09	1.2
20000	5.95979E+14	5.95995E+14	7.88993E+10	0.2

A.2.2 Quartic couplings in two Z and two W boson cross sections

$W^+W^- \rightarrow ZZ$ $\text{Abs}(\cos(\theta)) < 0.95$ anomalous coupling $a_{4,6} = 0.1$				
$\sqrt{s}[\text{GeV}]$	$\sigma_{an}(s)[fb]$	$\sigma_{num}(s)[fb]$	Error[fb]	Pull
200	2.60619E+05	2.60650E+05	2.03633E+01	1.52
300	2.19684E+05	2.19622E+05	4.75063E+01	-1.3
400	1.99585E+05	1.99622E+05	4.50490E+01	0.811
500	1.93794E+05	1.93782E+05	4.03087E+01	-0.296
700	3.51755E+05	3.51993E+05	8.92007E+01	2.66
1000	2.10743E+06	2.10801E+06	3.00890E+02	1.93
2000	1.34318E+08	1.34341E+08	1.27899E+04	1.77
5000	3.32738E+10	3.32690E+10	4.79322E+06	-1.01
7000	2.50925E+11	2.50981E+11	2.68852E+07	2.07
10000	2.13461E+12	2.13434E+12	2.58236E+08	-1.03
20000	1.36698E+14	1.36727E+14	1.49072E+10	1.91

$W^+W^- \rightarrow ZZ$
 $\text{Abs}(\cos(\theta)) < 0.99$
anomalous coupling $a_{4,6} = 0.1$

$\sqrt{s}[\text{GeV}]$	$\sigma_{an}(s)[fb]$	$\sigma_{num}(s)[fb]$	Error[fb]	Pull
200	2.77109E+05	2.77103E+05	1.74448E+01	-0.353
300	2.68649E+05	2.68553E+05	4.69132E+01	-2.05
400	2.79984E+05	2.79977E+05	5.55498E+01	-0.132
500	3.00109E+05	3.00052E+05	6.44204E+01	-0.883
700	5.03996E+05	5.04022E+05	1.08155E+02	0.24
1000	2.43931E+06	2.43938E+06	1.70539E+02	0.391
2000	1.46691E+08	1.46703E+08	7.42455E+03	1.66
5000	3.62691E+10	3.62770E+10	2.21664E+06	3.56
7000	2.73497E+11	2.73509E+11	1.79812E+07	0.678
10000	2.32658E+12	2.32667E+12	1.49902E+08	0.573
20000	1.48990E+14	1.48987E+14	9.79196E+09	-0.294

$W^+W^- \rightarrow ZZ$
 $\text{Abs}(\cos(\theta)) < 0.95$
anomalous coupling $a_{5,7} = 0.1$

$\sqrt{s}[\text{GeV}]$	$\sigma_{an}(s)[fb]$	$\sigma_{num}(s)[fb]$	Error[fb]	Pull
200	2.54398E+05	2.54327E+05	2.19848E+01	-3.23
300	2.28741E+05	2.28679E+05	4.94370E+01	-1.25
400	2.59910E+05	2.59949E+05	4.92220E+01	0.783
500	4.28833E+05	4.28775E+05	5.31947E+01	-1.1
700	2.19914E+06	2.19934E+06	1.85551E+02	1.1
1000	1.84539E+07	1.84523E+07	1.16632E+03	-1.39
2000	1.22131E+09	1.22131E+09	7.32080E+04	0.0309
5000	3.01919E+11	3.01930E+11	2.30124E+07	0.47
7000	2.27608E+12	2.27606E+12	1.59153E+08	-0.129
10000	1.93589E+13	1.93591E+13	1.50879E+09	0.148
20000	1.23955E+15	1.23945E+15	9.60414E+10	-1.09

$W^+W^- \rightarrow ZZ$
 $\text{Abs}(\cos(\theta)) < 0.99$
anomalous coupling $a_{5,7} = 0.1$

$\sqrt{s}[\text{GeV}]$	$\sigma_{an}(s)[fb]$	$\sigma_{num}(s)[fb]$	Error[fb]	Pull
200	2.70580E+05	2.70588E+05	1.46857E+01	0.561
300	2.78123E+05	2.78275E+05	4.96453E+01	3.06
400	3.43580E+05	3.43471E+05	6.75681E+01	-1.61
500	5.46816E+05	5.46636E+05	9.44566E+01	-1.9
700	2.42946E+06	2.42941E+06	1.57453E+02	-0.303
1000	1.94110E+07	1.94108E+07	8.00063E+02	-0.221
2000	1.27319E+09	1.27329E+09	6.18908E+04	1.64
5000	3.14634E+11	3.14661E+11	1.70141E+07	1.58
7000	2.37192E+12	2.37193E+12	1.34593E+08	0.0677
10000	2.01740E+13	2.01750E+13	1.29446E+09	0.782
20000	1.29174E+15	1.29172E+15	7.89103E+10	-0.272

$ZZ \rightarrow W^+W^-$
 $\text{Abs}(\cos(\theta)) < 0.95$
anomalous coupling $a_{4,6} = 0.1$

$\sqrt{s}[\text{GeV}]$	$\sigma_{an}(s)[fb]$	$\sigma_{num}(s)[fb]$	Error[fb]	Pull
200	1.09302E+06	1.09320E+06	9.11545E+01	1.93
300	4.96611E+05	4.96609E+05	1.05439E+02	-0.0165
400	4.22451E+05	4.22613E+05	9.98219E+01	1.63
500	4.00808E+05	4.00682E+05	8.16789E+01	-1.54
700	7.14896E+05	7.14984E+05	1.85531E+02	0.475
1000	4.24708E+06	4.24663E+06	5.88878E+02	-0.766
2000	2.69137E+08	2.69249E+08	2.79247E+04	4.02
5000	6.65672E+10	6.65541E+10	9.78366E+06	-1.34
7000	5.01925E+11	5.02090E+11	5.64989E+07	2.92
10000	4.26954E+12	4.27048E+12	5.30018E+08	1.78
20000	2.73402E+14	2.73447E+14	3.04043E+10	1.49

$ZZ \rightarrow W^+W^-$
 $\text{Abs}(\cos(\theta)) < 0.99$
anomalous coupling $a_{4,6} = 0.1$

$\sqrt{s}[\text{GeV}]$	$\sigma_{an}(s)[fb]$	$\sigma_{num}(s)[fb]$	Error[fb]	Pull
200	1.16218E+06	1.16234E+06	7.62163E+01	2.05
300	6.07301E+05	6.07425E+05	1.09198E+02	1.13
400	5.92629E+05	5.92644E+05	1.21980E+02	0.124
500	6.20690E+05	6.20570E+05	1.39459E+02	-0.858
700	1.02431E+06	1.02461E+06	2.19631E+02	1.37
1000	4.91593E+06	4.91481E+06	3.27809E+02	-3.41
2000	2.93929E+08	2.93907E+08	1.46766E+04	-1.52
5000	7.25596E+10	7.25599E+10	4.45392E+06	0.0751
7000	5.47078E+11	5.47133E+11	3.50375E+07	1.57
10000	4.65351E+12	4.65387E+12	2.84826E+08	1.26
20000	2.97985E+14	2.98012E+14	1.96371E+10	1.36

$ZZ \rightarrow W^+W^-$
 $\text{Abs}(\cos(\theta)) < 0.95$
anomalous coupling $a_{5,7} = 0.1$

$\sqrt{s}[\text{GeV}]$	$\sigma_{an}(s)[fb]$	$\sigma_{num}(s)[fb]$	Error[fb]	Pull
200	1.06693E+06	1.06691E+06	9.01924E+01	-0.27
300	5.17085E+05	5.17026E+05	1.06958E+02	-0.548
400	5.50140E+05	5.50076E+05	1.08027E+02	-0.59
500	8.86919E+05	8.86867E+05	1.07666E+02	-0.483
700	4.46947E+06	4.46917E+06	3.67532E+02	-0.809
1000	3.71900E+07	3.71964E+07	2.34924E+03	2.72
2000	2.44717E+09	2.44740E+09	1.47852E+05	1.59
5000	6.04016E+11	6.03919E+11	4.84267E+07	-2
7000	4.55284E+12	4.55318E+12	3.16886E+08	1.08
10000	3.87207E+13	3.87243E+13	3.00257E+09	1.21
20000	2.47915E+15	2.47923E+15	1.91959E+11	0.417

$ZZ \rightarrow W^+W^-$ $\text{Abs}(\cos(\theta)) < 0.99$ anomalous coupling $a_{5,7} = 0.1$				
$\sqrt{s}[\text{GeV}]$	$\sigma_{an}(s)[fb]$	$\sigma_{num}(s)[fb]$	Error[fb]	Pull
200	1.13479E+06	1.13485E+06	7.38127E+01	0.846
300	6.28717E+05	6.28523E+05	1.09029E+02	-1.78
400	7.27239E+05	7.27152E+05	1.36572E+02	-0.64
500	1.13093E+06	1.13105E+06	1.91920E+02	0.65
700	4.93756E+06	4.93715E+06	3.21030E+02	-1.27
1000	3.91188E+07	3.91194E+07	1.64128E+03	0.394
2000	2.55113E+09	2.55131E+09	1.24840E+05	1.41
5000	6.29454E+11	6.29459E+11	3.42011E+07	0.145
7000	4.74455E+12	4.74434E+12	2.70312E+08	-0.764
10000	4.03510E+13	4.03486E+13	2.61732E+09	-0.928
20000	2.58354E+15	2.58390E+15	1.60235E+11	2.25

$W^-Z \rightarrow W^-Z$ $\text{Abs}(\cos(\theta)) < 0.95$ anomalous coupling $a_{4,6} = 0.1$				
$\sqrt{s}[\text{GeV}]$	$\sigma_{an}(s)[fb]$	$\sigma_{num}(s)[fb]$	Error[fb]	Pull
200	1.78772E+05	1.78792E+05	3.33947E+01	0.591
300	1.71797E+05	1.71844E+05	4.99982E+01	0.936
400	1.91784E+05	1.91872E+05	5.95092E+01	1.48
500	3.22655E+05	3.22607E+05	7.85003E+01	-0.607
700	1.86481E+06	1.86541E+06	2.65882E+02	2.26
1000	1.65901E+07	1.65925E+07	2.10714E+03	1.15
2000	1.11952E+09	1.11932E+09	1.32947E+05	-1.53
5000	2.77135E+11	2.77121E+11	3.92629E+07	-0.358
7000	2.08931E+12	2.08904E+12	2.62351E+08	-1.03
10000	1.77705E+13	1.77670E+13	2.36733E+09	-1.48
20000	1.13785E+15	1.13810E+15	1.53683E+11	1.66

$W^-Z \rightarrow W^-Z$ $\text{Abs}(\cos(\theta)) < 0.99$ anomalous coupling $a_{4,6} = 0.1$				
$\sqrt{s}[\text{GeV}]$	$\sigma_{an}(s)[fb]$	$\sigma_{num}(s)[fb]$	Error[fb]	Pull
200	1.93772E+05	1.93812E+05	3.52484E+01	1.13
300	2.16633E+05	2.16577E+05	4.37060E+01	-1.28
400	2.67176E+05	2.67181E+05	6.33949E+01	0.0789
500	4.26910E+05	4.26938E+05	9.47873E+01	0.294
700	2.07146E+06	2.07193E+06	2.62656E+02	1.8
1000	1.76007E+07	1.76038E+07	1.05809E+03	2.94
2000	1.18213E+09	1.18209E+09	7.36549E+04	-0.577
5000	2.92653E+11	2.92662E+11	2.00897E+07	0.458
7000	2.20629E+12	2.20652E+12	1.54161E+08	1.51
10000	1.87655E+13	1.87694E+13	1.34476E+09	2.88
20000	1.20156E+15	1.20158E+15	9.10300E+10	0.22

$W^- Z \rightarrow W^- Z$				
$\text{Abs}(\cos(\theta)) < 0.95$				
anomalous coupling $a_{5,7} = 0.1$				
$\sqrt{s}[\text{GeV}]$	$\sigma_{an}(s)[fb]$	$\sigma_{num}(s)[fb]$	Error[fb]	Pull
200	1.80969E+05	1.80955E+05	3.03538E+01	-0.465
300	1.68191E+05	1.68187E+05	5.13641E+01	-0.0691
400	1.63386E+05	1.63472E+05	5.64999E+01	1.52
500	1.99360E+05	1.99317E+05	5.87062E+01	-0.737
700	7.99995E+05	8.00019E+05	2.29624E+02	0.105
1000	6.78736E+06	6.79069E+06	1.44461E+03	2.31
2000	4.54411E+08	4.54361E+08	8.12172E+04	-0.621
5000	1.12093E+11	1.12108E+11	2.58778E+07	0.569
7000	8.44735E+11	8.44726E+11	1.62419E+08	-0.0534
10000	7.18335E+12	7.18373E+12	1.62386E+09	0.232
20000	4.59882E+14	4.59926E+14	9.92286E+10	0.445

$W^- Z \rightarrow W^- Z$				
$\text{Abs}(\cos(\theta)) < 0.99$				
anomalous coupling $a_{5,7} = 0.1$				
$\sqrt{s}[\text{GeV}]$	$\sigma_{an}(s)[fb]$	$\sigma_{num}(s)[fb]$	Error[fb]	Pull
200	1.96030E+05	1.95996E+05	3.25670E+01	-1.03
300	2.12429E+05	2.12454E+05	5.11108E+01	0.497
400	2.36185E+05	2.36230E+05	6.43185E+01	0.694
500	2.96327E+05	2.96273E+05	8.33144E+01	-0.653
700	9.69543E+05	9.69652E+05	2.21204E+02	0.492
1000	7.54665E+06	7.54918E+06	8.70959E+02	2.9
2000	5.02475E+08	5.02458E+08	5.76882E+04	-0.296
5000	1.24061E+11	1.24064E+11	1.55294E+07	0.193
7000	9.34968E+11	9.35196E+11	1.12358E+08	2.03
10000	7.95083E+12	7.95240E+12	9.73672E+08	1.61
20000	5.09023E+14	5.08849E+14	6.54218E+10	-2.65

A.2.3 Quartic couplings in four Z -boson cross section

$ZZ \rightarrow ZZ$				
$\text{Abs}(\cos(\theta)) < 0.95$				
anomalous coupling $a_{4,5} = 0.1$				
$\sqrt{s}[\text{GeV}]$	$\sigma_{an}(s)[fb]$	$\sigma_{num}(s)[fb]$	Error[fb]	Pull
200	3.14426E+04	3.14486E+04	4.47162E+00	1.35
300	2.81248E+04	2.81232E+04	5.21215E+00	-0.311
400	1.34163E+05	1.34201E+05	2.16344E+01	1.73
500	5.94156E+05	5.94555E+05	1.13028E+02	3.53
700	5.27596E+06	5.27573E+06	9.06492E+02	-0.255
1000	4.89795E+07	4.90007E+07	8.81887E+03	2.4
2000	3.33275E+09	3.33315E+09	5.37456E+05	0.75
5000	8.27318E+11	8.27110E+11	1.50530E+08	-1.38
7000	6.23892E+12	6.24116E+12	1.16702E+09	1.92
10000	5.30733E+13	5.30682E+13	9.69145E+09	-0.528
20000	3.39869E+15	3.39856E+15	6.26552E+11	-0.2

$ZZ \rightarrow ZZ$				
$\text{Abs}(\cos(\theta)) < 0.99$				
anomalous coupling $a_{4,5} = 0.1$				
$\sqrt{s}[\text{GeV}]$	$\sigma_{an}(s)[fb]$	$\sigma_{num}(s)[fb]$	Error[fb]	Pull
200	3.28095E+04	3.28107E+04	4.75283E+00	0.261
300	3.01176E+04	3.01209E+04	5.14181E+00	0.642
400	1.43711E+05	1.43719E+05	2.33653E+01	0.339
500	6.33186E+05	6.33198E+05	8.04759E+01	0.149
700	5.60208E+06	5.60159E+06	8.79301E+02	-0.552
1000	5.19408E+07	5.19484E+07	5.10405E+03	1.49
2000	3.53206E+09	3.53228E+09	5.21962E+05	0.416
5000	8.76672E+11	8.76686E+11	1.09897E+08	0.131
7000	6.61102E+12	6.61029E+12	1.09409E+09	-0.671
10000	5.62383E+13	5.62368E+13	9.05954E+09	-0.165
20000	3.60135E+15	3.60174E+15	5.00981E+11	0.78

$ZZ \rightarrow ZZ$				
$\text{Abs}(\cos(\theta)) < 0.95$				
anomalous coupling $a_{6,7,10} = 0.1$				
$\sqrt{s}[\text{GeV}]$	$\sigma_{an}(s)[fb]$	$\sigma_{num}(s)[fb]$	Error[fb]	Pull
200	4.73265E+04	4.73274E+04	6.73939E+00	0.136
300	8.87616E+04	8.87385E+04	1.70575E+01	-1.36
400	5.42351E+05	5.42322E+05	9.34373E+01	-0.315
500	2.41541E+06	2.41548E+06	4.31437E+02	0.154
700	2.12309E+07	2.12279E+07	4.02582E+03	-0.749
1000	1.96237E+08	1.96194E+08	3.58263E+04	-1.19
2000	1.33325E+10	1.33354E+10	2.36512E+06	1.22
5000	3.30928E+12	3.30906E+12	5.94784E+08	-0.37
7000	2.49557E+13	2.49635E+13	4.58591E+09	1.69
10000	2.12293E+14	2.12254E+14	3.95893E+10	-0.985
20000	1.35948E+16	1.35928E+16	2.19993E+12	-0.93

$ZZ \rightarrow ZZ$				
$\text{Abs}(\cos(\theta)) < 0.99$				
anomalous coupling $a_{6,7,10} = 0.1$				
$\sqrt{s}[\text{GeV}]$	$\sigma_{an}(s)[fb]$	$\sigma_{num}(s)[fb]$	Error[fb]	Pull
200	4.93905E+04	4.93829E+04	6.76094E+00	-1.13
300	9.48090E+04	9.48185E+04	1.40032E+01	0.678
400	5.78660E+05	5.78694E+05	7.94701E+01	0.431
500	2.56955E+06	2.56940E+06	3.93156E+02	-0.37
700	2.25340E+07	2.25327E+07	3.86773E+03	-0.324
1000	2.08085E+08	2.08037E+08	3.05230E+04	-1.58
2000	1.41298E+10	1.41318E+10	1.57227E+06	1.27
5000	3.50670E+12	3.50644E+12	4.37951E+08	-0.598
7000	2.64441E+13	2.64457E+13	4.09448E+09	0.384
10000	2.24953E+14	2.24970E+14	3.12907E+10	0.538
20000	1.44054E+16	1.44042E+16	1.89207E+12	-0.628

A.2.4 Triple gauge boson couplings

$W^-W^- \rightarrow W^-W^-$				
$\text{Abs}(\cos(\theta)) < 0.95$				
anomalous coupling $g_a^1 = 0.1$				
$\sqrt{s}[\text{GeV}]$	$\sigma_{an}(s)[fb]$	$\sigma_{num}(s)[fb]$	Error[fb]	Pull
200	2.16235E+06	2.16372E+06	1.11615E+03	1.23
300	6.73036E+05	6.73333E+05	3.24701E+02	0.914
400	4.51239E+05	4.51782E+05	2.43010E+02	2.24
500	3.37467E+05	3.37436E+05	1.77525E+02	-0.174
700	2.12321E+05	2.12223E+05	1.01854E+02	-0.959
1000	1.25367E+05	1.25328E+05	6.73464E+01	-0.581
2000	5.79336E+04	5.79405E+04	3.08389E+01	0.223
5000	1.43379E+05	1.43411E+05	3.14824E+01	1.02
7000	2.70094E+05	2.70045E+05	4.23747E+01	-1.15
10000	5.43687E+05	5.43538E+05	6.88444E+01	-2.16
20000	2.15984E+06	2.16083E+06	2.57679E+02	-3.84

$W^-W^- \rightarrow W^-W^-$				
$\text{Abs}(\cos(\theta)) < 0.99$				
anomalous coupling $g_A^1 = 0.1$				
$\sqrt{s}[\text{GeV}]$	$\sigma_{an}(s)[fb]$	$\sigma_{num}(s)[fb]$	Error[fb]	Pull
200	8.53189E+06	8.52194E+06	7.98511E+03	-1.25
300	2.00511E+06	2.00729E+06	1.25497E+03	1.74
400	1.21994E+06	1.21977E+06	8.90734E+02	-0.186
500	9.00587E+05	9.00271E+05	5.74286E+02	-0.549
700	6.00049E+05	6.00291E+05	4.19185E+02	0.577
1000	3.93775E+05	3.93158E+05	2.97631E+02	-2.07
2000	1.68663E+05	1.68939E+05	1.54687E+02	1.79
5000	1.72514E+05	1.72664E+05	7.63563E+01	1.96
7000	2.94621E+05	2.94475E+05	6.00694E+01	-2.43
10000	5.74742E+05	5.74748E+05	4.76294E+01	0.116
20000	2.25949E+06	2.25925E+06	1.91345E+02	-1.26

$W^-W^- \rightarrow W^-W^-$				
$\text{Abs}(\cos(\theta)) < 0.95$				
anomalous coupling $g_Z^1 = 0.1$				
$\sqrt{s}[\text{GeV}]$	$\sigma_{an}(s)[fb]$	$\sigma_{num}(s)[fb]$	Error[fb]	Pull
200	1.84748E+06	1.84721E+06	8.79086E+02	-0.302
300	6.96872E+05	6.96935E+05	2.95663E+02	0.212
400	5.07768E+05	5.08170E+05	2.36694E+02	1.7
500	4.02509E+05	4.02634E+05	1.90455E+02	0.658
700	2.84447E+05	2.84334E+05	1.46862E+02	-0.766
1000	2.16667E+05	2.16594E+05	9.78243E+01	-0.748
2000	3.16042E+05	3.16072E+05	9.66924E+01	0.309
5000	1.66935E+06	1.66967E+06	2.44724E+02	1.32
7000	3.25112E+06	3.25126E+06	4.50713E+02	0.322
10000	6.61765E+06	6.61759E+06	8.13145E+02	-0.0704
20000	2.64290E+07	2.64363E+07	3.12196E+03	2.34

$W^-W^- \rightarrow W^-W^-$				
$\text{Abs}(\cos(\theta)) < 0.99$				
anomalous coupling $g_Z^1 = 0.1$				
$\sqrt{s}[\text{GeV}]$	$\sigma_{an}(s)[fb]$	$\sigma_{num}(s)[fb]$	Error[fb]	Pull
200	6.35841E+06	6.36165E+06	5.03605E+03	0.644
300	1.73042E+06	1.72733E+06	1.19087E+03	-2.6
400	1.16043E+06	1.16027E+06	7.11017E+02	-0.221
500	9.18349E+05	9.18171E+05	4.79615E+02	-0.372
700	6.79697E+05	6.79995E+05	4.18870E+02	0.713
1000	5.16375E+05	5.16326E+05	3.06564E+02	-0.16
2000	4.62284E+05	4.62327E+05	2.47719E+02	0.173
5000	1.77565E+06	1.77572E+06	2.10262E+02	0.351
7000	3.41540E+06	3.41606E+06	3.10296E+02	2.14
10000	6.92492E+06	6.92541E+06	5.20918E+02	0.943
20000	2.76143E+07	2.76204E+07	2.28853E+03	2.68

$W^-W^- \rightarrow W^-W^-$				
$\text{Abs}(\cos(\theta)) < 0.95$				
anomalous coupling $\kappa_A = 0.1$				
$\sqrt{s}[\text{GeV}]$	$\sigma_{an}(s)[fb]$	$\sigma_{num}(s)[fb]$	Error[fb]	Pull
200	1.60485E+06	1.60321E+06	7.95336E+02	-2.06
300	5.73691E+05	5.73452E+05	2.50624E+02	-0.954
400	4.58639E+05	4.58488E+05	2.14512E+02	-0.702
500	5.07930E+05	5.08341E+05	2.19189E+02	1.87
700	1.52282E+06	1.52276E+06	3.04112E+02	-0.208
1000	1.08484E+07	1.08504E+07	9.57779E+02	2.07
2000	6.80161E+08	6.80202E+08	5.24700E+04	0.789
5000	1.66404E+11	1.66412E+11	1.51645E+07	0.496
7000	1.25335E+12	1.25324E+12	1.09754E+08	-0.968
10000	1.06552E+13	1.06559E+13	9.09751E+08	0.723
20000	6.82021E+14	6.82023E+14	5.75695E+10	0.027

$W^-W^- \rightarrow W^-W^-$				
$\text{Abs}(\cos(\theta)) < 0.99$				
anomalous coupling $\kappa_A = 0.1$				
$\sqrt{s}[\text{GeV}]$	$\sigma_{an}(s)[fb]$	$\sigma_{num}(s)[fb]$	Error[fb]	Pull
200	6.01376E+06	6.01289E+06	5.82237E+03	-0.15
300	1.53515E+06	1.53417E+06	1.10531E+03	-0.888
400	1.04295E+06	1.04214E+06	6.35897E+02	-1.28
500	9.62626E+05	9.62915E+05	4.60629E+02	0.626
700	1.90140E+06	1.90022E+06	5.78425E+02	-2.05
1000	1.14063E+07	1.14062E+07	7.72741E+02	-0.0671
2000	6.97060E+08	6.96998E+08	4.15954E+04	-1.5
5000	1.70442E+11	1.70447E+11	1.10897E+07	0.476
7000	1.28375E+12	1.28391E+12	8.59368E+07	1.87
10000	1.09137E+13	1.09139E+13	7.05339E+08	0.285
20000	6.98568E+14	6.98538E+14	4.83024E+10	-0.625

$W^-W^- \rightarrow W^-W^-$ $\text{Abs}(\cos(\theta)) < 0.95$ anomalous coupling $\kappa_Z = 0.1$				
$\sqrt{s}[\text{GeV}]$	$\sigma_{an}(s)[fb]$	$\sigma_{num}(s)[fb]$	Error[fb]	Pull
200	1.59137E+06	1.59089E+06	8.25984E+02	-0.582
300	6.37274E+05	6.37695E+05	2.31702E+02	1.82
400	8.62617E+05	8.61751E+05	3.13853E+02	-2.76
500	2.11113E+06	2.11091E+06	3.70907E+02	-0.601
700	1.43175E+07	1.43174E+07	1.26058E+03	-0.0644
1000	1.24541E+08	1.24542E+08	9.90657E+03	0.0886
2000	8.24291E+09	8.24359E+09	6.40365E+05	1.06
5000	2.03475E+12	2.03456E+12	1.86111E+08	-1.05
7000	1.53370E+13	1.53366E+13	1.32087E+09	-0.299
10000	1.30436E+14	1.30411E+14	1.15067E+10	-2.21
20000	8.35131E+15	8.35262E+15	7.19401E+11	1.82

$W^-W^- \rightarrow W^-W^-$ $\text{Abs}(\cos(\theta)) < 0.99$ anomalous coupling $\kappa_Z = 0.1$				
$\sqrt{s}[\text{GeV}]$	$\sigma_{an}(s)[fb]$	$\sigma_{num}(s)[fb]$	Error[fb]	Pull
200	5.99011E+06	5.99360E+06	4.90997E+03	0.71
300	1.59584E+06	1.59558E+06	1.13257E+03	-0.233
400	1.46234E+06	1.46215E+06	6.66445E+02	-0.288
500	2.62311E+06	2.62149E+06	5.52854E+02	-2.94
700	1.50564E+07	1.50577E+07	1.20776E+03	1.06
1000	1.27956E+08	1.27963E+08	7.10477E+03	1
2000	8.44310E+09	8.44341E+09	5.03990E+05	0.614
5000	2.08409E+12	2.08397E+12	1.34586E+08	-0.915
7000	1.57090E+13	1.57104E+13	1.04705E+09	1.35
10000	1.33600E+14	1.33594E+14	8.52143E+09	-0.71
20000	8.55392E+15	8.55448E+15	5.87719E+11	0.947

$W^-W^- \rightarrow W^-W^-$ $\text{Abs}(\cos(\theta)) < 0.95$ anomalous coupling $\kappa_Z^5 = 0.1$				
$\sqrt{s}[\text{GeV}]$	$\sigma_{an}(s)[fb]$	$\sigma_{num}(s)[fb]$	Error[fb]	Pull
200	1.61407E+06	1.61276E+06	8.04783E+02	-1.63
300	5.50539E+05	5.50805E+05	2.22597E+02	1.2
400	3.86017E+05	3.86509E+05	1.96283E+02	2.51
500	2.98998E+05	2.98756E+05	1.45009E+02	-1.67
700	2.05278E+05	2.05095E+05	1.03314E+02	-1.77
1000	1.53356E+05	1.53301E+05	6.93291E+01	-0.79
2000	2.30322E+05	2.30415E+05	6.69545E+01	1.39
5000	1.26119E+06	1.26122E+06	1.87693E+02	0.151
7000	2.46529E+06	2.46575E+06	3.48122E+02	1.32
10000	5.02789E+06	5.02759E+06	6.09257E+02	-0.497
20000	2.01078E+07	2.01097E+07	2.37860E+03	0.814

$W^-W^- \rightarrow W^-W^-$ $\text{Abs}(\cos(\theta)) < 0.99$ anomalous coupling $\kappa_Z^5 = 0.1$				
$\sqrt{s}[\text{GeV}]$	$\sigma_{an}(s)[fb]$	$\sigma_{num}(s)[fb]$	Error[fb]	Pull
200	6.02559E+06	6.02979E+06	5.21919E+03	0.805
300	1.50663E+06	1.50569E+06	1.04620E+03	-0.9
400	9.58748E+05	9.58735E+05	6.40320E+02	-0.0203
500	7.32638E+05	7.32464E+05	4.40825E+02	-0.395
700	5.18830E+05	5.19116E+05	3.39872E+02	0.842
1000	3.80385E+05	3.80503E+05	2.39763E+02	0.491
2000	3.35222E+05	3.34917E+05	1.78809E+02	-1.71
5000	1.33827E+06	1.33810E+06	1.52074E+02	-1.13
7000	2.58749E+06	2.58806E+06	2.29060E+02	2.5
10000	5.26037E+06	5.26049E+06	3.92004E+02	0.3
20000	2.10154E+07	2.10194E+07	1.75694E+03	2.28

$W^-W^- \rightarrow W^-W^-$ $\text{Abs}(\cos(\theta)) < 0.95$ anomalous coupling $\lambda_A = 0.1$				
$\sqrt{s}[\text{GeV}]$	$\sigma_{an}(s)[fb]$	$\sigma_{num}(s)[fb]$	Error[fb]	Pull
200	1.65100E+06	1.65136E+06	8.45988E+02	0.42
300	5.72377E+05	5.72423E+05	2.71192E+02	0.168
400	4.24966E+05	4.25408E+05	2.07335E+02	2.13
500	4.00879E+05	4.01004E+05	1.57079E+02	0.795
700	8.71435E+05	8.71443E+05	2.66841E+02	0.0294
1000	5.76370E+06	5.76555E+06	6.93554E+02	2.67
2000	3.63120E+08	3.63135E+08	3.63452E+04	0.415
5000	8.89900E+10	8.89957E+10	1.09639E+07	0.518
7000	6.70303E+11	6.70450E+11	8.09957E+07	1.81
10000	5.69900E+12	5.69867E+12	6.26855E+08	-0.529
20000	3.64800E+14	3.64804E+14	3.74107E+10	0.109

$W^-W^- \rightarrow W^-W^-$ $\text{Abs}(\cos(\theta)) < 0.99$ anomalous coupling $\lambda_A = 0.1$				
$\sqrt{s}[\text{GeV}]$	$\sigma_{an}(s)[fb]$	$\sigma_{num}(s)[fb]$	Error[fb]	Pull
200	6.07510E+06	6.07273E+06	5.65093E+03	-0.419
300	1.53610E+06	1.53660E+06	1.06600E+03	0.468
400	1.00640E+06	1.00696E+06	6.36247E+02	0.886
500	8.46910E+05	8.47752E+05	4.26390E+02	1.97
700	1.22260E+06	1.22320E+06	4.83214E+02	1.25
1000	6.22600E+06	6.22557E+06	5.63427E+02	-0.77
2000	3.77410E+08	3.77417E+08	2.43615E+04	0.297
5000	9.24700E+10	9.24790E+10	6.46959E+06	1.4
7000	6.96600E+11	6.96446E+11	5.03788E+07	-3.05
10000	5.92200E+12	5.92305E+12	4.04126E+08	2.61
20000	3.79100E+14	3.79095E+14	2.83168E+10	-0.188

$W^-W^- \rightarrow W^-W^-$
 $\text{Abs}(\cos(\theta)) < 0.95$
anomalous coupling $\lambda_Z = 0.1$

$\sqrt{s}[\text{GeV}]$	$\sigma_{an}(s)[fb]$	$\sigma_{num}(s)[fb]$	Error[fb]	Pull
200	1.67522E+06	1.67575E+06	7.72556E+02	0.685
300	6.44261E+05	6.44493E+05	2.69177E+02	0.861
400	6.80966E+05	6.81019E+05	2.77708E+02	0.19
500	1.30505E+06	1.30511E+06	3.52486E+02	0.167
700	7.79874E+06	7.79751E+06	9.51792E+02	-1.3
1000	6.68348E+07	6.68293E+07	6.76410E+03	-0.806
2000	4.41222E+09	4.41159E+09	4.38964E+05	-1.44
5000	1.08845E+12	1.08884E+12	1.34500E+08	2.91
7000	8.20367E+12	8.20522E+12	9.76274E+08	1.59
10000	6.97670E+13	6.97886E+13	7.58195E+09	2.85
20000	4.46680E+15	4.46757E+15	4.66149E+11	1.66

$W^-W^- \rightarrow W^-W^-$
 $\text{Abs}(\cos(\theta)) < 0.99$
anomalous coupling $\lambda_Z = 0.1$

$\sqrt{s}[\text{GeV}]$	$\sigma_{an}(s)[fb]$	$\sigma_{num}(s)[fb]$	Error[fb]	Pull
200	6.10739E+06	6.10713E+06	5.14714E+03	-0.0506
300	1.62272E+06	1.62206E+06	1.12152E+03	-0.587
400	1.28641E+06	1.28575E+06	6.46854E+02	-1.02
500	1.80189E+06	1.80049E+06	5.31092E+02	-2.64
700	8.43527E+06	8.43409E+06	9.63168E+02	-1.23
1000	6.96746E+07	6.96774E+07	4.04596E+03	0.694
2000	4.58432E+09	4.58414E+09	2.91534E+05	-0.605
5000	1.13110E+12	1.13098E+12	7.95289E+07	-1.52
7000	8.52534E+12	8.52601E+12	6.19666E+08	1.08
10000	7.25035E+13	7.25057E+13	4.82382E+09	0.449
20000	4.64205E+15	4.64218E+15	3.47180E+11	0.369

$W^+W^- \rightarrow W^+W^-$
 $\text{Abs}(\cos(\theta)) < 0.95$
anomalous coupling $g_1^A = 0.1$

$\sqrt{s}[\text{GeV}]$	$\sigma_{an}(s)[fb]$	$\sigma_{num}(s)[fb]$	Error[fb]	Pull
200	2.07759E+06	2.07613E+06	8.29874E+02	-1.76
300	6.07501E+05	6.07677E+05	2.43695E+02	0.721
400	3.93426E+05	3.93518E+05	1.49667E+02	0.616
500	2.90627E+05	2.90553E+05	1.21716E+02	-0.605
700	1.81686E+05	1.81668E+05	1.04314E+02	-0.174
1000	1.07482E+05	1.07464E+05	5.85553E+01	-0.315
2000	5.28299E+04	5.28311E+04	2.85578E+01	0.0414
5000	1.47997E+05	1.47976E+05	2.62666E+01	-0.795
7000	2.81668E+05	2.81716E+05	3.97224E+01	1.21
10000	5.69413E+05	5.69515E+05	7.67442E+01	1.33
20000	2.26842E+06	2.26863E+06	3.36535E+02	0.619

$W^+W^- \rightarrow W^+W^-$
 $\text{Abs}(\cos(\theta)) < 0.99$
anomalous coupling $g_A^1 = 1.1$

$\sqrt{s}[\text{GeV}]$	$\sigma_{an}(s)[fb]$	$\sigma_{num}(s)[fb]$	Error[fb]	Pull
200	8.42620E+06	8.42050E+06	5.06336E+03	-1.13
300	1.93820E+06	1.93644E+06	1.59020E+03	-1.11
400	1.15872E+06	1.15862E+06	8.35465E+02	-0.125
500	8.49406E+05	8.48557E+05	5.67632E+02	-1.5
700	5.64709E+05	5.64917E+05	4.09982E+02	0.508
1000	3.71800E+05	3.72215E+05	2.80845E+02	1.48
2000	1.61815E+05	1.61914E+05	1.36730E+02	0.728
5000	1.78535E+05	1.78363E+05	7.03500E+01	-2.45
7000	3.09608E+05	3.09686E+05	6.23929E+01	1.25
10000	6.07844E+05	6.07835E+05	6.27841E+01	-0.142
20000	2.39684E+06	2.39758E+06	2.43755E+02	-3.036

$W^+W^- \rightarrow W^+W^-$
 $\text{Abs}(\cos(\theta)) < 0.95$
anomalous coupling $g_1^Z = 1.1$

$\sqrt{s}[\text{GeV}]$	$\sigma_{an}(s)[fb]$	$\sigma_{num}(s)[fb]$	Error[fb]	Pull
200	1.74242E+06	1.74353E+06	7.58156E+02	1.47
300	6.16453E+05	6.16102E+05	2.53656E+02	-1.39
400	4.38948E+05	4.38626E+05	1.99300E+02	-1.62
500	3.47295E+05	3.47221E+05	1.59283E+02	-0.463
700	2.48886E+05	2.48930E+05	8.75848E+01	0.498
1000	1.97289E+05	1.97252E+05	8.77055E+01	-0.421
2000	3.20325E+05	3.20467E+05	9.18647E+01	-1.55
5000	1.74848E+06	1.74881E+06	2.40154E+02	1.37
7000	3.41109E+06	3.41125E+06	4.65948E+02	0.336
10000	6.94868E+06	6.95040E+06	1.08127E+03	1.59
20000	2.77663E+07	2.77667E+07	3.98778E+03	0.11

$W^+W^- \rightarrow W^+W^-$
 $\text{Abs}(\cos(\theta)) < 0.99$
anomalous coupling $g_Z^1 = 1.1$

$\sqrt{s}[\text{GeV}]$	$\sigma_{an}(s)[fb]$	$\sigma_{num}(s)[fb]$	Error[fb]	Pull
200	6.22792E+06	6.22985E+06	4.14091E+03	0.466
300	1.64554E+06	1.64464E+06	1.17641E+03	-0.767
400	1.08625E+06	1.08782E+06	6.31909E+02	2.49
500	8.57395E+05	8.57140E+05	4.88949E+02	-0.522
700	6.38684E+05	6.38347E+05	3.89390E+02	-0.866
1000	4.92911E+05	4.93429E+05	3.11255E+02	1.67
2000	4.67795E+05	4.67670E+05	2.01481E+02	-0.622
5000	1.87726E+06	1.87749E+06	2.48984E+02	0.905
7000	3.62032E+06	3.61992E+06	3.55733E+02	-1.11
10000	7.34831E+06	7.34769E+06	5.81193E+02	-1.07
20000	2.93196E+07	2.93270E+07	2.88130E+03	2.57

$W^+W^- \rightarrow W^+W^-$ $\text{Abs}(\cos(\theta)) < 0.95$ anomalous coupling $\kappa_A = 0.1$				
$\sqrt{s}[\text{GeV}]$	$\sigma_{an}(s)[fb]$	$\sigma_{num}(s)[fb]$	Error[fb]	Pull
200	1.53467E+06	1.53482E+06	6.52422E+02	0.225
300	4.83514E+05	4.83419E+05	1.80170E+02	-0.529
400	3.57900E+05	3.57773E+05	1.79089E+02	-0.707
500	4.15610E+05	4.15599E+05	1.62759E+02	-0.0678
700	1.62739E+06	1.62730E+06	3.26122E+02	-0.282
1000	1.30600E+07	1.30596E+07	2.56978E+03	-0.168
2000	8.41085E+08	8.40783E+08	1.98875E+05	-1.52
5000	2.05743E+11	2.05704E+11	4.56419E+07	-0.848
7000	1.54938E+12	1.54915E+12	2.93898E+08	-0.772
10000	1.31706E+13	1.31644E+13	3.09635E+09	-2
20000	8.42961E+14	8.43096E+14	2.12690E+11	0.634

$W^+W^- \rightarrow W^+W^-$ $\text{Abs}(\cos(\theta)) < 0.99$ anomalous coupling $\kappa_A = 1.1$				
$\sqrt{s}[\text{GeV}]$	$\sigma_{an}(s)[fb]$	$\sigma_{num}(s)[fb]$	Error[fb]	Pull
200	5.92750E+06	5.92659E+06	3.83818E+03	-0.238
300	1.43418E+06	1.43282E+06	1.08503E+03	-1.25
400	9.21565E+05	9.21611E+05	5.33712E+02	0.0864
500	8.44024E+05	8.44047E+05	4.16810E+02	0.0561
700	2.02460E+06	2.02459E+06	5.77163E+02	-0.0101
1000	1.43079E+07	1.43093E+07	1.60894E+03	0.863
2000	9.14231E+08	9.14311E+08	1.10409E+05	0.723
5000	2.23862E+11	2.23825E+11	3.01139E+07	-1.24
7000	1.68597E+12	1.68543E+12	2.36408E+08	-2.28
10000	1.43322E+13	1.43288E+13	1.83948E+09	-1.83
20000	9.17337E+14	9.17277E+14	1.47259E+11	-0.407

$W^+W^- \rightarrow W^+W^-$ $\text{Abs}(\cos(\theta)) < 0.95$ anomalous coupling $\kappa_Z = 1.1$				
$\sqrt{s}[\text{GeV}]$	$\sigma_{an}(s)[fb]$	$\sigma_{num}(s)[fb]$	Error[fb]	Pull
200	1.50323E+06	1.50302E+06	6.63739E+02	-0.312
300	5.18405E+05	5.18337E+05	2.23450E+02	-0.304
400	8.37784E+05	8.37829E+05	2.84803E+02	0.159
500	2.50728E+06	2.50831E+06	5.77739E+02	1.78
700	1.84278E+07	1.84304E+07	2.84248E+03	0.914
1000	1.58993E+08	1.58981E+08	3.41460E+04	-0.366
2000	1.02903E+10	1.02933E+10	2.45012E+06	1.22
5000	2.51907E+12	2.51939E+12	5.55672E+08	0.578
7000	1.89720E+13	1.89808E+13	3.75476E+09	2.34
10000	1.61280E+14	1.61278E+14	3.62691E+10	-0.0601
20000	1.03228E+16	1.03253E+16	2.58613E+12	0.981

$W^+W^- \rightarrow W^+W^-$ $\text{Abs}(\cos(\theta)) < 0.99$ anomalous coupling $\kappa_Z = 1.1$				
$\sqrt{s}[\text{GeV}]$	$\sigma_{an}(s)[fb]$	$\sigma_{num}(s)[fb]$	Error[fb]	Pull
200	5.87785E+06	5.87459E+06	3.83380E+03	-0.85
300	1.44602E+06	1.44574E+06	9.98810E+02	-0.279
400	1.40127E+06	1.40184E+06	7.13979E+02	0.799
500	3.05083E+06	3.05131E+06	7.01077E+02	0.687
700	2.01328E+07	2.01292E+07	2.12915E+03	-1.71
1000	1.72557E+08	1.72564E+08	1.68594E+04	0.397
2000	1.11901E+10	1.11921E+10	1.37289E+06	1.49
5000	2.74106E+12	2.74092E+12	3.72240E+08	-0.382
7000	2.06450E+13	2.06391E+13	2.90448E+09	-2.03
10000	1.75507E+14	1.75485E+14	2.35248E+10	-0.928
20000	1.12337E+16	1.12283E+16	1.81050E+12	-2.96

$W^+W^- \rightarrow W^+W^-$ $\text{Abs}(\cos(\theta)) < 0.95$ anomalous coupling $\kappa_5^A = 0.1$				
$\sqrt{s}[\text{GeV}]$	$\sigma_{an}(s)[fb]$	$\sigma_{num}(s)[fb]$	Error[fb]	Pull
200	1.54180E+06	1.54149E+06	6.66363E+02	-0.47
300	4.85882E+05	4.86083E+05	1.86547E+02	1.07
400	3.25808E+05	3.26001E+05	1.36987E+02	1.41
500	2.45242E+05	2.45278E+05	9.27697E+01	0.387
700	1.55965E+05	1.55929E+05	8.91646E+01	-0.406
1000	9.27124E+04	9.27453E+04	5.07625E+01	0.649
2000	4.40407E+04	4.40396E+04	2.31398E+01	-0.0468
5000	1.20227E+05	1.20218E+05	2.23018E+01	-0.391
7000	2.29353E+05	2.29390E+05	3.13785E+01	1.17
10000	4.64528E+05	4.64567E+05	7.08000E+01	0.556
20000	1.85390E+06	1.85333E+06	2.77964E+02	-2.06

$W^+W^- \rightarrow W^+W^-$ $\text{Abs}(\cos(\theta)) < 0.99$ anomalous coupling $\kappa_A^5 = 0.1$				
$\sqrt{s}[\text{GeV}]$	$\sigma_{an}(s)[fb]$	$\sigma_{num}(s)[fb]$	Error[fb]	Pull
200	5.93590E+06	5.94150E+06	3.84630E+03	1.46
300	1.44010E+06	1.43917E+06	1.13117E+03	-0.823
400	8.94985E+05	8.94743E+05	6.13601E+02	-0.394
500	6.74411E+05	6.73604E+05	4.56338E+02	-1.77
700	4.64214E+05	4.64275E+05	2.89410E+02	0.212
1000	3.13760E+05	3.13215E+05	2.22117E+02	-2.45
2000	1.38358E+05	1.38093E+05	1.30613E+02	-2.03
5000	1.45635E+05	1.45595E+05	5.79227E+01	-0.687
7000	2.51826E+05	2.51834E+05	5.09788E+01	0.154
10000	4.94992E+05	4.95114E+05	5.01190E+01	2.44
20000	1.95665E+06	1.95681E+06	1.92057E+02	-0.83

$W^+W^- \rightarrow W^+W^-$
 $\text{Abs}(\cos(\theta)) < 0.95$
anomalous coupling $\lambda_A = 0.1$

$\sqrt{s}[\text{GeV}]$	$\sigma_{an}(s)[fb]$	$\sigma_{num}(s)[fb]$	Error[fb]	Pull
200	1.56680E+06	1.56690E+06	6.91153E+02	0.147
300	5.12640E+05	5.12777E+05	2.15102E+02	0.638
400	3.85497E+05	3.85223E+05	1.83352E+02	-1.49
500	4.13199E+05	4.13375E+05	1.90561E+02	0.926
700	1.25960E+06	1.25948E+06	2.67122E+02	-0.442
1000	9.17430E+06	9.17310E+06	1.57631E+03	-0.759
2000	5.72030E+08	5.72274E+08	1.01723E+05	2.4
5000	1.39000E+11	1.39033E+11	2.07040E+07	1.58
7000	1.04600E+12	1.04603E+12	1.57640E+08	0.174
10000	8.89100E+12	8.89228E+12	1.47130E+09	0.867
20000	5.68900E+14	5.68562E+14	1.02024E+11	-3.31

$W^+W^- \rightarrow W^+W^-$
 $\text{Abs}(\cos(\theta)) < 0.99$
anomalous coupling $\lambda_A = 0.1$

$\sqrt{s}[\text{GeV}]$	$\sigma_{an}(s)[fb]$	$\sigma_{num}(s)[fb]$	Error[fb]	Pull
200	5.96750E+06	5.96505E+06	3.90530E+03	-0.627
300	1.47200E+06	1.47001E+06	1.13195E+03	-1.76
400	9.61563E+05	9.61217E+05	5.28077E+02	-0.655
500	8.55455E+05	8.56155E+05	4.68609E+02	1.49
700	1.64000E+06	1.63999E+06	4.71943E+02	-0.0171
1000	1.00090E+07	1.00073E+07	1.00098E+03	-1.72
2000	6.12980E+08	6.12941E+08	5.25387E+04	-0.736
5000	1.49100E+11	1.49105E+11	1.36182E+07	0.333
7000	1.12200E+12	1.12230E+12	1.04547E+08	2.91
10000	9.53700E+12	9.53674E+12	8.54259E+08	-0.307
20000	6.10300E+14	6.10326E+14	6.90722E+10	0.376

$W^+W^- \rightarrow W^+W^-$
 $\text{Abs}(\cos(\theta)) < 0.95$
anomalous coupling $\lambda_5^A = 0.1$

$\sqrt{s}[\text{GeV}]$	$\sigma_{an}(s)[fb]$	$\sigma_{num}(s)[fb]$	Error[fb]	Pull
200	1.54360E+06	1.54383E+06	6.77328E+02	0.341
300	5.14193E+05	5.13955E+05	1.97206E+02	-1.21
400	4.87128E+05	4.87256E+05	2.32364E+02	0.553
500	8.55308E+05	8.55551E+05	2.73771E+02	0.887
700	4.66020E+06	4.65927E+06	6.86630E+02	-1.36
1000	3.77300E+07	3.77289E+07	5.82593E+03	-0.195
2000	2.37010E+09	2.37014E+09	3.96465E+05	0.0984
5000	5.75600E+11	5.75468E+11	9.59682E+07	-1.38
7000	4.33200E+12	4.33181E+12	6.25360E+08	-0.308
10000	3.68100E+13	3.68121E+13	5.78385E+09	0.361
20000	2.35500E+15	2.35617E+15	3.68755E+11	3.18

$W^+W^- \rightarrow W^+W^-$
 $\text{Abs}(\cos(\theta)) < 0.99$
anomalous coupling $\lambda_A^5 = 0.1$

$\sqrt{s}[\text{GeV}]$	$\sigma_{an}(s)[fb]$	$\sigma_{num}(s)[fb]$	Error[fb]	Pull
200	5.93750E+06	5.93497E+06	3.86302E+03	-0.655
300	1.46810E+06	1.46855E+06	1.02204E+03	0.437
400	1.06070E+06	1.06065E+06	6.23521E+02	-0.0806
500	1.31170E+06	1.31208E+06	5.13365E+02	0.736
700	5.23650E+06	5.23740E+06	8.57017E+02	1.05
1000	4.04710E+07	4.04783E+07	3.18790E+03	2.28
2000	2.54010E+09	2.54038E+09	2.24510E+05	1.27
5000	6.17500E+11	6.17565E+11	6.10760E+07	1.06
7000	4.64800E+12	4.64755E+12	4.47085E+08	-1.01
10000	3.94900E+13	3.94947E+13	3.64168E+09	1.3
20000	2.52700E+15	2.52741E+15	2.85437E+11	1.42

$W^+W^- \rightarrow ZZ$
 $\text{Abs}(\cos(\theta)) < 0.99$
anomalous coupling $g_Z^1 = 1.1$

$\sqrt{s}[\text{GeV}]$	$\sigma_{an}(s)[fb]$	$\sigma_{num}(s)[fb]$	Error[fb]	Pull
200	3.08391E+05	3.08380E+05	1.85195E+01	-0.579
300	3.59810E+05	3.59793E+05	5.99073E+01	-0.278
400	6.10528E+05	6.10785E+05	8.35478E+01	3.08
500	1.45006E+06	1.45031E+06	1.20784E+02	2.07
700	9.16448E+06	9.16637E+06	4.42060E+02	4.27
1000	7.80132E+07	7.80189E+07	3.99787E+03	1.42
2000	5.11924E+09	5.11977E+09	2.96172E+05	1.78
5000	1.26114E+12	1.26114E+12	8.74562E+07	-0.0306
7000	9.50416E+12	9.50440E+12	7.03334E+08	0.343
10000	8.08219E+13	8.08335E+13	6.33822E+09	1.83
20000	5.17435E+15	5.17474E+15	4.61482E+11	0.852

$W^+W^- \rightarrow ZZ$
 $\text{Abs}(\cos(\theta)) < 0.99$
anomalous coupling $\kappa_Z = 1.1$

$\sqrt{s}[\text{GeV}]$	$\sigma_{an}(s)[fb]$	$\sigma_{num}(s)[fb]$	Error[fb]	Pull
200	3.22585E+05	3.22608E+05	1.80057E+01	1.29
300	3.23397E+05	3.23292E+05	6.00864E+01	-1.74
400	3.32583E+05	3.32492E+05	6.74426E+01	-1.34
500	3.27428E+05	3.27531E+05	7.51628E+01	1.37
700	3.01346E+05	3.01496E+05	8.72054E+01	1.72
1000	2.59662E+05	2.59809E+05	8.35125E+01	1.76
2000	2.35711E+05	2.35509E+05	7.24410E+01	-2.8
5000	8.48788E+05	8.48855E+05	5.73730E+01	1.16
7000	1.62652E+06	1.62660E+06	9.83667E+01	0.849
10000	3.29345E+06	3.29346E+06	2.07223E+02	0.0316
20000	1.31247E+07	1.31234E+07	8.07103E+02	-1.55

$W^+W^- \rightarrow ZZ$				
Abs(cos(θ)) < 0.99				
anomalous coupling $\kappa_Z^5 = 0.1$				
\sqrt{s} [GeV]	$\sigma_{an}(s)[fb]$	$\sigma_{num}(s)[fb]$	Error[fb]	Pull
200	2.68024E+05	2.68047E+05	1.56712E+01	1.5
300	2.62916E+05	2.63019E+05	4.71788E+01	2.18
400	2.68244E+05	2.68141E+05	5.83385E+01	-1.77
500	2.62606E+05	2.62599E+05	6.06995E+01	-0.108
700	2.39595E+05	2.39605E+05	6.54949E+01	0.146
1000	2.04058E+05	2.04004E+05	6.46634E+01	-0.832
2000	1.79179E+05	1.79314E+05	5.98016E+01	2.25
5000	6.41504E+05	6.41500E+05	4.39004E+01	-0.0974
7000	1.23236E+06	1.23229E+06	7.44232E+01	-0.993
10000	2.49946E+06	2.49975E+06	1.58217E+02	1.82
20000	9.97384E+06	9.97455E+06	6.01821E+02	1.17

$W^+W^- \rightarrow ZZ$				
Abs(cos(θ)) < 0.99				
anomalous coupling $g_Z^4 = 0.1$				
\sqrt{s} [GeV]	$\sigma_{an}(s)[fb]$	$\sigma_{num}(s)[fb]$	Error[fb]	Pull
200	2.64208E+05	2.64200E+05	1.61021E+01	-0.472
300	2.60000E+05	2.60062E+05	4.14639E+01	1.49
400	3.02258E+05	3.02221E+05	5.95989E+01	-0.622
500	7.44545E+05	7.44660E+05	1.06353E+02	1.09
700	1.75387E+07	1.75398E+07	1.10050E+03	1.04
1000	6.65491E+08	6.65551E+08	3.89559E+04	1.54
2000	7.16345E+11	7.16271E+11	4.74111E+07	-1.56
5000	6.92244E+15	6.92243E+15	5.61258E+11	-0.0196
7000	2.00480E+17	2.00500E+17	1.69501E+13	1.19
10000	7.10187E+18	7.10161E+18	5.66375E+14	-0.457
20000	7.27572E+21	7.27704E+21	6.27242E+17	2.1

$W^+W^- \rightarrow ZZ$				
Abs(cos(θ)) < 0.95				
anomalous coupling $g_Z^1 = 1.1$				
\sqrt{s} [GeV]	$\sigma_{an}(s)[fb]$	$\sigma_{num}(s)[fb]$	Error[fb]	Pull
200	2.89721E+05	2.89775E+05	2.50005E+01	2.16
300	3.01065E+05	3.01036E+05	6.41695E+01	-0.447
400	5.07650E+05	5.07667E+05	6.92608E+01	0.248
500	1.29538E+06	1.29551E+06	8.34478E+01	1.53
700	8.78182E+06	8.78197E+06	4.95651E+02	0.297
1000	7.59529E+07	7.59614E+07	4.24500E+03	2.01
2000	4.99772E+09	4.99798E+09	2.95820E+05	0.875
5000	1.23128E+12	1.23131E+12	8.23462E+07	0.352
7000	9.27909E+12	9.27870E+12	6.49949E+08	-0.593
10000	7.89077E+13	7.89203E+13	5.92643E+09	2.13
20000	5.05179E+15	5.05167E+15	4.20874E+11	-0.281

$W^+W^- \rightarrow ZZ$				
$\text{Abs}(\cos(\theta)) < 0.95$				
anomalous coupling $\kappa_Z = 1.1$				
$\sqrt{s}[\text{GeV}]$	$\sigma_{an}(s)[fb]$	$\sigma_{num}(s)[fb]$	Error[fb]	Pull
200	3.03223E+05	3.03259E+05	2.56085E+01	1.41
300	2.63858E+05	2.63747E+05	5.77667E+01	-1.93
400	2.35391E+05	2.35430E+05	5.75256E+01	0.676
500	2.02491E+05	2.02572E+05	4.13984E+01	1.95
700	1.50862E+05	1.50842E+05	5.37573E+01	-0.377
1000	1.14360E+05	1.14398E+05	3.88353E+01	0.967
2000	1.54316E+05	1.54325E+05	2.52799E+01	0.36
5000	7.95030E+05	7.95151E+05	6.94936E+01	1.74
7000	1.54688E+06	1.54708E+06	1.09612E+02	1.82
10000	3.14749E+06	3.14749E+06	2.45036E+02	-0.00704
20000	1.25680E+07	1.25679E+07	9.80082E+02	-0.121

$W^+W^- \rightarrow ZZ$				
$\text{Abs}(\cos(\theta)) < 0.95$				
anomalous coupling $\kappa_Z^5 = 0.1$				
$\sqrt{s}[\text{GeV}]$	$\sigma_{an}(s)[fb]$	$\sigma_{num}(s)[fb]$	Error[fb]	Pull
200	2.51974E+05	2.52011E+05	2.09542E+01	1.76
300	2.14733E+05	2.14751E+05	4.62015E+01	0.393
400	1.89993E+05	1.89948E+05	4.60632E+01	-0.983
500	1.62261E+05	1.62294E+05	3.24206E+01	1.02
700	1.19098E+05	1.19011E+05	4.28164E+01	-2.03
1000	8.81707E+04	8.81430E+04	2.96504E+01	-0.934
2000	1.15430E+05	1.15412E+05	1.86159E+01	-0.942
5000	6.01435E+05	6.01547E+05	5.17875E+01	2.16
7000	1.17287E+06	1.17298E+06	8.33315E+01	1.27
10000	2.38955E+06	2.38954E+06	1.94265E+02	-0.0439
20000	9.55073E+06	9.55153E+06	7.67497E+02	1.04

$W^+W^- \rightarrow ZZ$				
$\text{Abs}(\cos(\theta)) < 0.95$				
anomalous coupling $g_Z^4 = 0.1$				
$\sqrt{s}[\text{GeV}]$	$\sigma_{an}(s)[fb]$	$\sigma_{num}(s)[fb]$	Error[fb]	Pull
200	2.48365E+05	2.48388E+05	2.09310E+01	1.1
300	2.12989E+05	2.13019E+05	4.54398E+01	0.657
400	2.24810E+05	2.24690E+05	4.61509E+01	-2.6
500	6.03627E+05	6.03724E+05	6.91472E+01	1.41
700	1.54168E+07	1.54124E+07	2.18772E+03	-2
1000	5.83696E+08	5.83859E+08	9.18594E+04	1.78
2000	6.26534E+11	6.26585E+11	8.80794E+07	0.579
5000	6.05104E+15	6.05077E+15	9.59505E+11	-0.28
7000	1.75234E+17	1.75244E+17	2.32132E+13	0.417
10000	6.20738E+18	6.20867E+18	9.72783E+14	1.33
20000	6.35920E+21	6.35827E+21	9.76848E+17	-0.953

$W^- Z \rightarrow W^- Z$				
Abs(cos(θ)) < 0.99				
anomalous coupling $g_Z^1 = 1.1$				
\sqrt{s} [GeV]	$\sigma_{an}(s)$ [fb]	$\sigma_{num}(s)$ [fb]	Error[fb]	Pull
200	2.49057E+05	2.48991E+05	4.38394E+01	-1.51
300	3.09518E+05	3.09466E+05	6.55759E+01	-0.787
400	6.39512E+05	6.39462E+05	1.27726E+02	-0.395
500	1.78584E+06	1.78569E+06	2.64953E+02	-0.564
700	1.22658E+07	1.22660E+07	1.16185E+03	0.168
1000	1.04600E+08	1.04595E+08	8.47611E+03	-0.646
2000	6.76960E+09	6.76989E+09	6.25286E+05	0.457
5000	1.65806E+12	1.65848E+12	1.68676E+08	2.49
7000	1.24881E+13	1.24916E+13	1.41182E+09	2.46
10000	1.06163E+14	1.06148E+14	1.16514E+10	-1.29
20000	6.79519E+15	6.79494E+15	8.12518E+11	-0.303

$W^- Z \rightarrow W^- Z$				
Abs(cos(θ)) < 0.99				
anomalous coupling $\kappa_Z = 1.1$				
\sqrt{s} [GeV]	$\sigma_{an}(s)$ [fb]	$\sigma_{num}(s)$ [fb]	Error[fb]	Pull
200	2.69001E+05	2.69015E+05	4.26598E+01	0.334
300	2.84218E+05	2.84159E+05	6.25247E+01	-0.94
400	3.02457E+05	3.02515E+05	7.98236E+01	0.723
500	3.03765E+05	3.03854E+05	8.92072E+01	1
700	2.85851E+05	2.85798E+05	1.25659E+02	-0.421
1000	2.49952E+05	2.49953E+05	1.28413E+02	0.00769
2000	2.28482E+05	2.28285E+05	1.03905E+02	-1.9
5000	8.16485E+05	8.16482E+05	1.01085E+02	-0.0261
7000	1.56317E+06	1.56334E+06	1.42778E+02	1.19
10000	3.16375E+06	3.16395E+06	2.47241E+02	0.812
20000	1.26045E+07	1.26047E+07	9.68397E+02	0.225

$W^- Z \rightarrow W^- Z$				
Abs(cos(θ)) < 0.99				
anomalous coupling $\kappa_Z^5 = 0.1$				
\sqrt{s} [GeV]	$\sigma_{an}(s)$ [fb]	$\sigma_{num}(s)$ [fb]	Error[fb]	Pull
200	2.06097E+05	2.06160E+05	3.70832E+01	1.7
300	2.22906E+05	2.22914E+05	4.80824E+01	0.157
400	2.38543E+05	2.38511E+05	6.53177E+01	-0.483
500	2.39847E+05	2.39919E+05	6.35678E+01	1.14
700	2.25387E+05	2.25350E+05	9.80622E+01	-0.38
1000	1.96071E+05	1.96002E+05	9.30512E+01	-0.737
2000	1.76384E+05	1.76586E+05	8.12860E+01	2.48
5000	6.33739E+05	6.33761E+05	8.02486E+01	0.28
7000	1.21662E+06	1.21687E+06	1.06310E+02	2.35
10000	2.46642E+06	2.46670E+06	1.82487E+02	1.55
20000	9.83882E+06	9.83809E+06	7.56255E+02	-0.966

$W^- Z \rightarrow W^- Z$				
$\text{Abs}(\cos(\theta)) < 0.99$				
anomalous coupling $g_Z^4 = 0.1$				
$\sqrt{s}[\text{GeV}]$	$\sigma_{an}(s)[fb]$	$\sigma_{num}(s)[fb]$	Error[fb]	Pull
200	2.03444E+05	2.03417E+05	3.49292E+01	-0.762
300	2.22178E+05	2.22211E+05	4.83593E+01	0.674
400	4.05549E+05	4.05609E+05	8.07824E+01	0.743
500	2.39534E+06	2.39497E+06	2.59484E+02	-1.44
700	7.58189E+07	7.58219E+07	3.80878E+03	0.786
1000	2.90685E+09	2.90716E+09	1.39168E+05	2.24
2000	3.14341E+12	3.14344E+12	1.63541E+08	0.172
5000	3.04265E+16	3.04258E+16	1.82439E+12	-0.401
7000	8.81318E+17	8.81389E+17	5.48583E+13	1.29
10000	3.12227E+19	3.12271E+19	1.92482E+15	2.3
20000	3.19889E+22	3.19907E+22	2.09831E+18	0.872

$W^- Z \rightarrow W^- Z$				
$\text{Abs}(\cos(\theta)) < 0.95$				
anomalous coupling $g_Z^1 = 1.1$				
$\sqrt{s}[\text{GeV}]$	$\sigma_{an}(s)[fb]$	$\sigma_{num}(s)[fb]$	Error[fb]	Pull
200	2.30375E+05	2.30381E+05	4.38531E+01	0.14
300	2.54609E+05	2.54702E+05	6.66084E+01	1.39
400	5.33280E+05	5.33407E+05	1.17319E+02	1.09
500	1.57947E+06	1.57944E+06	2.29092E+02	-0.118
700	1.12690E+07	1.12688E+07	1.79042E+03	-0.135
1000	9.64515E+07	9.64597E+07	1.58166E+04	0.517
2000	6.22695E+09	6.22710E+09	1.06375E+06	0.141
5000	1.52385E+12	1.52370E+12	3.03129E+08	-0.485
7000	1.14763E+13	1.14744E+13	2.13738E+09	-0.875
10000	9.75584E+13	9.75602E+13	1.93188E+10	0.0929
20000	6.24425E+15	6.24545E+15	1.32023E+12	0.912

$W^- Z \rightarrow W^- Z$				
$\text{Abs}(\cos(\theta)) < 0.95$				
anomalous coupling $\kappa_Z = 1.1$				
$\sqrt{s}[\text{GeV}]$	$\sigma_{an}(s)[fb]$	$\sigma_{num}(s)[fb]$	Error[fb]	Pull
200	2.49077E+05	2.49118E+05	4.58883E+01	0.894
300	2.26690E+05	2.26650E+05	6.68140E+01	-0.6
400	2.08035E+05	2.08236E+05	7.48627E+01	2.69
500	1.81850E+05	1.81880E+05	6.77671E+01	0.436
700	1.38182E+05	1.38218E+05	5.24957E+01	0.681
1000	1.06652E+05	1.06576E+05	4.58470E+01	-1.66
2000	1.46741E+05	1.46758E+05	4.08729E+01	0.406
5000	7.54953E+05	7.55142E+05	1.13055E+02	1.67
7000	1.46803E+06	1.46790E+06	1.88722E+02	-0.694
10000	2.98602E+06	2.98512E+06	4.02636E+02	-2.24
20000	1.19201E+07	1.19220E+07	1.50340E+03	1.27

$W^- Z \rightarrow W^- Z$				
Abs(cos(θ)) < 0.95				
anomalous coupling $\kappa_Z^5 = 0.1$				
\sqrt{s} [GeV]	$\sigma_{an}(s)$ [fb]	$\sigma_{num}(s)$ [fb]	Error[fb]	Pull
200	1.90488E+05	1.90542E+05	3.19252E+01	1.68
300	1.77240E+05	1.77280E+05	5.34647E+01	0.753
400	1.63374E+05	1.63513E+05	5.80495E+01	2.39
500	1.42698E+05	1.42794E+05	5.19689E+01	1.86
700	1.07737E+05	1.07710E+05	3.80389E+01	-0.711
1000	8.21676E+04	8.21371E+04	3.55442E+01	-0.858
2000	1.12428E+05	1.12454E+05	2.76139E+01	0.934
5000	5.87165E+05	5.87241E+05	8.48653E+01	0.892
7000	1.14416E+06	1.14396E+06	1.44678E+02	-1.38
10000	2.32995E+06	2.32970E+06	3.26954E+02	-0.76
20000	9.30894E+06	9.30922E+06	1.34223E+03	0.208

$W^- Z \rightarrow W^- Z$				
Abs(cos(θ)) < 0.95				
anomalous coupling $g_Z^4 = 0.1$				
\sqrt{s} [GeV]	$\sigma_{an}(s)$ [fb]	$\sigma_{num}(s)$ [fb]	Error[fb]	Pull
200	1.88029E+05	1.88032E+05	2.89829E+01	0.1
300	1.77714E+05	1.77693E+05	5.48046E+01	-0.374
400	3.31323E+05	3.31315E+05	8.11927E+01	-0.104
500	2.25573E+06	2.25597E+06	2.17837E+02	1.1
700	7.35573E+07	7.35509E+07	6.27013E+03	-1.02
1000	2.81825E+09	2.81805E+09	2.51975E+05	-0.8
2000	3.04523E+12	3.04537E+12	2.85342E+08	0.498
5000	2.94713E+16	2.94676E+16	3.14333E+12	-1.19
7000	8.53636E+17	8.53580E+17	8.51225E+13	-0.658
10000	3.02418E+19	3.02463E+19	3.27314E+15	1.36
20000	3.09837E+22	3.09793E+22	3.39946E+18	-1.29

$ZZ \rightarrow W^+ W^-$				
Abs(cos(θ)) < 0.99				
anomalous coupling $g_Z^1 = 1.1$				
\sqrt{s} [GeV]	$\sigma_{an}(s)$ [fb]	$\sigma_{num}(s)$ [fb]	Error[fb]	Pull
200	1.29337E+06	1.29352E+06	7.83788E+01	1.94
300	8.13376E+05	8.13342E+05	1.31153E+02	-0.256
400	1.29228E+06	1.29208E+06	1.93921E+02	-1.01
500	2.99903E+06	2.99850E+06	2.45348E+02	-2.18
700	1.86256E+07	1.86272E+07	9.23007E+02	1.68
1000	1.57220E+08	1.57247E+08	8.08788E+03	3.34
2000	1.02576E+10	1.02572E+10	6.05914E+05	-0.651
5000	2.52304E+12	2.52292E+12	1.76435E+08	-0.659
7000	1.90112E+13	1.90116E+13	1.40741E+09	0.299
10000	1.61656E+14	1.61669E+14	1.26150E+10	1.05
20000	1.03489E+16	1.03499E+16	9.21487E+11	1.1

$ZZ \rightarrow W^+W^-$
 $\text{Abs}(\cos(\theta)) < 0.99$
anomalous coupling $\kappa_Z = 1.1$

\sqrt{s} [GeV]	$\sigma_{an}(s)[fb]$	$\sigma_{num}(s)[fb]$	Error[fb]	Pull
200	1.35290E+06	1.35308E+06	8.92350E+01	2.07
300	7.31062E+05	7.31152E+05	1.26572E+02	0.714
400	7.03962E+05	7.04063E+05	1.42014E+02	0.711
500	6.77190E+05	6.77399E+05	1.62224E+02	1.29
700	6.12447E+05	6.12254E+05	1.67457E+02	-1.15
1000	5.23296E+05	5.23600E+05	1.64353E+02	1.85
2000	4.72301E+05	4.72108E+05	1.40271E+02	-1.38
5000	1.69808E+06	1.69835E+06	1.15680E+02	2.37
7000	3.25353E+06	3.25331E+06	1.95124E+02	-1.14
10000	6.58738E+06	6.58715E+06	4.17640E+02	-0.562
20000	2.62497E+07	2.62474E+07	1.58408E+03	-1.47

$ZZ \rightarrow W^+W^-$
 $\text{Abs}(\cos(\theta)) < 0.99$
anomalous coupling $\kappa_Z^5 = 0.1$

\sqrt{s} [GeV]	$\sigma_{an}(s)[fb]$	$\sigma_{num}(s)[fb]$	Error[fb]	Pull
200	1.12407E+06	1.12417E+06	7.26965E+01	1.35
300	5.94340E+05	5.94411E+05	1.05252E+02	0.676
400	5.67779E+05	5.67666E+05	1.16226E+02	-0.975
500	5.43126E+05	5.43163E+05	1.25887E+02	0.292
700	4.86945E+05	4.86901E+05	1.37768E+02	-0.316
1000	4.11236E+05	4.11294E+05	1.29238E+02	0.447
2000	3.59025E+05	3.59218E+05	1.19739E+02	1.61
5000	1.28339E+06	1.28349E+06	8.86248E+01	1.14
7000	2.46508E+06	2.46503E+06	1.49139E+02	-0.342
10000	4.99929E+06	4.99902E+06	3.14210E+02	-0.875
20000	1.99479E+07	1.99514E+07	1.21973E+03	2.89

$ZZ \rightarrow W^+W^-$
 $\text{Abs}(\cos(\theta)) < 0.99$
anomalous coupling $g_Z^4 = 0.1$

\sqrt{s} [GeV]	$\sigma_{an}(s)[fb]$	$\sigma_{num}(s)[fb]$	Error[fb]	Pull
200	1.10807E+06	1.10825E+06	7.28113E+01	2.52
300	5.87748E+05	5.87783E+05	1.02569E+02	0.342
400	6.39776E+05	6.40064E+05	1.19990E+02	2.4
500	1.53988E+06	1.54027E+06	2.14148E+02	1.81
700	3.56452E+07	3.56395E+07	2.42874E+03	-2.33
1000	1.34116E+09	1.34130E+09	7.72763E+04	1.8
2000	1.43536E+12	1.43564E+12	9.60400E+07	2.92
5000	1.38490E+16	1.38479E+16	1.11120E+12	-0.956
7000	4.01021E+17	4.01068E+17	3.43154E+13	1.38
10000	1.42048E+19	1.42069E+19	1.15439E+15	1.83
20000	1.45517E+22	1.45505E+22	1.30687E+18	-0.944

$ZZ \rightarrow W^+W^-$
 $\text{Abs}(\cos(\theta)) < 0.95$
anomalous coupling $g_Z^1 = 1.1$

\sqrt{s} [GeV]	$\sigma_{an}(s)[fb]$	$\sigma_{num}(s)[fb]$	Error[fb]	Pull
200	1.21507E+06	1.21505E+06	1.04891E+02	-0.22
300	6.80580E+05	6.80697E+05	1.40888E+02	0.832
400	1.07452E+06	1.07488E+06	1.41067E+02	2.54
500	2.67913E+06	2.67934E+06	1.72878E+02	1.22
700	1.78479E+07	1.78485E+07	1.01517E+03	0.573
1000	1.53067E+08	1.53068E+08	8.53936E+03	0.0945
2000	1.00141E+10	1.00144E+10	5.95199E+05	0.471
5000	2.46330E+12	2.46322E+12	1.66625E+08	-0.492
7000	1.85610E+13	1.85577E+13	1.31322E+09	-2.54
10000	1.57827E+14	1.57840E+14	1.22803E+10	1.09
20000	1.01038E+16	1.01036E+16	8.27931E+11	-0.273

$ZZ \rightarrow W^+W^-$
 $\text{Abs}(\cos(\theta)) < 0.95$
anomalous coupling $\kappa_Z = 1.1$

\sqrt{s} [GeV]	$\sigma_{an}(s)[fb]$	$\sigma_{num}(s)[fb]$	Error[fb]	Pull
200	1.27169E+06	1.27183E+06	1.07515E+02	1.32
300	5.96471E+05	5.96495E+05	1.36134E+02	0.176
400	4.98241E+05	4.98335E+05	1.18572E+02	0.791
500	4.18795E+05	4.18671E+05	9.08881E+01	-1.36
700	3.06607E+05	3.06866E+05	1.15726E+02	2.24
1000	2.30469E+05	2.30517E+05	7.63072E+01	0.633
2000	3.09207E+05	3.09118E+05	4.71665E+01	-1.89
5000	1.59053E+06	1.59054E+06	1.39934E+02	0.0805
7000	3.09422E+06	3.09459E+06	2.17513E+02	1.7
10000	6.29544E+06	6.29712E+06	4.97407E+02	3.38
20000	2.51365E+07	2.51355E+07	2.02981E+03	-0.507

$ZZ \rightarrow W^+W^-$
 $\text{Abs}(\cos(\theta)) < 0.95$
anomalous coupling $\kappa_Z^5 = 0.1$

\sqrt{s} [GeV]	$\sigma_{an}(s)[fb]$	$\sigma_{num}(s)[fb]$	Error[fb]	Pull
200	1.05676E+06	1.05684E+06	8.68696E+01	0.941
300	4.85421E+05	4.85561E+05	1.07126E+02	1.31
400	4.02150E+05	4.02379E+05	9.35038E+01	2.45
500	3.35591E+05	3.35505E+05	7.26165E+01	-1.18
700	2.42050E+05	2.41987E+05	9.35680E+01	-0.676
1000	1.77690E+05	1.77826E+05	6.56053E+01	2.08
2000	2.31290E+05	2.31208E+05	3.50391E+01	-2.33
5000	1.20323E+06	1.20319E+06	1.03567E+02	-0.432
7000	2.34609E+06	2.34624E+06	1.69883E+02	0.864
10000	4.77946E+06	4.77860E+06	3.82047E+02	-2.25
20000	1.91019E+07	1.91023E+07	1.50505E+03	0.283

$ZZ \rightarrow W^+W^-$				
$\text{Abs}(\cos(\theta)) < 0.95$				
anomalous coupling $g_Z^4 = 0.1$				
$\sqrt{s}[\text{GeV}]$	$\sigma_{an}(s)[fb]$	$\sigma_{num}(s)[fb]$	Error[fb]	Pull
200	1.04162E+06	1.04158E+06	8.01450E+01	-0.532
300	4.81477E+05	4.81511E+05	1.06096E+02	0.319
400	4.75845E+05	4.76003E+05	9.73026E+01	1.62
500	1.24843E+06	1.24871E+06	1.41755E+02	1.96
700	3.13327E+07	3.13214E+07	4.36270E+03	-2.58
1000	1.17632E+09	1.17654E+09	1.85065E+05	1.2
2000	1.25540E+12	1.25596E+12	1.72832E+08	3.25
5000	1.21057E+16	1.21034E+16	2.10949E+12	-1.11
7000	3.50521E+17	3.50466E+17	4.93291E+13	-1.12
10000	1.24157E+19	1.24186E+19	2.07691E+15	1.39
20000	1.27186E+22	1.27197E+22	2.11092E+18	0.505

A.3 $W^-W^- \rightarrow W^-W^-$ with different seeds and iterations

$W^-W^- \rightarrow W^-W^-$				
$\text{Abs}(\cos(\theta)) < 0.99$				
$\sqrt{s}[\text{GeV}]$	$\sigma_{an}(s)[fb]$	$\sigma_{num}(s)[fb]$	Error[fb]	Pull
200	6.02473E+06	6.01834E+06	4.76452E+03	-1.34
300	1.50374E+06	1.50317E+06	1.11675E+03	-0.508
400	9.52232E+05	9.52053E+05	6.47708E+02	-0.276
500	7.21275E+05	7.21625E+05	4.44478E+02	0.787
700	4.94506E+05	4.94500E+05	3.37920E+02	-0.0174
1000	3.28773E+05	3.28616E+05	2.33688E+02	-0.672
2000	1.25114E+05	1.25047E+05	1.31623E+02	-0.51
5000	2.44119E+04	2.43407E+04	3.80533E+01	-1.87
7000	1.27323E+04	1.27180E+04	1.70132E+01	-0.843
10000	6.31059E+03	6.30398E+03	8.49266E+00	-0.779

$W^-W^- \rightarrow W^-W^-$				
$\text{Abs}(\cos(\theta)) < 0.95$				
seed = 143				
$\sqrt{s}[\text{GeV}]$	$\sigma_{an}(s)[fb]$	$\sigma_{num}(s)[fb]$	Error[fb]	Pull
200	6.02473E+06	6.02666E+06	5.38571E+03	0.358
300	1.50374E+06	1.50261E+06	1.09640E+03	-1.03
400	9.52232E+05	9.51966E+05	6.22091E+02	-0.428
500	7.21275E+05	7.20854E+05	4.35449E+02	-0.966
700	4.94506E+05	4.94780E+05	3.31276E+02	0.827
1000	3.28773E+05	3.28552E+05	2.40749E+02	-0.919
2000	1.25114E+05	1.25126E+05	1.30568E+02	0.0898
5000	2.44119E+04	2.44002E+04	3.40681E+01	-0.344
7000	1.27323E+04	1.27614E+04	1.94763E+01	1.5
10000	6.31059E+03	6.31311E+03	7.77477E+00	0.324

$W^-W^- \rightarrow W^-W^-$ $\text{Abs}(\cos(\theta)) < 0.95$ seed = 13				
$\sqrt{s}[\text{GeV}]$	$\sigma_{an}(s)[fb]$	$\sigma_{num}(s)[fb]$	Error[fb]	Pull
200	6.02473E+06	6.04114E+06	4.96208E+03	3.31
300	1.50374E+06	1.50428E+06	1.11105E+03	0.482
400	9.52232E+05	9.53261E+05	5.97353E+02	1.72
500	7.21275E+05	7.21316E+05	4.04198E+02	0.101
700	4.94506E+05	4.94607E+05	3.32999E+02	0.305
1000	3.28773E+05	3.28633E+05	2.50213E+02	-0.559
2000	1.25114E+05	1.24918E+05	1.30772E+02	-1.5
5000	2.44119E+04	2.43715E+04	3.76269E+01	-1.07
7000	1.27323E+04	1.26960E+04	1.74925E+01	-2.07
10000	6.31059E+03	6.29221E+03	7.82351E+00	-2.35

$W^-W^- \rightarrow W^-W^-$ $\text{Abs}(\cos(\theta)) < 0.95$ 2 : 1000000 iterations				
$\sqrt{s}[\text{GeV}]$	$\sigma_{an}(s)[fb]$	$\sigma_{num}(s)[fb]$	Error[fb]	Pull
200	6.02473E+06	6.02508E+06	8.50217E+02	0.416
300	1.50374E+06	1.50384E+06	1.54055E+02	0.625
400	9.52232E+05	9.52135E+05	9.31004E+01	-1.04
500	7.21275E+05	7.21272E+05	7.16969E+01	-0.0439
700	4.94506E+05	4.94525E+05	4.64403E+01	0.415
1000	3.28773E+05	3.28764E+05	3.21158E+01	-0.292
2000	1.25114E+05	1.25144E+05	1.49582E+01	2
5000	2.44119E+04	2.44132E+04	5.47947E+00	0.243
7000	1.27323E+04	1.27295E+04	3.09156E+00	-0.898
10000	6.31059E+03	6.31591E+03	1.34290E+00	3.96

A.4 Scan of anomalous couplings at c.m. energy 1 TeV

$W^+W^- \rightarrow W^+W^-$ $\text{Abs}(\cos(\theta)) < 0.95$ $\sqrt{s} = 1 \text{ TeV}$				
g_A^1	$\sigma_{an}(s)[fb]$	$\sigma_{num}(s)[fb]$	Error[fb]	Pull
0.9	81475.5	81559.1	45.8555	1.82
0.92	81872.5	81869.2	45.1309	-0.0724
0.94	82691	82562.2	51.4468	-2.5
0.96	83955.3	84028.9	51.9984	1.42
0.98	85690.5	85719.4	55.5626	0.521
1	87922.2	87990.3	58.8676	1.16
1.02	90677	90655.9	60.0496	-0.352
1.04	93982	93922.4	61.418	-0.972
1.06	97865.4	97875.4	61.7306	0.163
1.08	102356	102381	58.5796	0.439
1.1	107482	107506	61.1451	0.387

$W^+W^- \rightarrow W^+W^-$ $\text{Abs}(\cos(\theta)) < 0.95$ $\sqrt{s} = 1 \text{ TeV}$				
g_Z^1	$\sigma_{an}(s)[fb]$	$\sigma_{num}(s)[fb]$	Error[fb]	Pull
0.9	119327	119429	56.3229	1.8
0.92	103554	103520	51.8185	-0.656
0.94	92249	92202	42.9	-1.09
0.96	85685.3	85685.2	51.0141	-0.00137
0.98	84146	84183.4	51.172	0.729
1	87922.2	87833.1	57.9622	-1.54
1.02	97312.8	97411.9	55.5521	1.78
1.04	112625	112858	64.4131	3.61
1.06	134175	134246	65.6944	1.09
1.08	162286	162182	80.3163	-1.29
1.1	197289	197220	92.3616	-0.752

$W^+W^- \rightarrow W^+W^-$ $\text{Abs}(\cos(\theta)) < 0.95$ $\sqrt{s} = 1 \text{ TeV}$				
κ_A	$\sigma_{an}(s)[fb]$	$\sigma_{num}(s)[fb]$	Error[fb]	Pull
0.9	1.08585e+07	1.08593e+07	2128.72	0.37
0.92	7.13891e+06	7.13998e+06	1467.2	0.731
0.94	4.14868e+06	4.15018e+06	922.142	1.62
0.96	1.94062e+06	1.94046e+06	458.353	-0.341
0.98	568665	568508	174.002	-0.899
1	87922.2	88022.9	57.7549	1.74
1.02	554616	554936	176.667	1.81
1.04	2.02611e+06	2.02618e+06	416.546	0.167
1.06	4.5609e+06	4.56045e+06	948.72	-0.479
1.08	8.21862e+06	8.2177e+06	1559.16	-0.587
1.1	1.306e+07	1.30605e+07	2653.39	0.193

$W^+W^- \rightarrow W^+W^-$ $\text{Abs}(\cos(\theta)) < 0.95$ $\sqrt{s} = 1 \text{ TeV}$				
κ_Z	$\sigma_{an}(s)[fb]$	$\sigma_{num}(s)[fb]$	Error[fb]	Pull
0.9	1.30755e+08	1.30765e+08	26331.6	0.393
0.92	8.55253e+07	8.55254e+07	17715.6	0.00551
0.94	4.91934e+07	4.91842e+07	9921.12	-0.926
0.96	2.24025e+07	2.23984e+07	4279.54	-0.955
0.98	5.81021e+06	5.8097e+06	1302.48	-0.393
1	87922.2	87942.6	58.8302	0.346
1.02	5.92084e+06	5.92267e+06	1187.32	1.54
1.04	2.4008e+07	2.40119e+07	4921.24	0.8
1.06	5.50623e+07	5.50945e+07	11326.9	2.84
1.08	9.98103e+07	9.98525e+07	20683.1	2.04
1.1	1.58993e+08	1.59006e+08	35158.6	0.395

$W^+W^- \rightarrow W^+W^-$ $\text{Abs}(\cos(\theta)) < 0.95$ $\sqrt{s} = 1 \text{ TeV}$				
λ_Z	$\sigma_{an}(s)[fb]$	$\sigma_{num}(s)[fb]$	Error[fb]	Pull
-0.1	1.11007e+08	1.11034e+08	18725.6	1.44
-0.08	7.07037e+07	7.06958e+07	11333.3	-0.7
-0.06	3.9629e+07	3.96304e+07	6538.62	0.213
-0.04	1.75908e+07	1.75877e+07	3108.51	-0.977
-0.02	4.44342e+06	4.44226e+06	830.751	-1.4
0	87922.2	87892.5	57.8664	-0.512
0.02	4.47184e+06	4.47205e+06	826.083	0.259
0.04	1.75894e+07	1.75845e+07	3152.18	-1.56
0.06	3.94815e+07	3.94799e+07	6855.88	-0.229
0.08	7.02355e+07	7.02599e+07	11712.5	2.09
0.1	1.09986e+08	1.10005e+08	18511.6	1.03

$W^+W^- \rightarrow W^+W^-$ $\text{Abs}(\cos(\theta)) < 0.95$ $\sqrt{s} = 1 \text{ TeV}$				
λ_A	$\sigma_{an}(s)[fb]$	$\sigma_{num}(s)[fb]$	Error[fb]	Pull
-0.1	9.21711e+06	9.22082e+06	1571.89	2.36
-0.08	5.89699e+06	5.89788e+06	950.16	0.935
-0.06	3.33786e+06	3.33717e+06	590.571	-1.17
-0.04	1.52396e+06	1.5239e+06	321.209	-0.171
-0.02	443343	443470	135.861	0.938
0	87922.2	87869.6	59.5326	-0.884
0.02	453444	453541	129.582	0.748
0.04	1.5395e+06	1.53963e+06	340.993	0.401
0.06	3.3495e+06	3.34924e+06	623.199	-0.432
0.08	5.89074e+06	5.88971e+06	967.614	-1.06
0.1	9.1743e+06	9.17681e+06	1502.88	1.67

$W^+W^- \rightarrow W^+W^-$ $\text{Abs}(\cos(\theta)) < 0.95$ $\sqrt{s} = 1 \text{ TeV}$				
λ_Z^5	$\sigma_{an}(s)[fb]$	$\sigma_{num}(s)[fb]$	Error[fb]	Pull
-0.1	4.56435e+08	4.56493e+08	70643	0.818
-0.08	2.8767e+08	2.87653e+08	42758.7	-0.394
-0.06	1.59892e+08	1.59832e+08	25850.9	-2.35
-0.04	7.04899e+07	7.04834e+07	11489.5	-0.569
-0.02	1.75951e+07	1.75954e+07	3100.57	0.101
0	87922.2	87914	58.4317	-0.14
0.02	1.75951e+07	1.75993e+07	3136.54	1.34
0.04	7.04899e+07	7.05048e+07	11648.2	1.28
0.06	1.59892e+08	1.59876e+08	25799.3	-0.628
0.08	2.8767e+08	2.87635e+08	45084	-0.769
0.1	4.56435e+08	4.56487e+08	62861.6	0.837

$W^+W^- \rightarrow W^+W^-$ $\text{Abs}(\cos(\theta)) < 0.95$ $\sqrt{s} = 1 \text{ TeV}$				
λ_A^5	$\sigma_{an}(s)[fb]$	$\sigma_{num}(s)[fb]$	Error[fb]	Pull
-0.1	3.7731e+07	3.77319e+07	5943.14	0.141
-0.08	2.38106e+07	2.38079e+07	3976.92	-0.689
-0.06	1.32705e+07	1.3275e+07	2326.89	1.92
-0.04	5.89563e+06	5.89441e+06	983.051	-1.24
-0.02	1.53216e+06	1.5327e+06	330.217	1.62
0	87922.2	88005.6	56.7624	1.47
0.02	1.53216e+06	1.53266e+06	330.326	1.51
0.04	5.89563e+06	5.896e+06	984.371	0.378
0.06	1.32705e+07	1.32722e+07	2297.68	0.729
0.08	2.38106e+07	2.38066e+07	4128.01	-0.985
0.1	3.7731e+07	3.7732e+07	5925.95	0.157

$W^+W^- \rightarrow W^+W^-$ $\text{Abs}(\cos(\theta)) < 0.95$ $\sqrt{s} = 1 \text{ TeV}$				
κ_Z^5	$\sigma_{an}(s)[fb]$	$\sigma_{num}(s)[fb]$	Error[fb]	Pull
-0.1	147388	147375	66.97	-0.201
-0.08	125938	126075	61.5835	2.22
-0.06	109288	109301	56.0012	0.235
-0.04	97412.1	97454.5	58.4463	0.726
-0.02	90293.8	90255.9	55.9346	-0.678
0	87922.2	87943.6	58.2712	0.367
0.02	90293.8	90272.8	54.0307	-0.388
0.04	97412.1	97434.4	55.3233	0.404
0.06	109288	109284	55.4555	-0.0577
0.08	125938	125940	61.528	0.0311
0.1	147388	147424	67.4524	0.526

$W^+W^- \rightarrow W^+W^-$ $\text{Abs}(\cos(\theta)) < 0.95$ $\sqrt{s} = 1 \text{ TeV}$				
κ_A^5	$\sigma_{an}(s)[fb]$	$\sigma_{num}(s)[fb]$	Error[fb]	Pull
-0.1	92712.4	92657.8	49.9409	-1.09
-0.08	90984.3	90967.6	53.3815	-0.313
-0.06	89643	89646.8	55.6408	0.0679
-0.04	88686.5	88707	58.8036	0.349
-0.02	88113.2	88110.6	59.0836	-0.0442
0	87922.2	87930.8	59.1834	0.145
0.02	88113.2	88164.6	57.5947	0.893
0.04	88686.5	88752.5	56.864	1.16
0.06	89643	89611	55.2623	-0.58
0.08	90984.3	90953.7	52.7051	-0.58
0.1	92712.4	92728.3	53.4638	0.298

$W^+W^- \rightarrow W^+W^-$
 $\text{Abs}(\cos(\theta)) < 0.95$
 $\sqrt{s} = 1 \text{ TeV}$

a_5	$\sigma_{an}(s)[fb]$	$\sigma_{num}(s)[fb]$	Error[fb]	Pull
-0.1	6.72629e+07	6.72455e+07	10426.5	-1.67
-0.08	4.30551e+07	4.30609e+07	6735.16	0.857
-0.06	2.42338e+07	2.42269e+07	3904.88	-1.77
-0.04	1.07988e+07	1.07986e+07	1535.94	-0.0886
-0.02	2.75015e+06	2.7505e+06	445.854	0.783
0	87922.2	87830.9	60.0335	-1.52
0.02	2.81207e+06	2.81124e+06	487.314	-1.71
0.04	1.09226e+07	1.09195e+07	1623.44	-1.93
0.06	2.44195e+07	2.44267e+07	3559.2	2.03
0.08	4.33028e+07	4.33e+07	6799.42	-0.409
0.1	6.75725e+07	6.75344e+07	10580.4	-3.61

$W^+W^- \rightarrow W^+W^-$
 $\text{Abs}(\cos(\theta)) < 0.95$
 $\sqrt{s} = 1 \text{ TeV}$

a_4	$\sigma_{an}(s)[fb]$	$\sigma_{num}(s)[fb]$	Error[fb]	Pull
-0.1	3.64774e+07	3.64725e+07	5814.71	-0.833
-0.08	2.33396e+07	2.33389e+07	3847.32	-0.18
-0.06	1.31317e+07	1.31284e+07	2123.25	-1.56
-0.04	5.85386e+06	5.85428e+06	1052.88	0.407
-0.02	1.50591e+06	1.5064e+06	314.097	1.54
0	87922.2	87797.4	58.9444	-2.12
0.02	1.59988e+06	1.60009e+06	328.719	0.632
0.04	6.04179e+06	6.04182e+06	1178.08	0.0208
0.06	1.34137e+07	1.34137e+07	2367.75	0.0363
0.08	2.37155e+07	2.37195e+07	4253.72	0.944
0.1	3.69472e+07	3.69591e+07	6213.51	1.91

$W^-W^- \rightarrow W^-W^-$
 $\text{Abs}(\cos(\theta)) < 0.95$
 $\sqrt{s} = 1 \text{ TeV}$

g_A^1	$\sigma_{an}(s)[fb]$	$\sigma_{num}(s)[fb]$	Error[fb]	Pull
0.9	95200.2	95288.4	46.4689	1.9
0.92	96132.7	96095.5	50.052	-0.743
0.94	97466.8	97468.3	50.9091	0.0287
0.96	99224.2	99103.2	67.6587	-1.79
0.98	101427	101310	67.0202	-1.75
1	104100	104117	65.4769	0.265
1.02	107265	107431	69.6193	2.38
1.04	110949	110985	66.2402	0.545
1.06	115176	115157	65.1881	-0.285
1.08	119973	119905	60.7041	-1.11
1.1	125367	125335	78.7602	-0.406

$W^-W^- \rightarrow W^-W^-$
 $\text{Abs}(\cos(\theta)) < 0.95$
 $\sqrt{s} = 1 \text{ TeV}$

g_Z^1	$\sigma_{an}(s)[fb]$	$\sigma_{num}(s)[fb]$	Error[fb]	Pull
0.9	123936	123936	55.8072	0.00288
0.92	110936	110933	53.3853	-0.0656
0.94	102210	102268	52.2141	1.11
0.96	97996	98105.4	54.2622	2.02
0.98	98540.7	98528.9	53.0763	-0.222
1	104100	103906	63.4854	-3.05
1.02	114938	114880	62.9	-0.926
1.04	131328	131206	76.1297	-1.59
1.06	153551	153587	78.3583	0.459
1.08	181898	181910	76.8524	0.161
1.1	216667	216661	91.6131	-0.0671

$W^-W^- \rightarrow W^-W^-$
 $\text{Abs}(\cos(\theta)) < 0.95$
 $\sqrt{s} = 1 \text{ TeV}$

κ_A	$\sigma_{an}(s)[fb]$	$\sigma_{num}(s)[fb]$	Error[fb]	Pull
0.9	8.44804e+06	8.44897e+06	705.137	1.32
0.92	5.51795e+06	5.51835e+06	481.281	0.835
0.94	3.17601e+06	3.17642e+06	300.954	1.37
0.96	1.46428e+06	1.46439e+06	191.357	0.627
0.98	425689	425721	117.867	0.27
1	104100	104059	58.2036	-0.707
1.02	544248	544113	147.378	-0.918
1.04	1.79177e+06	1.79236e+06	269.505	2.19
1.06	3.8932e+06	3.89216e+06	430.442	-2.41
1.08	6.89595e+06	6.8962e+06	677.673	0.363
1.1	1.08484e+07	1.08495e+07	955.731	1.21

$W^-W^- \rightarrow W^-W^-$
 $\text{Abs}(\cos(\theta)) < 0.95$
 $\sqrt{s} = 1 \text{ TeV}$

κ_Z	$\sigma_{an}(s)[fb]$	$\sigma_{num}(s)[fb]$	Error[fb]	Pull
0.9	1.00561e+08	1.00554e+08	7667.68	-0.846
0.92	6.56133e+07	6.56161e+07	5086.31	0.548
0.94	3.75924e+07	3.7593e+07	2924.35	0.216
0.96	1.69943e+07	1.69957e+07	1316.95	1.05
0.98	4.3258e+06	4.32677e+06	393.984	2.47
1	104100	104005	62.0533	-1.52
1.02	4.85702e+06	4.85731e+06	511.677	0.566
1.04	1.91229e+07	1.91197e+07	1647.71	-1.99
1.06	4.34508e+07	4.34551e+07	3554.63	1.21
1.08	7.84001e+07	7.84184e+07	6368	2.86
1.1	1.24541e+08	1.24547e+08	9852.08	0.568

$W^-W^- \rightarrow W^-W^-$ $\text{Abs}(\cos(\theta)) < 0.95$ $\sqrt{s} = 1 \text{ TeV}$				
λ_Z	$\sigma_{an}(s)[fb]$	$\sigma_{num}(s)[fb]$	Error[fb]	Pull
-0.1	6.633e+07	6.63491e+07	6737.98	2.83
-0.08	4.23028e+07	4.23072e+07	4276.5	1.03
-0.06	2.37569e+07	2.37518e+07	2500.36	-2.06
-0.04	1.05856e+07	1.05847e+07	1120.16	-0.806
-0.02	2.7149e+06	2.71568e+06	382.13	2.03
0	104100	104030	56.6779	-1.23
0.02	2.74545e+06	2.74576e+06	400.887	0.76
0.04	1.06643e+07	1.0664e+07	1139.33	-0.277
0.06	2.3919e+07	2.39164e+07	2594.16	-1.01
0.08	4.2601e+07	4.25879e+07	4388.75	-2.99
0.1	6.68348e+07	6.68482e+07	6890.64	1.95

$W^-W^- \rightarrow W^-W^-$ $\text{Abs}(\cos(\theta)) < 0.95$ $\sqrt{s} = 1 \text{ TeV}$				
λ_A	$\sigma_{an}(s)[fb]$	$\sigma_{num}(s)[fb]$	Error[fb]	Pull
-0.1	5.69296e+06	5.69368e+06	697.577	1.03
-0.08	3.66302e+06	3.66361e+06	483.351	1.24
-0.06	2.09679e+06	2.09741e+06	330.574	1.87
-0.04	985258	985213	202.269	-0.222
-0.02	322176	322245	107.803	0.641
0	104100	103992	62.2724	-1.73
0.02	330376	330282	122.363	-0.763
0.04	1.00314e+06	1.00333e+06	215.835	0.88
0.06	2.12734e+06	2.12723e+06	328.45	-0.311
0.08	3.71068e+06	3.71035e+06	502.588	-0.648
0.1	5.76369e+06	5.76465e+06	719.542	1.33

$W^+W^- \rightarrow W^+W^-$ $\text{Abs}(\cos(\theta)) < 0.95$ $\sqrt{s} = 1 \text{ TeV}$				
λ_5^Z	$\sigma_{an}(s)[fb]$	$\sigma_{num}(s)[fb]$	Error[fb]	Pull
-0.1	2.76086e+08	2.76124e+08	27889.1	1.34
-0.08	1.73558e+08	1.73576e+08	17400.3	1.03
-0.06	9.62835e+07	9.6278e+07	9916.42	-0.562
-0.04	4.24097e+07	4.2425e+07	4364.55	3.52
-0.02	1.06144e+07	1.06138e+07	1189.35	-0.441
0	104100	104173	53.9001	1.36
0.02	1.06144e+07	1.06146e+07	1131.99	0.174
0.04	4.24097e+07	4.24168e+07	4390.79	1.63
0.06	9.62835e+07	9.6288e+07	9799.6	0.453
0.08	1.73558e+08	1.73541e+08	17198.9	-1.01
0.1	2.76086e+08	2.76059e+08	27346.4	-0.979

$W^-W^- \rightarrow W^-W^-$ Abs($\cos(\theta)$) < 0.95 $\sqrt{s} = 1$ TeV				
λ_A^5	$\sigma_{an}(s)[fb]$	$\sigma_{num}(s)[fb]$	Error[fb]	Pull
-0.1	2.34517e+07	2.34543e+07	2451.42	1.07
-0.08	1.47784e+07	1.47827e+07	1585.55	2.71
-0.06	8.24104e+06	8.23998e+06	948.049	-1.11
-0.04	3.68327e+06	3.68419e+06	487.719	1.9
-0.02	993304	993147	211.248	-0.748
0	104100	104134	64.381	0.536
0.02	993304	993149	206.968	-0.753
0.04	3.68327e+06	3.68351e+06	479.606	0.509
0.06	8.24104e+06	8.24255e+06	939.163	1.61
0.08	1.47784e+07	1.47767e+07	1604.3	-1.02
0.1	2.34517e+07	2.34519e+07	2480.1	0.0982

$W^-W^- \rightarrow W^-W^-$ Abs($\cos(\theta)$) < 0.95 $\sqrt{s} = 1$ TeV				
κ_Z^5	$\sigma_{an}(s)[fb]$	$\sigma_{num}(s)[fb]$	Error[fb]	Pull
-0.1	153356	153294	70.7035	-0.869
-0.08	135581	135526	65.4791	-0.839
-0.06	121789	121724	72.3607	-0.895
-0.04	111956	111888	67.5674	-1.01
-0.02	106063	106019	54.7046	-0.81
0	104100	104187	51.2017	1.7
0.02	106063	106050	62.3869	-0.211
0.04	111956	111951	56.7884	-0.0797
0.06	121789	121738	59.1886	-0.864
0.08	135581	135518	64.3096	-0.977
0.1	153356	153316	68.0438	-0.583

$W^-W^- \rightarrow W^-W^-$ Abs($\cos(\theta)$) < 0.95 $\sqrt{s} = 1$ TeV				
κ_A^5	$\sigma_{an}(s)[fb]$	$\sigma_{num}(s)[fb]$	Error[fb]	Pull
-0.1	108114	108112	58.5198	-0.0276
-0.08	106665	106549	61.363	-1.89
-0.06	105541	105546	54.0414	0.0804
-0.04	104740	104694	63.0139	-0.736
-0.02	104260	104344	62.2017	1.35
0	104100	104111	61.5661	0.186
0.02	104260	104308	67.1937	0.721
0.04	104740	104765	60.1636	0.422
0.06	105541	105603	60.1299	1.03
0.08	106665	106590	66.8097	-1.12
0.1	108114	108216	64.5377	1.58

$W^-W^- \rightarrow W^-W^-$ Abs(cos(θ)) < 0.95 $\sqrt{s} = 1$ TeV				
a_4	$\sigma_{an}(s)[fb]$	$\sigma_{num}(s)[fb]$	Error[fb]	Pull
-0.1	3.28151e+07	3.28143e+07	4650.27	-0.185
-0.08	2.11214e+07	2.11252e+07	3086.34	1.24
-0.06	1.20034e+07	1.20073e+07	1810.36	2.16
-0.04	5.46117e+06	5.46042e+06	910.828	-0.833
-0.02	1.49475e+06	1.49446e+06	301.93	-0.965
0	104100	104015	55.0084	-1.54
0.02	1.28923e+06	1.28963e+06	267.135	1.5
0.04	5.05014e+06	5.04981e+06	736.538	-0.443
0.06	1.13868e+07	1.13835e+07	1544.34	-2.18
0.08	2.02993e+07	2.03026e+07	2710.41	1.21
0.1	3.17875e+07	3.17937e+07	4257.98	1.45

$W^-W^- \rightarrow W^-W^-$ Abs(cos(θ)) < 0.95 $\sqrt{s} = 1$ TeV				
a_5	$\sigma_{an}(s)[fb]$	$\sigma_{num}(s)[fb]$	Error[fb]	Pull
-0.1	8.36629e+06	8.3675e+06	1576.59	0.77
-0.08	5.43482e+06	5.436e+06	1069.22	1.1
-0.06	3.14287e+06	3.14344e+06	658.574	0.875
-0.04	1.49043e+06	1.49063e+06	338.335	0.606
-0.02	477507	477199	145.059	-2.12
0	104100	104178	54.1096	1.44
0.02	370208	370306	119.02	0.825
0.04	1.27583e+06	1.27635e+06	263.922	1.95
0.06	2.82097e+06	2.82083e+06	516.499	-0.272
0.08	5.00562e+06	5.00467e+06	889.907	-1.07
0.1	7.82979e+06	7.83142e+06	1330.37	1.23

$W^+W^- \rightarrow ZZ$ Abs(cos(θ)) < 0.95 $\sqrt{s} = 1$ TeV				
a_4	$\sigma_{an}(s)[fb]$	$\sigma_{num}(s)[fb]$	Error[fb]	Pull
-0.1	1.96307e+06	1.96292e+06	239.869	-0.591
-0.08	1.26741e+06	1.26744e+06	168.901	0.179
-0.06	729560	729785	114.574	1.96
-0.04	349504	349466	72.9729	-0.517
-0.02	127244	127205	42.5713	-0.917
0	62781.3	62822.6	26.2481	1.58
0.02	156116	156056	48.571	-1.23
0.04	407248	407262	92.8279	0.154
0.06	816176	816163	145.882	-0.0906
0.08	1.3829e+06	1.38251e+06	213.924	-1.84
0.1	2.10743e+06	2.10733e+06	297.559	-0.314

$W^+W^- \rightarrow ZZ$ Abs($\cos(\theta)$) < 0.95 $\sqrt{s} = 1$ TeV				
a_5	$\sigma_{an}(s)[fb]$	$\sigma_{num}(s)[fb]$	Error[fb]	Pull
-0.1	1.80675e+07	1.80688e+07	1116.49	1.1
-0.08	1.15549e+07	1.15549e+07	722.531	-0.0737
-0.06	6.49812e+06	6.49854e+06	417.367	0.99
-0.04	2.89717e+06	2.89728e+06	197.989	0.514
-0.02	752061	752057	70.1554	-0.0502
0	62781.3	62848	26.5013	2.52
0.02	829336	829409	92.7498	0.784
0.04	3.05173e+06	3.05197e+06	230.135	1.05
0.06	6.72995e+06	6.72975e+06	455.724	-0.429
0.08	1.1864e+07	1.18645e+07	775.18	0.69
0.1	1.84539e+07	1.8456e+07	1152.68	1.83

$W^+W^- \rightarrow ZZ$ Abs($\cos(\theta)$) < 0.95 $\sqrt{s} = 1$ TeV				
a_6	$\sigma_{an}(s)[fb]$	$\sigma_{num}(s)[fb]$	Error[fb]	Pull
-0.1	1.96307e+06	1.96237e+06	244.109	-2.85
-0.08	1.26741e+06	1.26736e+06	167.204	-0.319
-0.06	729560	729955	113.434	3.48
-0.04	349504	349468	71.1293	-0.504
-0.02	127244	127331	44.2039	1.96
0	62781.3	62804.1	25.6498	0.888
0.02	156116	156100	50.8452	-0.308
0.04	407248	407260	91.9724	0.138
0.06	816176	815949	146.321	-1.55
0.08	1.3829e+06	1.38308e+06	217.245	0.826
0.1	2.10743e+06	2.10794e+06	301.4	1.72

$W^+W^- \rightarrow ZZ$ Abs($\cos(\theta)$) < 0.95 $\sqrt{s} = 1$ TeV				
a_7	$\sigma_{an}(s)[fb]$	$\sigma_{num}(s)[fb]$	Error[fb]	Pull
-0.1	1.80675e+07	1.80676e+07	1110.68	0.103
-0.08	1.15549e+07	1.15564e+07	729.239	2.06
-0.06	6.49812e+06	6.49779e+06	412.065	-0.798
-0.04	2.89717e+06	2.89717e+06	198.397	-0.00621
-0.02	752061	752113	73.6768	0.708
0	62781.3	62720	25.8605	-2.37
0.02	829336	829363	95.1683	0.284
0.04	3.05173e+06	3.05129e+06	231.816	-1.86
0.06	6.72995e+06	6.73076e+06	462.62	1.76
0.08	1.1864e+07	1.18641e+07	789.635	0.102
0.1	1.84539e+07	1.84551e+07	1161.82	1.05

$W^+W^- \rightarrow ZZ$ Abs($\cos(\theta)$) < 0.95 $\sqrt{s} = 1$ TeV				
g_Z^1	$\sigma_{an}(s)[fb]$	$\sigma_{num}(s)[fb]$	Error[fb]	Pull
0.9	6.1548e+07	6.15556e+07	3440.43	2.2
0.92	4.01937e+07	4.01952e+07	2246.43	0.677
0.94	2.3059e+07	2.30592e+07	1279.8	0.151
0.96	1.04497e+07	1.04504e+07	575.813	1.15
0.98	2.67801e+06	2.67795e+06	164.091	-0.372
1	62781.3	62783.3	26.3188	0.077
1.02	2.92942e+06	2.92976e+06	190.66	1.79
1.04	1.16099e+07	1.16091e+07	648.924	-1.32
1.06	2.64428e+07	2.64454e+07	1527.98	1.67
1.08	4.77732e+07	4.77687e+07	2722.24	-1.68
1.1	7.59529e+07	7.59604e+07	4320.84	1.72

$W^+W^- \rightarrow ZZ$ Abs($\cos(\theta)$) < 0.95 $\sqrt{s} = 1$ TeV				
κ_Z	$\sigma_{an}(s)[fb]$	$\sigma_{num}(s)[fb]$	Error[fb]	Pull
0.9	74753	74763.4	26.0936	0.401
0.92	68187.9	68209.8	22.6465	0.964
0.94	63565.6	63572.4	25.3169	0.269
0.96	61026.2	61017.8	25.486	-0.332
0.98	60714.9	60708.6	24.4309	-0.257
1	62781.3	62825	26.3008	1.66
1.02	67380.1	67376.9	26.8858	-0.12
1.04	74670.8	74679.1	28.3788	0.294
1.06	84817.5	84847.7	28.1427	1.07
1.08	97989.3	98024	35.0895	0.989
1.1	114360	114240	41.3566	-2.89

$W^+W^- \rightarrow ZZ$ Abs($\cos(\theta)$) < 0.95 $\sqrt{s} = 1$ TeV				
g_Z^4	$\sigma_{an}(s)[fb]$	$\sigma_{num}(s)[fb]$	Error[fb]	Pull
-0.1	5.83696e+08	5.83806e+08	91736	1.2
-0.08	2.3892e+08	2.3901e+08	37204.2	2.4
-0.06	7.55033e+07	7.5504e+07	11845.1	0.0606
-0.04	1.48881e+07	1.48904e+07	2309.85	0.99
-0.02	963539	963380	133.652	-1.19
0	62781.3	62729.5	25.8483	-2
0.02	963539	963527	141.526	-0.0828
0.04	1.48881e+07	1.48851e+07	2326.16	-1.28
0.06	7.55033e+07	7.55272e+07	11871.2	2.01
0.08	2.3892e+08	2.38935e+08	37734.9	0.379
0.1	5.83696e+08	5.83734e+08	91959.4	0.418

$W^+W^- \rightarrow ZZ$				
$\text{Abs}(\cos(\theta)) < 0.95$				
$\sqrt{s} = 1 \text{ TeV}$				
κ_Z^5	$\sigma_{an}(s)[fb]$	$\sigma_{num}(s)[fb]$	Error[fb]	Pull
-0.1	88170.7	88126.4	29.0671	-1.52
-0.08	79009.3	79046.8	25.2955	1.48
-0.06	71900.3	71872.9	23.1316	-1.18
-0.04	66831.2	66893.6	25.2495	2.47
-0.02	63793.3	63846.5	27.9306	1.9
0	62781.3	62721.4	25.177	-2.38
0.02	63793.3	63776.4	25.6329	-0.66
0.04	66831.2	66816.3	29.9195	-0.5
0.06	71900.3	71909.3	24.6294	0.368
0.08	79009.3	78998.5	29.8333	-0.362
0.1	88170.7	88162.9	29.7117	-0.26

$W^-Z \rightarrow W^-Z$				
$\text{Abs}(\cos(\theta)) < 0.95$				
$\sqrt{s} = 1 \text{ TeV}$				
a_4	$\sigma_{an}(s)[fb]$	$\sigma_{num}(s)[fb]$	Error[fb]	Pull
-0.1	1.69259e+07	1.69258e+07	2049.85	-0.0631
-0.08	1.08797e+07	1.08823e+07	1269.35	2
-0.06	6.16965e+06	6.16809e+06	767.065	-2.03
-0.04	2.79571e+06	2.79587e+06	372.768	0.42
-0.02	757923	758036	132.476	0.851
0	56272.5	56283.5	29.9864	0.365
0.02	690763	690870	116.785	0.92
0.04	2.66139e+06	2.66097e+06	351.703	-1.19
0.06	5.96817e+06	5.96918e+06	731.524	1.38
0.08	1.06111e+07	1.06104e+07	1342.28	-0.485
0.1	1.65901e+07	1.65935e+07	2082.19	1.62

$W^-Z \rightarrow W^-Z$				
$\text{Abs}(\cos(\theta)) < 0.95$				
$\sqrt{s} = 1 \text{ TeV}$				
a_5	$\sigma_{an}(s)[fb]$	$\sigma_{num}(s)[fb]$	Error[fb]	Pull
-0.1	7.12164e+06	7.12429e+06	1479.98	1.79
-0.08	4.60485e+06	4.60454e+06	1082.71	-0.285
-0.06	2.63992e+06	2.63835e+06	670.07	-2.34
-0.04	1.22684e+06	1.22686e+06	367.32	0.0462
-0.02	365629	365610	123.165	-0.159
0	56272.5	56306.2	29.6089	1.14
0.02	298774	298616	92.2864	-1.71
0.04	1.09313e+06	1.09342e+06	259.306	1.12
0.06	2.43935e+06	2.43974e+06	518.324	0.76
0.08	4.33743e+06	4.3372e+06	933.489	-0.24
0.1	6.78736e+06	6.78491e+06	1318.59	-1.86

$W^- Z \rightarrow W^- Z$ Abs($\cos(\theta)$) < 0.95 $\sqrt{s} = 1$ TeV				
a_6	$\sigma_{an}(s)[fb]$	$\sigma_{num}(s)[fb]$	Error[fb]	Pull
-0.1	1.69259e+07	1.69267e+07	2077.61	0.373
-0.08	1.08797e+07	1.08812e+07	1317.58	1.12
-0.06	6.16965e+06	6.17005e+06	797.991	0.51
-0.04	2.79571e+06	2.79559e+06	369.783	-0.325
-0.02	757923	757851	136.33	-0.527
0	56272.5	56221.6	30.6258	-1.66
0.02	690763	690805	116.216	0.364
0.04	2.66139e+06	2.66117e+06	334.743	-0.676
0.06	5.96817e+06	5.96787e+06	736.286	-0.401
0.08	1.06111e+07	1.0608e+07	1316.17	-2.34
0.1	1.65901e+07	1.65897e+07	2039.53	-0.235

$W^- Z \rightarrow W^- Z$ Abs($\cos(\theta)$) < 0.95 $\sqrt{s} = 1$ TeV				
a_7	$\sigma_{an}(s)[fb]$	$\sigma_{num}(s)[fb]$	Error[fb]	Pull
-0.1	7.12164e+06	7.11959e+06	1536.44	-1.33
-0.08	4.60485e+06	4.60575e+06	1081.3	0.835
-0.06	2.63992e+06	2.64047e+06	573.952	0.956
-0.04	1.22684e+06	1.22679e+06	352.496	-0.153
-0.02	365629	365615	124.065	-0.119
0	56272.5	56276.3	29.9168	0.126
0.02	298774	298814	78.3791	0.52
0.04	1.09313e+06	1.09264e+06	270.725	-1.83
0.06	2.43935e+06	2.4402e+06	544.808	1.55
0.08	4.33743e+06	4.33774e+06	878.746	0.362
0.1	6.78736e+06	6.78837e+06	1508.17	0.673

$W^- Z \rightarrow W^- Z$ Abs($\cos(\theta)$) < 0.95 $\sqrt{s} = 1$ TeV				
g_Z^1	$\sigma_{an}(s)[fb]$	$\sigma_{num}(s)[fb]$	Error[fb]	Pull
0.9	7.89393e+07	7.89533e+07	12675.8	1.11
0.92	5.16085e+07	5.16088e+07	8445.56	0.0443
0.94	2.96602e+07	2.96675e+07	4896.36	1.49
0.96	1.34849e+07	1.34846e+07	2388.04	-0.12
0.98	3.48118e+06	3.48286e+06	647.852	2.59
1	56272.5	56271.5	29.8735	-0.0342
1.02	3.62569e+06	3.62491e+06	658.876	-1.19
1.04	1.46134e+07	1.4618e+07	2321.54	1.99
1.06	3.34517e+07	3.34559e+07	5583.14	0.749
1.08	6.05814e+07	6.05912e+07	10022.7	0.978
1.1	9.64515e+07	9.64564e+07	16381.3	0.295

$W^- Z \rightarrow W^- Z$ Abs(cos(θ)) < 0.95 $\sqrt{s} = 1$ TeV				
κ_Z	$\sigma_{an}(s)[fb]$	$\sigma_{num}(s)[fb]$	Error[fb]	Pull
0.9	66282.2	66320.3	27.5656	1.38
0.92	60501.4	60470.5	28.5236	-1.08
0.94	56449.4	56441.9	20.3014	-0.366
0.96	54283.1	54320.7	21.5201	1.75
0.98	54166.9	54150.8	28.2182	-0.574
1	56272.5	56284	29.9576	0.384
1.02	60778.9	60761.9	30.4227	-0.558
1.04	67872.6	67881.8	24.9693	0.368
1.06	77747.3	77763.1	30.0891	0.523
1.08	90604.4	90608.2	42.7269	0.0888
1.1	106652	106711	44.792	1.31

$W^- Z \rightarrow W^- Z$ Abs(cos(θ)) < 0.95 $\sqrt{s} = 1$ TeV				
g_Z^4	$\sigma_{an}(s)[fb]$	$\sigma_{num}(s)[fb]$	Error[fb]	Pull
-0.1	2.81825e+09	2.81809e+09	253483	-0.604
-0.08	1.15392e+09	1.15388e+09	104088	-0.358
-0.06	3.64826e+08	3.64899e+08	33476.8	2.19
-0.04	7.19293e+07	7.19257e+07	6551.85	-0.553
-0.02	4.48748e+06	4.48692e+06	439.951	-1.29
0	56272.5	56291.4	29.0878	0.65
0.02	4.48748e+06	4.48765e+06	454.5	0.36
0.04	7.19293e+07	7.19157e+07	6339.14	-2.14
0.06	3.64826e+08	3.64849e+08	33173.9	0.681
0.08	1.15392e+09	1.15403e+09	103346	1.11
0.1	2.81825e+09	2.81858e+09	259053	1.28

$W^- Z \rightarrow W^- Z$ Abs(cos(θ)) < 0.95 $\sqrt{s} = 1$ TeV				
κ_Z^5	$\sigma_{an}(s)[fb]$	$\sigma_{num}(s)[fb]$	Error[fb]	Pull
-0.1	82167.6	82174.6	35.4759	0.198
-0.08	72825.3	72821.8	33.0021	-0.107
-0.06	65574.7	65567.9	21.0465	-0.32
-0.04	60404	60364.5	26.206	-1.51
-0.02	57305	57344.4	28.0001	1.41
0	56272.5	56273.6	29.9234	0.0349
0.02	57305	57325.5	28.1946	0.728
0.04	60404	60380.4	24.4577	-0.964
0.06	65574.7	65588.3	22.9481	0.593
0.08	72825.3	72791.2	33.3775	-1.02
0.1	82167.6	82197.3	35.2098	0.843

$ZZ \rightarrow ZZ$ Abs(cos(θ)) < 0.95 $\sqrt{s} = 1$ TeV				
a_4	$\sigma_{an}(s)[fb]$	$\sigma_{num}(s)[fb]$	Error[fb]	Pull
-0.1	4.93003e+07	4.92976e+07	9161.14	-0.289
-0.08	3.1578e+07	3.15817e+07	5422.48	0.666
-0.06	1.77869e+07	1.77904e+07	3286.94	1.05
-0.04	7.927e+06	7.92662e+06	1332.53	-0.282
-0.02	1.9982e+06	1.99876e+06	268.706	2.08
0	544.211	544.288	0.0614543	1.26
0.02	1.93404e+06	1.9343e+06	318.622	0.817
0.04	7.79869e+06	7.79852e+06	1233.77	-0.135
0.06	1.75945e+07	1.7602e+07	3178.91	2.37
0.08	3.13214e+07	3.13261e+07	4842.06	0.962
0.1	4.89795e+07	4.89738e+07	8217.15	-0.696

$ZZ \rightarrow ZZ$ Abs(cos(θ)) < 0.95 $\sqrt{s} = 1$ TeV				
a_5	$\sigma_{an}(s)[fb]$	$\sigma_{num}(s)[fb]$	Error[fb]	Pull
-0.1	4.93003e+07	4.92996e+07	6709.71	-0.097
-0.08	3.1578e+07	3.1574e+07	5431.23	-0.744
-0.06	1.77869e+07	1.77924e+07	3342.03	1.63
-0.04	7.927e+06	7.92758e+06	1461.16	0.398
-0.02	1.9982e+06	1.99764e+06	345.612	-1.62
0	544.211	544.233	0.0577543	0.38
0.02	1.93404e+06	1.93385e+06	303.617	-0.624
0.04	7.79869e+06	7.79874e+06	1107.97	0.0451
0.06	1.75945e+07	1.75947e+07	3184.21	0.0809
0.08	3.13214e+07	3.13201e+07	5819.81	-0.228
0.1	4.89795e+07	4.89688e+07	7995.71	-1.34

$ZZ \rightarrow ZZ$ Abs(cos(θ)) < 0.95 $\sqrt{s} = 1$ TeV				
a_6	$\sigma_{an}(s)[fb]$	$\sigma_{num}(s)[fb]$	Error[fb]	Pull
-0.1	1.96879e+08	1.96908e+08	21672.3	1.33
-0.08	1.26054e+08	1.26049e+08	12740.9	-0.365
-0.06	7.09537e+07	7.09687e+07	12616.4	1.19
-0.04	3.1578e+07	3.15825e+07	5795.88	0.776
-0.02	7.927e+06	7.92862e+06	1424.58	1.14
0	544.211	544.253	0.0845464	0.497
0.02	7.79869e+06	7.80317e+06	1447.25	3.1
0.04	3.13214e+07	3.13251e+07	4841.2	0.757
0.06	7.05688e+07	7.05497e+07	13429.5	-1.42
0.08	1.25541e+08	1.25545e+08	14071.1	0.308
0.1	1.96237e+08	1.96232e+08	36102.2	-0.156

$ZZ \rightarrow ZZ$ Abs($\cos(\theta)$) < 0.95 $\sqrt{s} = 1$ TeV				
a_7	$\sigma_{an}(s)[fb]$	$\sigma_{num}(s)[fb]$	Error[fb]	Pull
-0.1	1.96879e+08	1.96913e+08	36733.9	0.93
-0.08	1.26054e+08	1.26012e+08	21357.8	-1.97
-0.06	7.09537e+07	7.09435e+07	11423.1	-0.888
-0.04	3.1578e+07	3.15873e+07	5798	1.59
-0.02	7.927e+06	7.92778e+06	1079.86	0.722
0	544.211	544.285	0.0805592	0.921
0.02	7.79869e+06	7.79682e+06	1431.46	-1.3
0.04	3.13214e+07	3.13103e+07	5818.09	-1.91
0.06	7.05688e+07	7.05943e+07	11973.6	2.14
0.08	1.25541e+08	1.25468e+08	21947.2	-3.31
0.1	1.96237e+08	1.96264e+08	22798.2	1.19

$ZZ \rightarrow ZZ$ Abs($\cos(\theta)$) < 0.95 $\sqrt{s} = 1$ TeV				
a_{10}	$\sigma_{an}(s)[fb]$	$\sigma_{num}(s)[fb]$	Error[fb]	Pull
-0.1	1.96879e+08	1.96857e+08	19934.5	-1.1
-0.08	1.26054e+08	1.26046e+08	22840	-0.331
-0.06	7.09537e+07	7.09562e+07	9891.12	0.257
-0.04	3.1578e+07	3.15774e+07	4861.55	-0.134
-0.02	7.927e+06	7.92589e+06	1444.65	-0.765
0	544.211	544.226	0.0770539	0.191
0.02	7.79869e+06	7.79834e+06	1054.66	-0.329
0.04	3.13214e+07	3.13301e+07	5831.67	1.48
0.06	7.05688e+07	7.0567e+07	7292.6	-0.241
0.08	1.25541e+08	1.25507e+08	18470.8	-1.82
0.1	1.96237e+08	1.96217e+08	29993.7	-0.669

Appendix B

Used Software

For the analytic calculation of total cross sections and the composition of this Thesis, the following software has been used :

- The square of the heavy gauge boson scattering amplitudes in terms of Mandelstam variables were calculated using the symbolic manipulation system FORM by J. Vermaseren. [10] <http://www.nikhef.nl/form/>
- The squared amplitudes were integrated using Wolfram's Mathematica 7. <http://www.wolfram.com/>
- Additionally, the cross section $e^+e^- \rightarrow W^+W^-$ was calculated using the Mathematica Package FeynCalc which can be found at <http://www.feyncalc.org/>
- The calculation of numeric cross sections was done using Whizard [12] (v2.0.3). <http://projects.hepforge.org/whizard/>
- The Feynman diagrams have been drawn using T.Ohl's \LaTeX package FeynMF, which can be found at <http://www.ctan.org/tex-archive/macros/latex/contrib/feynmf/>

Bibliography

- [1] Thomas Appellequist and Gong-Huo Wu. Electroweak chiral lagrangian and new precision experiments. *Physical Review D*, 48(7), 1993.
- [2] G. Arnison. Experimental observation of lepton pairs of invariant mass around 95-gev/c**2 at the cern sps collider. *Physics Letters*, B(126):398–410, 1983.
- [3] F. Bach. Phenomenology of the three site higgsless model at the atlas detector of the lhc. Master’s thesis, Wuerzburg, Oktober 2009.
- [4] DEPLHI Collaboration. Study of W boson polarisations and triple gauge boson couplings in the reaction $e^+e^- \rightarrow W^+W$ at LEP 2. 2008.
- [5] UA2 Collaboration. Evidence for Z0 at the CERN pp collider. *Physics Letters*, B(129):130–140, 1983.
- [6] M. Barner et al. Observation of single isolated electrons of high transverse momentum in events with missing transverse energy at the CERN anti-p p collider. *Physics Letters*, B(122):476–485, 1983.
- [7] Abbiendi et al. (Opal Collaboration). Constraints on anomalous quartic gauge boson couplings. *Physical Review D*, 70(032005), 2004.
- [8] J.F. Gunion, H. E. Haber, G. Kane, and Sally Dawson. *The Higgs Hunters Guide*. Addison-Wesley Publishing Company, 1990.
- [9] K. Hagiwara, R. D. Peccei, D. Zeppenfeld, and K. Hisaka. Probing the weak boson sector in $e^+e^- \rightarrow W^+W$. *Nuclear Physics B*, 282:253–307, 1986.
- [10] J.A.M.Vermaseren. New features of FORM. 2010.
- [11] W. Kilian. *Electroweak Symmetry Breaking: The bottom up approach*. Springer New York, 2003.
- [12] W. Kilian, T. Ohl, and J. Reuter. Whizard simulating multi particle processes at LHC and ILC. 2007.
- [13] A.C. Longhitano. Low energy impact of a heavy higgs boson sector. *Nuclear Physics B*, (188):118–154, 1980.
- [14] Mandl and Shaw. *Quantum Field Theory*. Wiley, 1984.
- [15] M. Moretti, T. Ohl, and J. Reuter. O’mega an optimizing matrix element generator. 2001.

- [16] T. Ohl. Vegas revisited: Adaptive multi channel integration beyond factorization. 1998.
- [17] Schroeder Peskin. *An Introduction to Quantum Field Theory*, volume 14. 1993.
- [18] C. Schwinn. *Gauge checks (...) of realistic scattering amplitudes*. PhD thesis, Darmstadt, hep-ph/0307057, 2003.
- [19] D.S. Sivia. *Data Analysis A Bayesian Tutorial*. Oxford University Press, 1996.
- [20] C.N. Yang and R.L. Mills. Conservation of isotopic spin and isotopic gauge invariance. *Physical Review*, 91:191, 1954.

Erklärung

Hiermit erkläre ich, dass ich die vorliegende Arbeit selbstständig verfasst und keine anderen als die angegebenen Quellen und Hilfsmittel verwendet habe.

Würzburg, 10. Oktober 2010

Felix Keller